C.P. No. 117
(14,698)
A R C Technical Report

MINISTRY OF SUPPLY

AERONAUTICAL RESEARCH COUNCIL

CURRENT PAPERS

Wake Survey and Strain-Gauge Measurements on an Inclined Propeller in the R.A.E. 24-ft Tunnel

Part I. Wake Survey

By

J. G Russell

LONDON : HER MAJESTY'S STATIONERY OFFICE

1953

NINE SHILLINGS NET

C.P. No.117

ROTOL LIMITED

GLOUCESTER

February, 1952

Performance Office Report No.648

PERFORMANCE OFFICE REPORT NO.648

WAKE SURVEY AND STRAINGAUGE MEASUREMENTS ON AN INCLINED PROPELLER IN THE R.A.E. 24 FT. TUNNEL

PART I – WAKE SURVEY

by

J. G. Russell

SUMMARY

It is well known that when the thrust axis of a propeller is inclined to the flight path the air loads on the blades vary in an approximately sinusoidal manner and give rise to vibratory stresses with a fundamental frequency equal to the propeller rotational speed.

This report describes tests carried out in the R.A.E. 24 ft. wind tunnel with a 16 ft. diameter, 4 bladed propeller, during October and November 1949. Wake survey and blade strain gauge measurements were made at tunnel speeds of 100 and 170 f.p.s. with the propeller axis inclined at angles of 0, 5, 10 and 15° to the airflow. The blade angles and propeller rotational speeds were also varied within the limits imposed by the 1,500 H.P. electric motor.

The lift grading curves at the points of maximum and minimum loading, derived from total head measurements made in the slipstream by means of a pitot comb, have been compared with estimated values, and estimated power absorption figures compared with measured values.

Despite the somewhat unsatisfactory nature of some of the test results it is concluded that the method of estimating the fluctuating lift loading put forward in this report is reasonably accurate.

A comparison of measured and estimated vibratory stresses is given in a companion report, – Project Stress Report No.418 "Wake Survey and Straingauge Measurements on an Inclined Propeller in the R.A.E. 24 ft. Tunnel." Part II.

CONTENTS

LIST OF ILLUSTRATIONS

I. INTRODUCTION

For fixed wing aircraft the airflow into the propeller is normal to the plane of rotation in certain flight conditions only; at all other times, due to changes in aircraft attitude with speed and power, the flow will be inclined at some angle and will give rise to periodic forces acting on the blades, with a fundamental frequency equal to the propeller rotational speed. The stresses induced in the propeller blades by the fluctuating loads are referred to as first propeller order or 1P stresses, since for uniform flow the higher orders are negligibly small. It should be mentioned here, perhaps, that aerodynamic excitation can also be caused by fuselage, nacelle or wing interference and in these cases the higher orders may be of considerable importance. In this report, however, attention will be confined to the case of the inclined propeller in a uniform flow.

Although the existence of these fluctuating loads has long been realised they have been of little concern to the propeller designer until recently, because it was found that providing the blades were designed to withstand engine crankshaft vibration and be free from flutter, no high blade stresses were encountered arising from this 1P excitation.

With the continual upward trend in flying speeds, engine powers and propeller diameters, and the constant urge to develop lighter propellers, the the 1P stresses have become of increasing concern in the last few years, and the advent of the turbine engine with its vibrationless characteristics has focussed additional attention on the problem, as aerodynamic excitation is almost the sole source of vibration with turbo-prop units.

Methods have been developed for calculating the variation in aerodynamic loading on a propeller blade in an inclined flow using an extension of Lock's propeller theory, and employing this fluctuating aerodynamic loading it is possible to estimate the magnitude of the vibratory stresses induced along a blade. Since at the time little experimental data was available to check the theories developed it was decided to carry out the wind tunnel tests described in this report, and measure simultaneously the total head in the wake and the vibratory stresses along the blades of an inclined propeller. The measured stresses and the lift grading curves deduced from the total head readings were then compared with estimated values for a range of operating conditions.

This report covers the calculation and measurement of the aerodynamic loadings while a companion report, Project Stress Report No.418 deals similarly with the stresses. The aerodynamic loadings are given in the form in which they are used in the stressing method, namely as variations of lift grading along the blade.

II. DESCRIPTION OF TEST EQUIPMENT

1. General

The tests were carried out in the 24 ft. Open Jet Tunnel at the R.A.E. A full description may be found in ref.1 but for convenience a line plan is included. Fig.1.

The propeller was driven by a 1,500 HP squirrel cage variable frequency induction motor which was enclosed in a nacelle supported by struts. (Fig.2.) The nacelle was inclined in a vertical plane by means of a screw jack at the base of the rear strut and the angle of inclination determined by a telescopic clinometer mounted on the gallery (Fig.2 and 3).

The power absorbed by the propeller could be measured by noting the input power to the motor and making allowance for losses.

The thrust on the propeller-nacelle unit could be measured on the normal tunnel balance.

2. Propeller

The Rotol propeller used in the test had the following characteristics.

Diameter	–	16 ft.
No. of blades	–	4
Max. Chord	–	12 ins.
Solidity at $r_c = 0.7$	–	0.113
Activity Factor	–	79 per blade
Section Type	–	NACA Series 16
$C_{L_{DES}}$ at $r_c = 0.7$	–	0.484
$tm/_c$ at $r_c = 0.7$	–	6.85%
$tm/_c$ at $r_c = 0.25$	–	24.1%
Blade Drawing No.	–	RA.25680
Rotation	–	Anticlockwise viewed from rear.

The blade angle could be adjusted manually when the propeller was stationary and was measured by a clinometer at the 0.7 fractional radius. Further particulars of the blades are given in Table I.

3. Wake Survey Apparatus

The pitot comb was composed of 13 tubes clamped to a streamlined spar which was secured at the inboard end by a strap around the motor nacelle and at the tip and mid span by rigging wires. (Figs. 2 and 3). The tubes were aligned parallel to the propeller axis with the open ends 16.5 inches behind the blade centre line and at radial intervals corresponding to $r_c^2 = 0.1$, 0.2, 0.3, ... 1.3 (Fig.4).

The pitot comb could be set in any angular position except over the bottom segment where the spar fouled the nacelle struts.

The pitots were connected to a multibank manometer in the balance house and the pressures were recorded by an observer.

4. Straingauge Equipment

Wire-wound electrical resistance straingauges were attached at predetermined positions around the roots and along the outboard portions of the propeller blades in such a manner as to measure the maximum alternating strains due to bending of the blades.

Recording of alternating stresses was by means of the Sperry M.I.T. 4-channel vibration measuring equipment which was installed in the balance room beneath the wind tunnel and connected to the straingauges via screened cables and sliprings mounted behind the propeller. The number of gauges from which records could be taken was limited by the slip rings to four during each run, the gauges being selected by means of a Yaxley switch mounted at the forward end of the propeller shaft so that the switch control rod protruded slightly through a hole in the nose of the spinner.

III. DETAILS OF TEST

1. Wake Traverse Measurements

The range of operating conditions covered in the test is summarised in the following tables:

Tunnel Speed (f.p.s.)	170		
Blade Angle @ r_c = .7	20°	23°	26°55'
Propeller R.P.M.	950	850	750
Inclination of Axis	0° 5° 10° 15°	5° 10° 15°	0° 5° 10° 15°

Tunnel Speed (f.p.s.)	100	170	100	100
Blade Angle @ r_c = .7	20°	20°	23°	26°55'
Inclination of Axis	10	10	5	15
Propeller R.P.M.	650 750 875	750 850	750	650

Since only a very limited time was available for the tests it was essential to keep the test schedule to a minimum, and hence only two spar positions were used for all test conditions with some readings being taken at 3 subsidiary positions as checks. The spar positions are designated by their angular position viz: 0°, 75°, 90°, 105°, 270°, (Fig.4), the two main positions being at 90° and 270°.

As the propeller rotation is anti-clockwise (viewed from rear) it was anticipated that the blade loading would reach a maximum at around 90°, and be a minimum at approx: 270°. In the vicinity of 0° and 180° the loading will have an intermediate value equal to that on an unpitched propeller, and which will be referred to as the 'mean' loading. Preliminary checks with spar positions 75°, 90° and 105°, under the same test conditions, showed that there was very little change in reading of the maximum loading with spar position, most of the variation lying within the limits of repeatability of the manometer readings. (There was a variation of total head outside the prop disc but see Sec.V regarding this.) As it was not possible to use more than two spar positions for the bulk of the tests, because of the limit on time available, it was decided to use 90° and 270°, and to regard the results as representing the true maximum and minimum loadings. For two conditions, readings were taken with the spar at 0° to check the calculated values of mean loading. It was not possible to rig the spar in the 180° position owing to the position of the nacelle struts as mentioned earlier.

In order to record all the straingauge groups it was necessary to repeat each running condition 12 times. As never more than four and, as stated in the last paragraph, usually only two spar positions were used for each condition, there were never less than three separate runs possible at the same condition for each spar position, enabling adequate check readings to be obtained from the manometers.

Because of the time factor no complete sets of readings were taken from the pitot tubes with the nacelle not inclined; this was unfortunate for reasons discussed later. The runs made with the nacelle at 0° incidence were primarily to provide a check on the vibratory stress level in the absence of pitch.

Some fluctuation in the manometer readings was experienced when the propeller was inclined to the flow but it is believed that the mean readings recorded over a short interval were sufficiently accurate. Damping could not be introduced owing to the limited period available for the tests.

The tunnel wind speed as given by the automatic control was checked at frequent intervals by a Chattock Gauge.

The power input to the motor driving the propeller was recorded for each run, and from this the mean power absorbed by the propeller for that condition was obtained.

For some conditions, when the nacelle was not inclined, thrust readings were obtained on the tunnel balance.

2. Straingauge Measurements

Blade and root stresses were recorded for all the conditions quoted in III.1, taking the gauges on one blade in sets of 4. Owing to time limitations it was not possible to survey more than one blade although check readings were made for two gauges on the diametrically opposite blade for every condition.

IV. NOTATION

a	Slope of curve of α against sC_L (assumed linear).
a_h	Speed of sound.
A_o	Slope of low speed lift curve $(dC_{Lo}/d\alpha)$.
b	Slope of curve $\emptyset$ against sC_L (assumed linear).
c	Chord of any blade element at radius r.
C_L	Lift coefficient of blade element.
$C_{L_{Des}}$	Design C_L value for any section.
C_{L_M}	Mean lift coefficient – see Ref. 7.
D	Propeller diameter.
h	Total head behind airscrew disc)
h_o	Total head in front of airscrew) at radius r
L	Lift Force.
M	Helical Mach number at blade element.
n	Rotational speed of propeller (revs. per sec.).
N	Propeller r.p.m.
r	Radius of blade element considered.
r_c	Fractional radius $(\frac{2r}{D})$.
s	Solidity = $(Zc/2\pi r)$.
t_m	Maximum thickness of any section.
V	Velocity of incident airflow.
W	Resultant air velocity at blade element.
W_o	Geometrical velocity of blade element.

Z Number of blades.

$\frac{dL}{dr}$ Lift of blade element between radii r and $(r + \delta r)$.

$\delta\frac{dL}{dr}$ Aerodynamic excitation lift force $\left(\frac{dL}{dr}\text{ Max} - \frac{dL}{dr}\text{ Mean}\right)$

$\Delta\frac{dL}{dr}$ " " " " $\left(\frac{dL}{dr}\text{ Max} - \frac{dL}{dr}\text{ Min}\right)$

α Incidence of blade element measured to chord line.

β Inflow angle $(\phi - \phi_o)$.

Γ Circulation taken over blade section at radius r.

γ_o Mean Low Speed Drag/Lift ratio. See Ref.7.

ε Zero-lift angle.

ζ Angle through which blade has turned from vertical.

θ Blade angle measured to chord line of any blade element or of element at 0.7 radius.

λ Inflow factor corresponding to helicoid angle ϕ.

λ_o Inflow factor corresponding to helicoid angle ϕ_o.

ρ Density of air.

ϕ Angle between plane of rotation and relative air velocity at blade element.

ϕ_o Angle between plane of rotation and geometrical velocity of blade element.

ψ Inclination of propeller axis to incident airstream.

Ω Rotational speed of propeller. (*radians per second.)

ωt Some function of time.

Suffices. 1, 2, 3 – are used to indicate 1st, 2nd and 3rd approximations.

ωt – to denote the general value of some quantity changing with time.

V. ANALYSIS OF TEST RESULTS

1. Determination of Aerodynamic Excitation Forces from Wake Survey

Using the Kutta-Joukowski relation we may write,

$$dL = \rho \Gamma W \, dr \qquad \text{(1)}$$

Lock shows (Ref.2) that, neglecting profile drag, the measured difference of total head across the propeller is given by

$$h - h_o = \frac{Z\rho\Gamma\Omega}{2\pi} \qquad \text{(2)}$$

Combining equations (1) and (2) we get

$$\frac{dL}{dr} = \frac{2\pi W}{Z\Omega}(h - h_o) \qquad \text{(3)}$$

The effect of profile drag on the thrust is generally negligible provided that the corresponding blade element is not stalled, and no account has been taken of it in this instance.

Experimental values of $\frac{dL}{dr}$ at the various spar positions may be derived from the test results by use of equation (3). The rotational speed is obtained from the known test conditions, h and h_o are obtained from the manometer readings as described below, and W is obtained theoretically (see section VI) from the geometry of the airflow.

No attempt was made to measure the total head upstream of the propeller disc since it was thought that the readings from the pitot tubes outside the propeller wake would be equivalent. When the tests were completed, however, it was realised that a considerable difference in total head existed on either side of the disc for the same tunnel conditions, indicating some variation across the working section. This was possibly due to the effect of the propeller slipstream on the flow around the tunnel, and it was therefore decided to assume arbitrarily that the free stream total head varied linearly across the disc to satisfy the two end conditions at the slipstream boundary. Figs. 5 and 6 show the measured total heads across the disc for several conditions, as given by spar positions 90° and 270° (for the horizontal plane) and also the readings obtained from spar positions 75° and 105°. It is remarkable that the readings from the two latter positions were identical outside the slipstream in all cases checked. The dashed lines on the figures indicate the assumed variation of free stream total head, while Figs. 7 and 8 show this more clearly for a number of cases.

Fig. 9 shows plots of the actual manometer readings taken for one spar position for one test condition, and indicates the amount of test scatter. Similar plots were made for each test condition, and values of h were read off from a faired curve drawn through the points for use in the evaluation of $\frac{dL}{dr}$ by means of equation (3). For this reason no test points are shown on the lift grading curves.

An estimate (Ref.3) of the blockage effect due to the presence of the motor nacelle indicated that the measured values of J should be increased by 0.4% but this was considered to be negligible.

To the thrust values measured on the tunnel balance, the drag of the nacelle in the absence of the propeller was added so as to give propulsive thrust figures. No other corrections were made.

VI. CALCULATION OF THEORETICAL VALUES

1. Estimation of Aerodynamic Loads

Consider a propeller with the axis inclined at an angle ψ to a uniform airstream having a velocity V. This velocity V may be resolved into components V cos ψ and V sin ψ perpendicular and parallel to the plane of rotation. (Fig. 10 a).

Fig. 10 (b) shows the propeller disc, viewed from the rear, when a blade has rotated through an angle ζ from the vertically upright position. The component V sin ψ, parallel to the propeller disc, may be resolved into two further components, V sin ψ sin ζ at right angles to the blade and in the direction of the rotational (tangential) velocity, and V sin ψ cos ζ in a radial direction along the blade. The component along the blade is considered to have a negligible effect on the aerodynamic characteristics of the blade elements, and is therefore neglected.

The effect of the component in the direction of the rotational velocity can be seen to vary with ζ. Its value when ζ = 0 and 180° is zero. When ζ = 90° the value is V sin ψ and is additive to the rotational velocity, and when ζ = 270° its value is also V sin ψ, but it subtracts from the rotational velocity. The velocity diagram for a blade element will thus change with ζ. Fig. 10 (c) shows the form of the diagram. The blade angle 'θ' is constant, but the magnitude and direction of 'W' will change with ζ, and will give rise to a fluctuating lift load on the element. With the assumption discussed in the next paragraph, this load will be a maximum when ζ = 90° and a minimum when ζ = 270°. For the 0° and 180° positions the loadings will be equal, and the same as that obtaining on an unpitched propeller operating in an airstream of velocity V cos ψ. This loading is referred to as the 'mean' loading.

From purely geometrical considerations it is possible to evaluate the values of $\emptyset_o$ and W_o (shown in Fig. 10 (c)) at any given instant, i.e. at any value of ωt and hence of ζ. Consideration of the fluctuating nature of the flow at any element leads to the conclusion that the frequency is sufficiently low for any oscillatory and lag effects on the section aerodynamic characteristics to be neglected. It is therefore assumed that normal steady state characteristics applicable to the instantaneous local values of incidence, Mach No. etc., may be employed, and that no lag effects are present.

If, therefore, the inflow velocities can be calculated for any given value of ζ, the loading on the blade can be determined. In this connection the assumption is made that, since at any point on the propeller disc the blade loading does not vary (each blade element as it passes will experience the same load at that point as those before and after it) the inflow velocities there may be obtained by considering all blade elements at that particular radius to be operating under the same conditions as apply to the one particular point, and evaluating the inflow velocities for the annulus in question in the normal way.

It can be shown, by taking a series of values of ζ, that the variation of loading on a blade element is very nearly sinusoidal in form, and hence it is reasonable for stressing purposes to calculate the Maximum and Minimum loadings only, and to take half the difference between them as representing the amplitude of a true sine wave fluctuation.

Alternatively, since in practice it is necessary to evaluate the mean condition in order to fix the blade angle on constant speeding propellers before the maximum or minimum loads can be evaluated, the amplitude of the sine wave may be taken as being the difference between the maximum and the mean loadings to save computation.

Assuming that the blade angle of any element is known, and also the local operating conditions, i.e. that $\emptyset_o$ is known, there are three conditions to be satisfied to enable the value of $\emptyset$, and hence of the blade loadings to be determined. (See equations (5), (6) and (7) of Ref. 4.) These conditions are:-

$$s C_L = 4 \lambda \tan \beta \sin \emptyset \qquad (4)$$

$$\theta = \alpha + \emptyset \qquad (5)$$

$$\emptyset = \emptyset_o + \beta \qquad (6)$$

Still following Ref. 4 it can be argued that, below the incidence stall, the lift curve slope may be assumed linear, so that

$$a\, s C_L = \alpha + \varepsilon \qquad (7)$$

where $$a = \frac{d\alpha}{d(s C_L)}$$

Now Ref. 4 (equations 43 and 44) shows that

$$\frac{d C_L}{d\alpha} = A_o (1-M^2) - 1/2 \quad \text{for sections less than 15\% thick.}$$

Ref. 5 shows that for such sections $A_o = 0.1$

hence substitution in equation (7) gives

$$a = \frac{0.1}{s} (1 - M^2) - 1/2 \qquad (8)$$

applicable to all sections less than 15% thick, that is to all working sections on normal modern blades.

Except in cases of very heavy disc loadings at low forward speeds, values of β are sufficiently small to justify the simplification

$$\tan \beta = \beta \qquad \text{(9)}$$

whence from (4) above we obtain

$$\beta = b \, s \, C_L \qquad \text{(10)}$$

where $$b = \frac{1}{4 \mathcal{K} \sin \phi}$$

From a combination of equations (5), (6), (7) and (10), it can be shown that

$$s \, C_L = \frac{\theta - \phi_o + \varepsilon}{a + b} \qquad \text{(11)}$$

Since it has been regarded as permissible to make the approximation given by equation (9) it follows that

$$W \doteq W_o \qquad \text{(12)}$$

as in fact $W = W_o \cos \beta$

and from fig. 10 (c) it can be seen that

$$W_{o_{\omega t}} = \left((\Omega r + V \sin \psi \sin \zeta)^2 + (V \cos \psi)^2 \right)^{1/2}$$

Now ref. 3 equation (38) gives

$$M = W_o / a_h$$

so that in equation (11) above all the terms on the right hand side can be regarded as known once the blade angle and operating conditions are known, with the exception of b.

For high J cases the approximation given by equation 10 of ref. 4 may be used, whence equation (11) can be solved explicitly. For low J values, as in the case of every condition tested during the present investigation, it is necessary to obtain b by successive approximations as follows:-

write $b_1 = \frac{1}{4 \mathcal{K}_o \sin \phi_o}$ as the first approx.

then evaluate $(sC_L)_1 = \frac{\theta - \phi_o + \varepsilon}{a + b_1}$

then $\beta_1 = b_1 (sC_L)1$

$\phi 1 = \phi_o + \beta 1$

$b_2 = \frac{1}{4 \mathcal{K}_1 \sin \phi_1}$

$(sC_L)_2 = \frac{\theta - \phi_o + \varepsilon}{a + b_2}$

etc:

'b' is quickly convergent and the value of b_3 will suffice as the true value in all reasonable circumstances, while in most cases b_2 will serve.

It must be remembered that at low J values the accuracy of equation (4) becomes doubtful as the assumptions on which it is based cannot be justified under such circumstances, and as all the above reasoning is founded on (4) this too must suffer in accuracy.

The lift on a blade element is, from first principles

$$\delta L = \tfrac{1}{2}\rho c\, W^2\, C_L\, \delta r$$

or

$$\frac{dL}{dr} = \tfrac{1}{2}\,\rho\, W^2 s\, C_L \frac{\pi\, Dr_c}{Z}$$

$$= sC_L\, W^2 r_c\, \frac{\pi\, D\rho}{2Z} \qquad (13)$$

It will be seen therefore that the theory above will enable $\frac{dL}{dr}$ to be obtained in any circumstances for any value of ζ once the blade angle is known. Test results, see ref. 6 for example, have shown that the power absorption of a propeller changes very little when its thrust axis is inclined to the airflow. If therefore normal strip analysis procedure is employed to determine the blade angle to absorb the correct power, assuming the whole propeller to be working under the 'mean' conditions as defined by J' this angle can be assumed to be that at which the propeller will settle down in the pitched condition.

Obviously the fluctuating drag load can be obtained as well as the lift load, but as the purpose of the evaluation of the loads is to enable stressing of the blades to be undertaken, and as the drag components, acting in the stiffest direction of the blade, produce negligible stresses, they are usually not evaluated.

The procedure followed to obtain theoretical values of $\frac{dL}{dr}$ for comparison with the measured was therefore as follows:-

(i) From the known blade angle for each test condition values of $\frac{dL}{dr}$ mean were computed by strip analysis procedure, as mentioned above, being determined by successive approximations.

(ii) The power absorbed, assuming the whole propeller to be operating under the mean conditions, was determined neglecting the drag terms.

(iii) Values of Maximum and Minimum $\frac{dL}{dr}$ were then calculated using the theory outlined above.

(iv) Values of $\Delta \frac{dL}{dr} = \frac{dL}{dr}\,\text{Max} - \frac{dL}{dr}\,\text{Min}$

were then obtained.

Since the propeller blades embodied NACA series 16 sections, the section data implied by equation (8) above is not necessarily strictly true, but is thought to be sufficiently representative of thin sections operating below their critical Mach No. to be used for the Series 16 sections. The no lift angle was in all cases assumed to be $7.3 \times C_L$Des.

2. Estimation of Propeller Thrust

Since some thrust measurements were available for a non-inclined propeller, it was decided to check the values given by the SBAC Standard Method of Propeller Performance Estimation for the same conditions against these. Ref. 7 gives details of the derivation and use of the SBAC Method and it is therefore not necessary to go into particulars in this report. The SBAC method as at present published is limited to blades with Clark Y sections, but provisional curves of $\gamma_o - C_{LM}$ have been derived for NACA Series 16 sections, allowing the method to cover these in addition. The particular $\gamma_o - C_{LM}$ curve used in the present calculations is given in Fig. 43 for reference. Using this and the known nacelle diameter, propulsive thrust figures were evaluated for the same conditions for which test

results existed, (i.e. known V, N and Power) the body correction factor being based on the nacelle-propeller diameter ratio.

VII. RESULTS

1. Blade Loading

Measured and calculated maximum and minimum lift grading curves for the various conditions covered by the tests are shown plotted in figs. 11 to 26, together with the variation of lift grading from minimum to maximum. Only two conditions were investigated with the spar in the 0° position, and the mean loadings resulting from this spar position are given in figs. 19 and 26. Pitot readings were obtained in two cases with the nacelle not inclined and these results are given in figs. 30 and 31. As readings were available for one spar position only in each case it is not possible to show any measured variation on these figures, and the theoretical variation is of course zero.

In order to show the effect of variation of angle of inclination and of rpm on the measured and calculated blade loadings figs. 32 to 36 have been prepared. The results covered by these figures are restricted to the Maximum loadings for reasons discussed below. Figs. 37, 38 and 39 show, each for one radius only, the effects of change of inclination on maximum, minimum and fluctuating lift gradings for three typical combinations of blade angle rpm and tunnel speed. The effect of taking the excitation as being a sine wave of amplitude $\delta \frac{dL}{dr}$ (i.e. $\frac{dL}{dr}$ Max $-$ $\frac{dL}{dr}$ mean) in place of a sine wave of amplitude

$$\frac{1}{2} \Delta \frac{dL}{dr} \left(\text{i.e. } \left(\frac{1}{2} \frac{dL}{dr} \text{ Max} - \frac{dL}{dr} \text{ Min} \right) \right) \text{ is shown by plots}$$

on figs. 19 and 26 and by Table II. As the difference is very small in all cases the figures are given for a limited number of conditions only.

2. Power Absorption

Figs. 40 and 41 give the measured and calculated values of the overall torque coefficient for the propeller, showing the variation with ψ, and with N.

3. Thrust

Fig. 42 shows the measured and calculated thrusts for various conditions for an unpitched propeller, the measured torque at the time the thrust readings were taken is also indicated.

VIII. DISCUSSION

1. Comparison of Estimated and Measured Aerodynamic Excitation Forces and Lift Grading along the Blade

(a) It can be seen from the majority of the maximum lift grading test results that whereas there is good agreement with the estimated values over most of the blade, the curves drop off very quickly beyond $r_c = 0.9$. This is probably due to a combination of slipstream contraction and distortion. Since the pitot comb was fairly close to the propeller disc and the thrust loading was low the contraction effect should not be large; the distortion effect due to the inclined airflow will have more significance but is less easily determined. Due to the method of supporting the spar the pitots were in actual fact not at the true 90° position, but, slightly beyond 90°, the actual value varying with radius. It is not considered that this small discrepancy had any measurable effect on the results.

The question of incidence stall at the tips was considered and the operating conditions of the blade elements were compared with the test data of ref. 8, but it was found that the blade elements inboard were more liable to stall than those outboard. Table IV is included to show the operating and estimated lift coefficients (at $r_c = 0.7$) for six typical conditions. The first condition (i.e. J = 0.422) shows the maximum C_L experienced during the tests. The estimated values of C_L are based on the assumption that the slope of the low speed $C_L - \alpha$ curve is 0.1 and that account is taken of the Glauert rise with increase of Mach No.

(b) It will be noted that in all cases the minimum loading results are less than the estimated values and while in some cases the agreement between the two sets of values is reasonable in others there is considerable discrepancy. This is thought to be due to the failure of the pitot tubes to record the full total head, and this view is supported by an estimate of the airflow angles at the pitot comb. As already mentioned the pitot tubes were fixed parallel to the propeller axis and consequently the angle between them and the incident airflow is composed of:

(a) The propeller inclination angle

and (b) The induced flow angle due to the bound and trailing vortices.

The accurate determination of (b) is not easy even for the uninclined propeller, but an approximate method due to Haines (ref. 9) for this latter case has been used to obtain an estimate of this effect. For an inclined propeller it is likely that the downwash induced in the wake will reduce the angle of incidence relative to the pitots.

The effect of the bound and trailing vortices has been calculated for two typical cases at positions of maximum and minimum loading. These results are tabulated in Table III. If the slipstream is assumed to approach the disc parallel to the propeller axis then at the point of maximum loading the incidence at $r_c = 0.7$ will be 19.9° for case A, whereas if the flow is assumed to remain parallel to the tunnel axis (i.e. no induced downwash) then the incidence will be only 9.9°. In actual fact the incidence will be somewhere between 9.9° and 19.9°, and since the pitots should record true total head up to about 15° (see ref. 3) we may consider this to be satisfactory.

At the point of minimum loading, however, the incidence is estimated to be between 17.7° and 27.7° and hence the test readings are almost certain to be low. Examination of fig. 22 (appropriate to case A) confirms that the maximum loading value is 4% low relative to the theoretical figure whereas the minimum loading result is 12.6% low.

In case B the maximum loading incidence lies between 9.8° and -5.2° and the minimum loading angle between 6° and 21°. As might be expected the measured and estimated total head values are coincident at the point of maximum loading as shown in fig. 13 but for minimum loading the test values are 4.5% low.

The consistent relationship between the percentage error and pitot incidence in these two cases may be taken as strong evidence in favour of this theory.

(c) The variation from maximum to minimum loading $\Delta\, dL/dr$, is the difference of two large quantities and therefore a small percentage error in either of them will induce a large percentage error in $\Delta\, dL/dr$. Thus, though the maximum and the minimum loading test results and theoretical values may agree fairly closely, the discrepancy in $\Delta\, dL/dr$ is sometimes a large percentage of the actual value.

(d) The theoretical values have been evaluated on the assumption that the free stream velocity is constant across the propeller disc, but since the total head values outside the slipstream on either side of the disc are not equal it is not unreasonable to suppose that the velocity distribution far upstream is not uniform. Three typical cases have therefore been re-analysed assuming the static pressure is equal to the atmospheric pressure, and thus the velocity head to vary as the assumed free stream total head. These cases are shown in figs. 27, 28 and 29.

It is interesting to note that in all three cases the values of $\Delta\, dL/dr$ are increased and in general agree more closely with the test results, although agreement with the actual Max and Min loadings is improved in only one case, being made worse in the others.

(e) The discrepancy between the measured and calculated mean values shown in figs. 19 and 26 is attributable to two causes. The spar in position 0° is most probably not in the correct position to measure the mean lift. The exact spar position is of little importance in measuring the maximum and minimum values of a sine wave, but will be of much more importance in the mean case. Some American results (ref. 10) which became available after the completion of these tests show an appreciable phase shift of measured values relative to those calculated, probably due to aerodynamic lag effects. In addition, the spar is mounted so that the pitots are inclined in the direction of the propeller axis (i.e. at ψ° to the incident flow.) The actual slipstream direction is probably at some angle between ψ and the normal axial flow direction so that a pitot will actually record the total head relative to a blade section further inboard than the radius at which the pitot is situated, and hence the measured mean values of figs. 19 and 26 should in fact be shifted inboard by some small amount. In view of these two factors it was concluded that the measured values of $\frac{dL}{dr}$ from spar position 0° could not be regarded as being mean values, and hence comparison with calculated mean values is really pointless.

It was pointed out in section VI above that the loading when the propeller was not inclined should be almost identical to that of the mean loading for an inclined case. In two instances the loadings were measured with the spar in positions 90° and 270° and with the nacelle not inclined. The comparison between the measured and calculated values for these cases is shown in Figs. 30 and 31, with the addition of a calculated mean loading for $\psi = 15^{\circ}$. In the case of Fig. 30 an incomplete set of readings was also taken with the spar in position 90°. The figures tended to show that the loading measured in the 270° position (i.e. the normal minimum) was slightly higher than that at 90°, suggesting that the airstream in the tunnel was not truly axial. Since the readings are incomplete however, no conclusions can be drawn and it must be emphasised that the effect, if any, was slight. It is known in fact that the airstream in the tunnel does deviate very slightly from axial. The agreement between the measured and calculated values for $\psi = 0^{\circ}$ is excellent in Fig. 30 and reasonable in Fig. 31. The small change of mean loading for 15° of pitch is also apparent and it is unfortunate that more readings were not taken with the nacelle at zero pitch as they would have provided additional, though indirect, backing for the method of calculation, in view of the doubts expressed above regarding the validity of the minimum loading curves.

(f) Figs. 32 to 36 have been restricted to the maximum values only, in view of the suggestion in VIII 1.(b) above. It can be seen that the theory effectively takes account of variation of ψ and of r.p.m. The agreement of measured and theoretical values is very good for the 20° and 23° blade angle settings, but not too good for 26°55', the measured values being consistently higher than those calculated in this instance, although the variation with ψ is consistent as figs. 37, 38 and 39 show. The reason for this is not known, a low measured value, relative to one calculated, may possibly be explained away, but a high value is difficult to account for unless the actual power absorption is higher than that calculated. Fig. 40 shows that in fact this was not the case. There was some confusion regarding the setting of the angle for the 26°55' tests (i.e. the original schedule called for 26°) but the discrepancy between the measured and calculated values of K_Q for the high angle tests is of the same order as those for the lower angles, which refutes any suggestion that the angle was in fact somewhat greater than 26°55'.

(g) Theoretically the aerodynamic excitation $\Delta \frac{dL}{dr}$ is proportional to the angle of inclination ψ, provided that ψ is small. Figs. 37, 38 and 39 show that for values of ψ up to 15° $\Delta\frac{dL}{dr}$ does vary linearly with ψ for the three radii and three blade angles covered, although in view of the suggestion in VIII 1.(b) above this is probably fortuitous.

2. Comparison of Estimated and Measured Power Absorption

From Figs. 40 and 41 it can be seen that the estimated values of K_Q for the propeller are always somewhat above those measured. The absolute magnitude of the discrepancy is not constant, it appears to increase slightly with blade angle and with forward speed, but a good deal of this variation

may be regarded as within the limits of accuracy of measurement or of computation. As the estimates of K_Q take account only of the lift terms and neglect the drag the actual discrepancies in each case will be slightly greater than figs. 40 and 41 suggest. Since the difference between measured and calculated values is much closer to a constant absolute value, rather than to a constant percentage value, it is considered that the no-lift angles used in the calculations are probably slightly incorrect, but that the values of $\frac{dC_L}{d\alpha}$ used are substantially correct.

It is most encouraging however to note from Fig. 40 that the rise of calculated and measured values with increase of ψ is nearly identical, thus justifying the method proposed in Section VI 1 above for determining the blade angle in the general case of a constant speeding propeller. This blade angle will be slightly too low if the same section data is used as employed in this report, but this is regarded as of very minor importance as the load distribution will be correct. It is also encouraging to note that change of r.p.m. is also successfully allowed for, see Fig. 41.

3. Comparison of Estimated and Measured Thrust Values

From Fig. 42 it can be seen that the calculated values are always higher than those measured but that the employment of a slightly more severe body correction factor would lead to very good agreement, except possibly for the $\theta = 26^\circ$ case at low r.p.m. It is of course not possible to make any very conclusive comment on the merit of the S.B.A.C. method as the range of conditions covered by the test is very limited, but except at the very low r.p.m. the variation of thrust with r.p.m. and K_Q is given quite adequately. The S.B.A.C. Method takes no account of blade angle in evaluating thrusts or efficiencies hence the values of θ given on Fig. 42 are purely for identification purposes.

It is perhaps worth pointing out that this propeller would in practise develop some 7000 lbs. thrust at full power at 900 r.p.m. at forward speeds of the order of 100 – 170'/sec and that normally it would never be analysed for such low values of K_Q. The absolute value of the discrepancy between measured and calculated values appears for any r.p.m. to be approximately constant and not to vary with power or thrust, hence for a higher thrust this discrepancy would not represent anything like the same percentage error that it does on Fig. 42.

IX. CONCLUSIONS

1. To obtain the blade angle on a pitched constant speeding propeller operating in a uniform flow under known conditions of power r.p.m. and forward speed, it is sufficient to regard the propeller as absorbing the known power at the given r.p.m. but operating normal to an airstream whose velocity is V cos ψ, and to evaluate the blade angle in the way normally used when strip analysing a propeller.

2. In view of the general agreement of the estimated maximum loading values of lift grading with those measured, and of the estimated power absorptions with those measured, the theoretical means of obtaining the fluctuating load on a pitched propeller put forward in section VI above, is regarded as reasonably justified, not withstanding the poor agreement between estimated and measured minimum lift gradings (and hence of fluctuating load) which can be explained by mis-alignment of the pitot tubes.

3. It is sufficiently accurate to take the excitation as being the difference between the 'maximum' and 'mean' loadings.

4. The conclusions above are strictly limited to low values of J, to low blade angles, to low operating Mach Numbers on the blade elements, and to operating section lift coefficients below the stall. However the theory given is not dependent on the values of J and θ being low, and it is considered that it should be reliable at higher values of J and θ than those tested.

5. The S.B.A.C. Standard Method of Propeller Performance Estimation gave, over the normal r.p.m. range for a propeller of this size, the correct variation of thrust with change of power, r.p.m. and forward speed over the range tested. The absolute calculated values of thrust were a little high but a somewhat more severe body correction factor would satisfactorily take account of this discrepancy.

Various members of the Performance Office have been concerned with the preparation of this report, in the actual conduct of the tests in conjunction with the R.A.E. Tunnel Staff, in analysis of the results and in the theoretical investigations made.

X. REFERENCES

No.	Author	Title etc.
1	Jennings, W. G., Terry, A., and Pearsall, P. J.	"Preliminary Calibration of the 24 foot Wind Tunnel, R.A.E., with a Short Description of the Tunnel." R and M 1720.
2	Lock, C. N. H. and Yeatman D. M.	"Periodic Flow behind an Airscrew". R and M 1483.
3	Monaghan, R. J.	"Blockage Effect on Propellers of Two Motor Nacelles used in the R.A.E. 24 ft. Tunnel." Tech. Note No. Aero 1590.
4	Lock, C. N. H., Pankhurst, R. C., and Conn, J. F. C.	"Strip Theory Method of Calculation for Airscrews on High Speed Aeroplanes". R and M 2035.
5	Haines, A. B. and Monaghan, R. J.	"High Speed Lift and Drag Data for Propeller Performance Calculations". R and M 2036.
6	Runckel, J. F.	"The effect of Pitch on Force and Moment Characteristics of full scale Propellers of Five Solidities". NACA. June 1942. ARC 6139.
7	-	"S.B.A.C. Standard Method of Propeller Performance Estimation". Published by the S.B.A.C., 32, Savile Row, London, W.1.
8	Lindsey, W. F., Stevenson, D. B., and Daley, N. D.	"Aerodynamic Characteristics of 24 NACA 16 - series aerofoils at Mach Nos. between 0.3 and 0.8". NACA TN 1546.
9	Haines, A. B.	"Fluctuation of Flow behind a Propeller at High Advance". Tech. Note No. Aero 1472.
10	Crigler, J. L. and Gilman, J. Jr.	"Calculation of Aerodynamic Forces on a Propeller in Pitch or yaw". NACA RM No. L8K26. (TIB/2074).

RADIUS FROM PROP. AXIS	INCHES	16	20	24	32	40	48	56	64	72	80	88	92	Tip
CHORD	INCHES	9.0	9.37	9.72	10.38	11.02	11.57	11.97	12.00	11.54	10.70	9.22	7.90	0
MAX. THICKNESS	INCHES	2.820	2.580	2.340	1.830	1.460	1.185	0.984	0.860	0.746	0.622	0.450	0.350	0
DESIGN LIFT COEFFICIENT		0	0.195	0.289	0.378	0.440	0.483	0.504	0.494	0.469	0.435	0.397	0.378	–
BLADE ANGLE	DEGREES	77.5	74.9	72.2	67.2	62.6	58.4	54.6	51.3	48.4	45.6	43.3	42.3	41.4
	Tip Radius is 96 inches. N.A.C.A. Series 16 Sections are used throughout.													

TABLE I. DETAILS OF BLADE TO DRAWING RA. 25680

CONDITIONS				Fractional radius r_c / lbs/ft. Fluctuating Load	0.30	0.45	0.60	0.70	0.80	0.90	0.95
V ft/sec	N R.P.M.	θ Degrees	ψ Degrees								
170	950	20	10	$\delta \frac{dL}{dr}$	26.1	36.5	46.0	46.0	42.2	34.5	28.0
				$\frac{1}{2} \Delta \frac{dL}{dr}$	24.6	36.3	43.9	44.1	41.0	32.6	26.5
170	850	23	15	$\delta \frac{dL}{dr}$	40.8	56.9	70.1	73.0	69.5	57.6	46.0
				$\frac{1}{2} \Delta \frac{dL}{dr}$	36.9	52.5	67.1	70.1	66.2	54.1	44.3
100	875	20	10	$\delta \frac{dL}{dr}$	13.8	22.9	26.4	28.6	27.0	20.9	16.8
				$\frac{1}{2} \Delta \frac{dL}{dr}$	13.6	21.4	26.3	27.4	25.5	20.8	16.3

NOTE:- $\delta \frac{dL}{dr} = \frac{dL}{dr}$ (Max) $- \frac{dL}{dr}$ (Mean) $\qquad \Delta \frac{dL}{dr} = \frac{dL}{dr}$ (Max) $- \frac{dL}{dr}$ (Min)

TABLE II: COMPARISON OF ALTERNATIVE THEORETICAL METHODS OF OBTAINING 1 P EXCITATION FOR STRESSING PURPOSES

TABLE II

		FRACTIONAL RADIUS r_c	0.3	0.45	0.6	0.7	0.8	0.9	0.95	0.975	
MAXIMUM LOADING SIDE	a	Effect of Trailing Vortices	8.9	8.9	7.8	6.6	5.5	4.3	4.0	3.86	CASE A CONDITIONS:- V = 100 θ = 20° ψ = 10° N = 875 RPM (see Fig. 22)
	b	" " Bound Vortices	7.2	11.0	13.4	13.3	11.9	9.2	7.3	5.87	
	c	Total Effect assuming Slipstream parallel to thrust line	16.1	19.9	21.2	19.9	17.4	13.5	11.3	9.73	
	d	Total Effect assuming Horizontal Slipstream	6.1	9.9	11.2	9.9	7.4	3.5	1.3	0.27	
MINIMUM LOADING SIDE	a	Effect of Trailing Vortices	6.8	8.4	6.9	6.0	5.0	3.9	3.7	3.5	
	b	" " Bound Vortices	5.3	9.4	11.6	11.7	10.6	8.2	6.5	5.2	
	c	Total Effect assuming Slipstream parallel to thrust Line	12.1	17.8	18.5	17.7	15.6	12.1	10.2	8.7	
	d	Total Effect assuming Horizontal Slipstream	22.1	27.8	28.5	27.7	25.6	22.1	20.2	18.7	
MAXIMUM LOADING SIDE	a	Effect of Trailing Vortices	4.66	4.9	4.3	3.6	2.8	2.1	1.9	1.73	CASE B CONDITIONS:- V = 170 ft/sec. θ = 20° ψ = 15° N = 950 RPM (See Fig. 13)
	b	" " Bound Vortices	3.54	5.6	6.5	6.2	5.4	3.7	2.7	2.07	
	c	Total Effect assuming Slipstream parallel to thrust line	8.2	10.5	10.8	9.8	8.2	5.8	4.6	3.8	
	d	Total Effect assuming Horizontal Slipstream	6.8	4.5	4.2	5.2	6.8	9.2	10.4	11.2	
MINIMUM LOADING SIDE	a	Effect of Trailing Vortices	.51	2.3	2.6	2.3	1.7	1.2	1.1	0.9	
	b	" " Bound Vortices	.37	2.6	3.7	3.7	3.0	2.1	1.4	1.1	
	c	Total Effect assuming Slipstream parallel to thrust Line	.88	4.9	6.3	6.0	4.7	3.3	2.5	2.0	
	d	Total Effect assuming Horizontal Slipstream	15.88	19.9	21.3	21.0	19.7	18.3	17.5	17.0	

Incidence of airflow relative to pitot tubes–degrees

TABLE III. ANGULAR FLUCTUATIONS IN THE WAKE DUE TO BOUND AND TRAILING VORTICES

CONDITIONS $\theta = 20^\circ$ $\psi = 10^\circ$ for all Cases.			All values refer to 0.7 radius								Reference to Figure giving Lift grading Curves
			LIFT GRADING – $\frac{dL}{dr}$ – lbs./ft.				LIFT COEFFICIENT – C_L				
V	N	J'	Maximum		Minimum		Maximum		Minimum		
ft/sec	R.P.M.		Estimated	Measured	Estimated	Measured	Estimated	Actual	Estimated	Actual	
100	875	0.422	307	295	252	221	0.90	0.865	0.842	0.804	Fig. 22
100	750	0.493	198	181	156	138	0.770	0.705	0.704	0.621	Fig. 21
100	650	0.568	129	125	93	84	0.655	0.634	0.559	0.503	Fig. 20
100	950	0.661	243	243	155	149	0.555	0.555	0.430	0.416	Fig. 12
170	850	0.739	156	155	87	68	0.431	0.430	0.298	0.233	Fig. 24
170	750	0.837	82	78	23	13	0.280	0.267	0.098	0.056	Fig. 23

TABLE IV. MAXIMUM AND MINIMUM ESTIMATED AND ACTUAL LIFE COEFFICIENTS

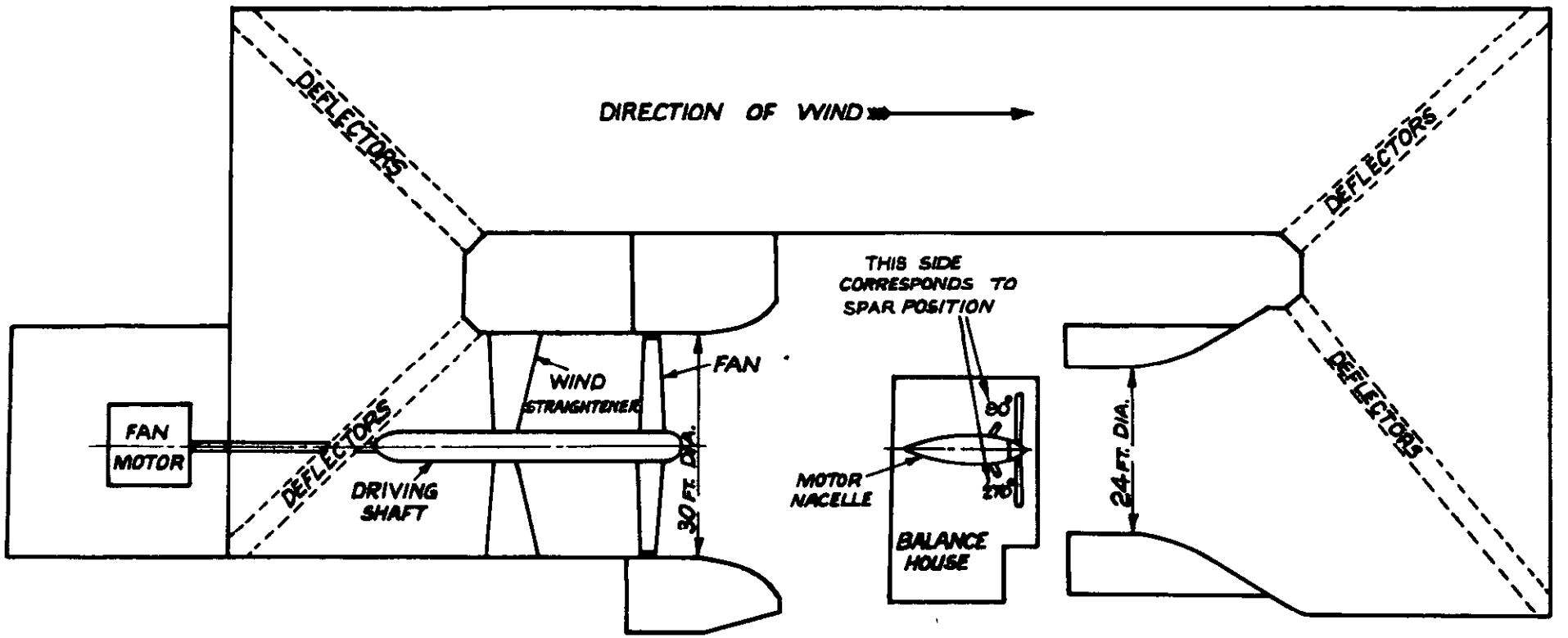

FIG. 1

FIG. 1 DIAGRAMMATIC PLAN OF R.A.E. 24FT. WIND TUNNEL

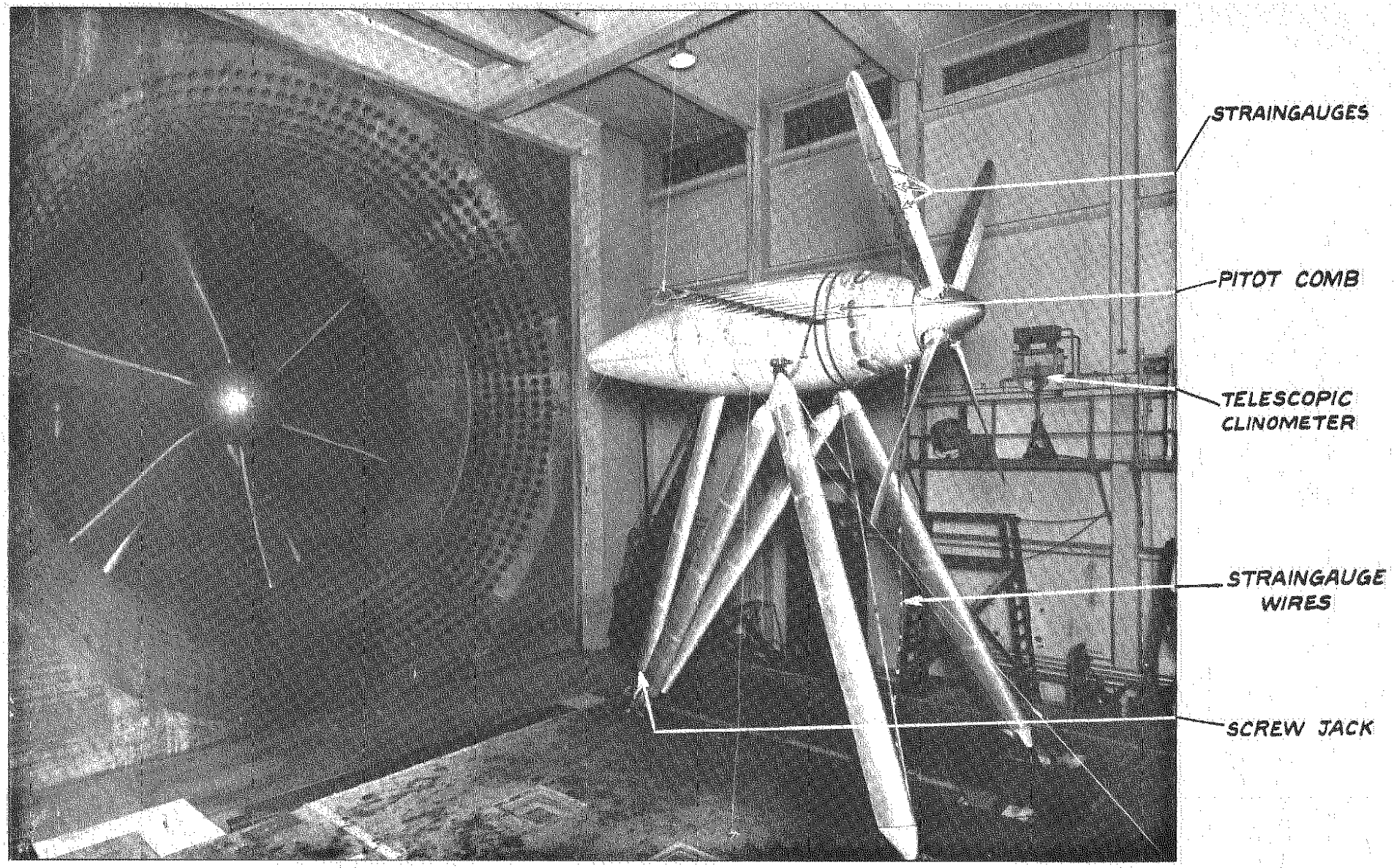

FIG. 2 VIEW OF NACELLE WHEN HORIZONTAL

FIG. 2

FIG. 3

FIG. 3 VIEW OF NACELLE WHEN INCLINED AT 15° TO HORIZONTAL

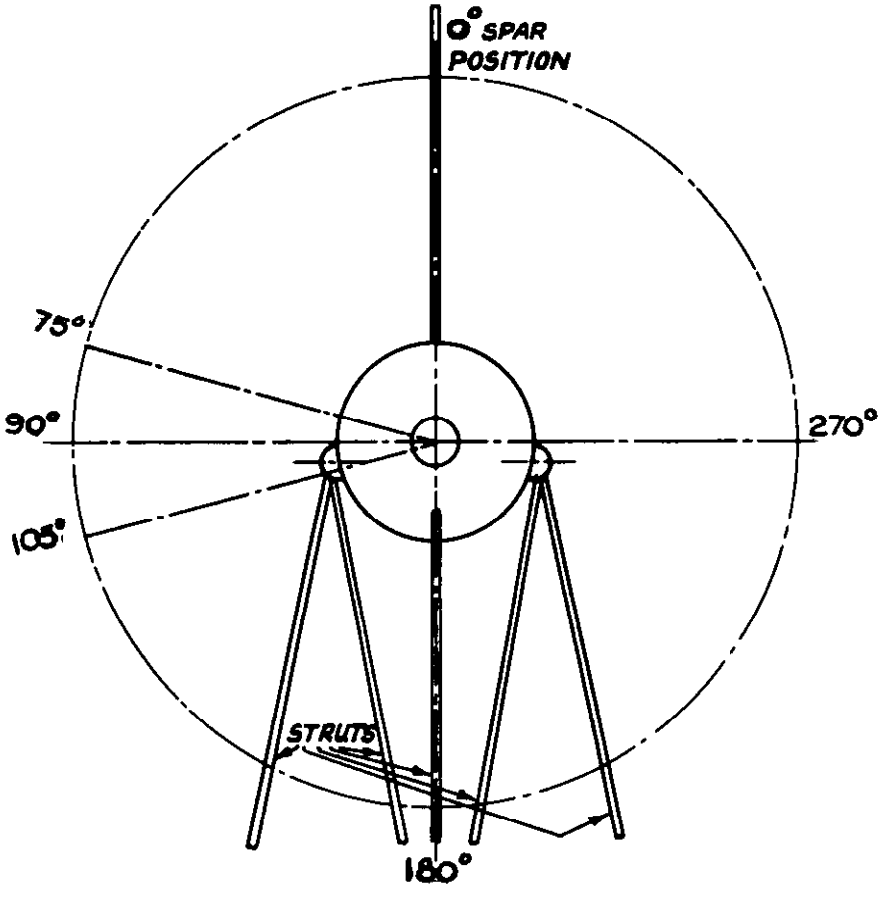

VIEWED FROM REAR

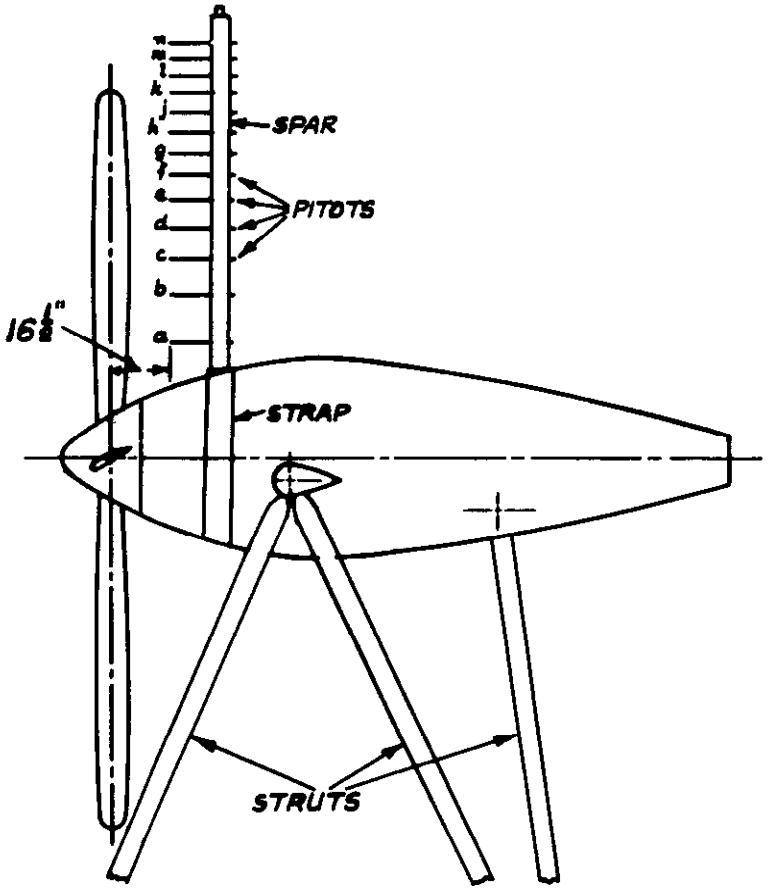

SIDE VIEW

PITOT POSITIONS			
PITOT	r_c^2	r_c	R (FT.)
a	0·1	0·3162	2·53
b	0·2	0·4472	3·578
c	0·3	0·5477	4·382
d	0·4	0·6325	5·06
e	0·5	0·7071	5·657
f	0·6	0·7746	6·197
g	0·7	0·8367	6·694
h	0·8	0·8944	7·155
j	0·9	0·9487	7·59
k	1·0	1·0	8·0
l	1·1	1·049	8·382
m	1·2	1·095	8·76
n	1·3	1·14	9·12

FIG. 4.

FIG.4. LINE DIAGRAM SHOWING POSITION OF SPAR & PITOTS

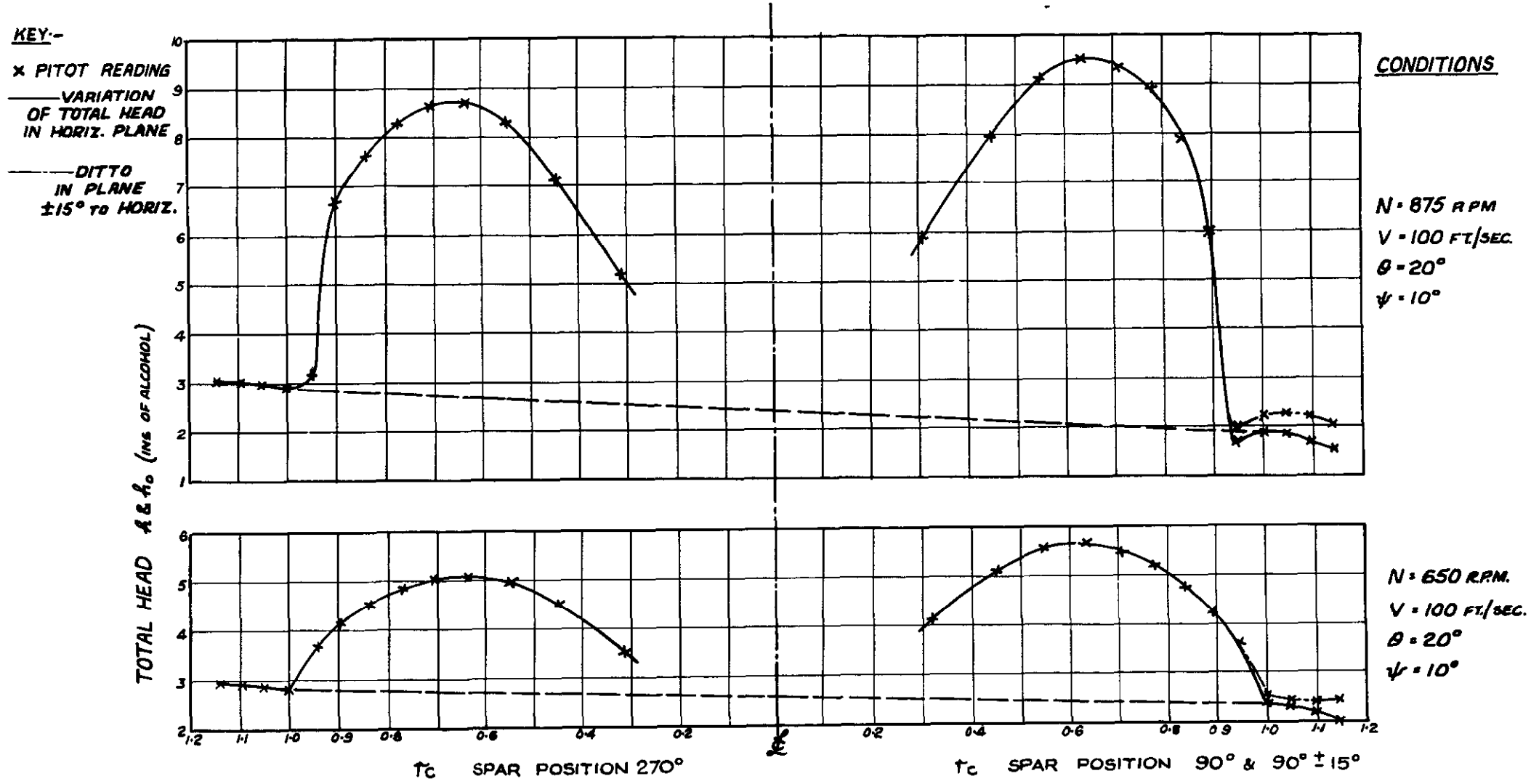

FIG. 5. VARIATION OF TOTAL HEAD IN FREE STREAM AND BEHIND PROPELLER DISC IN THE HORIZONTAL PLANE AND PLANES ±15° TO THE HORIZONTAL

FIG. 5.

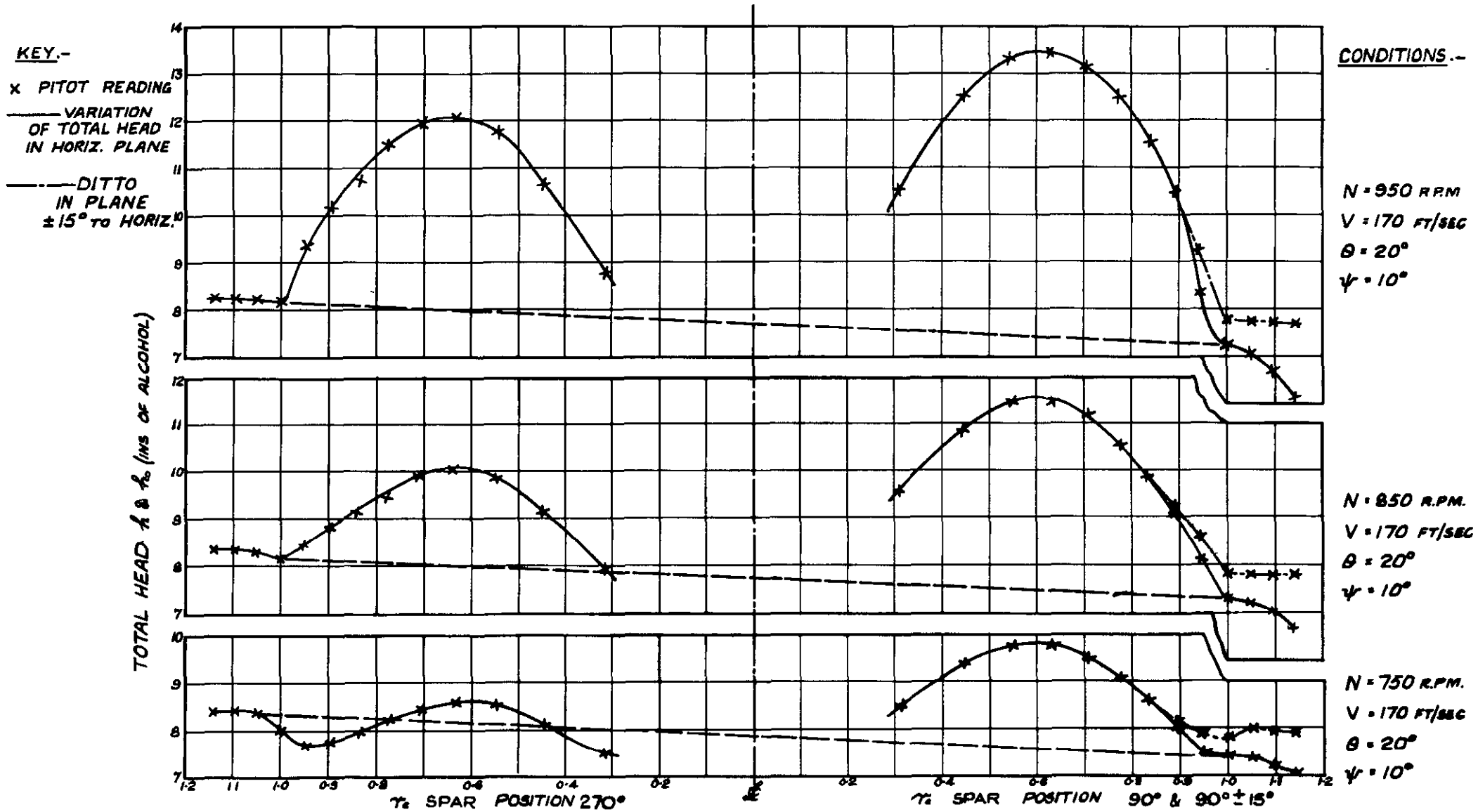

FIG. 6.

FIG. 6. VARIATION OF TOTAL HEAD IN FREE STREAM AND BEHIND PROPELLER DISC IN THE HORIZONTAL PLANE AND PLANES ±15° TO THE HORIZONTAL

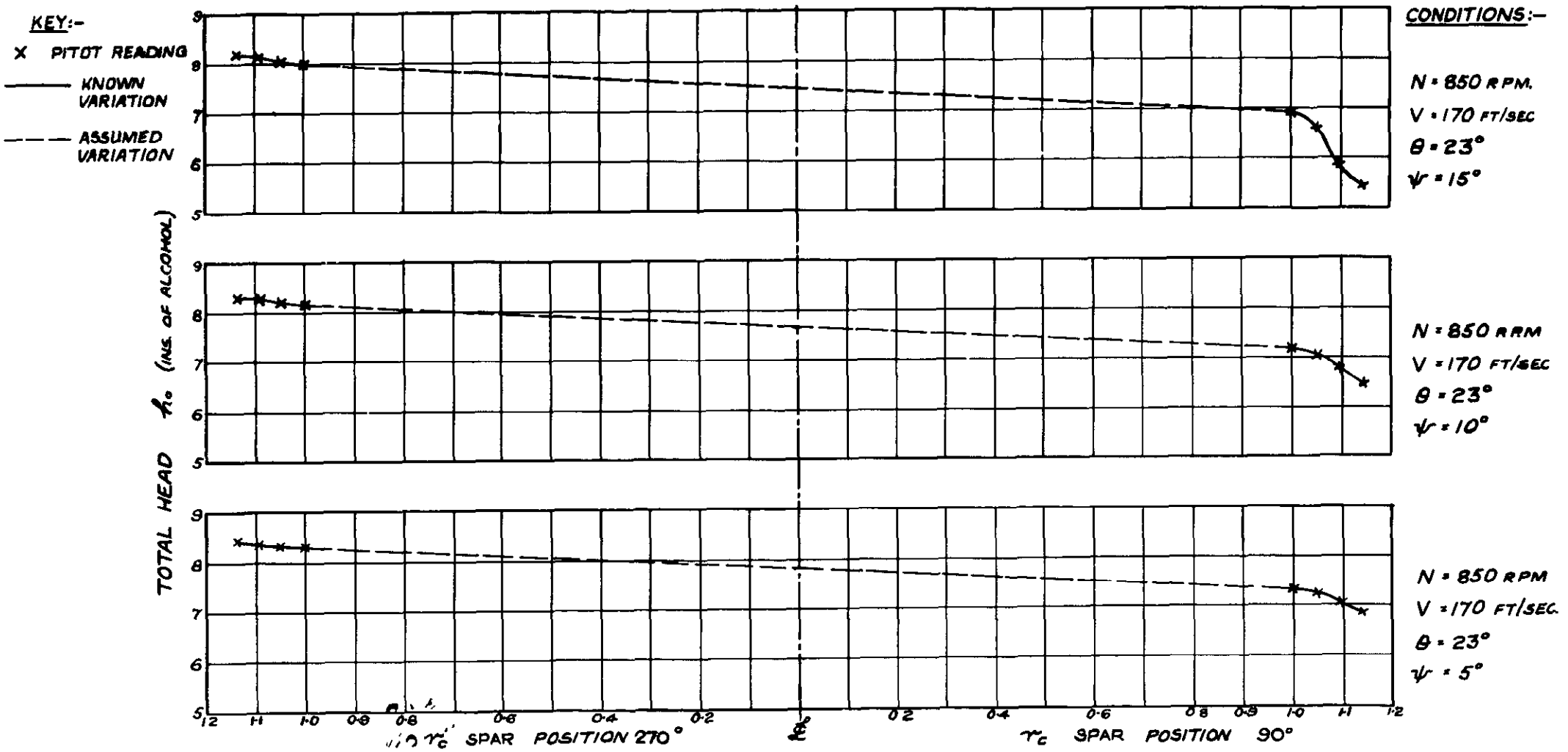

FIG. 7. ASSUMED VARIATION OF FREE STREAM TOTAL HEAD ACROSS PROPELLER DISC IN THE HORIZONTAL PLANE

FIG. 7.

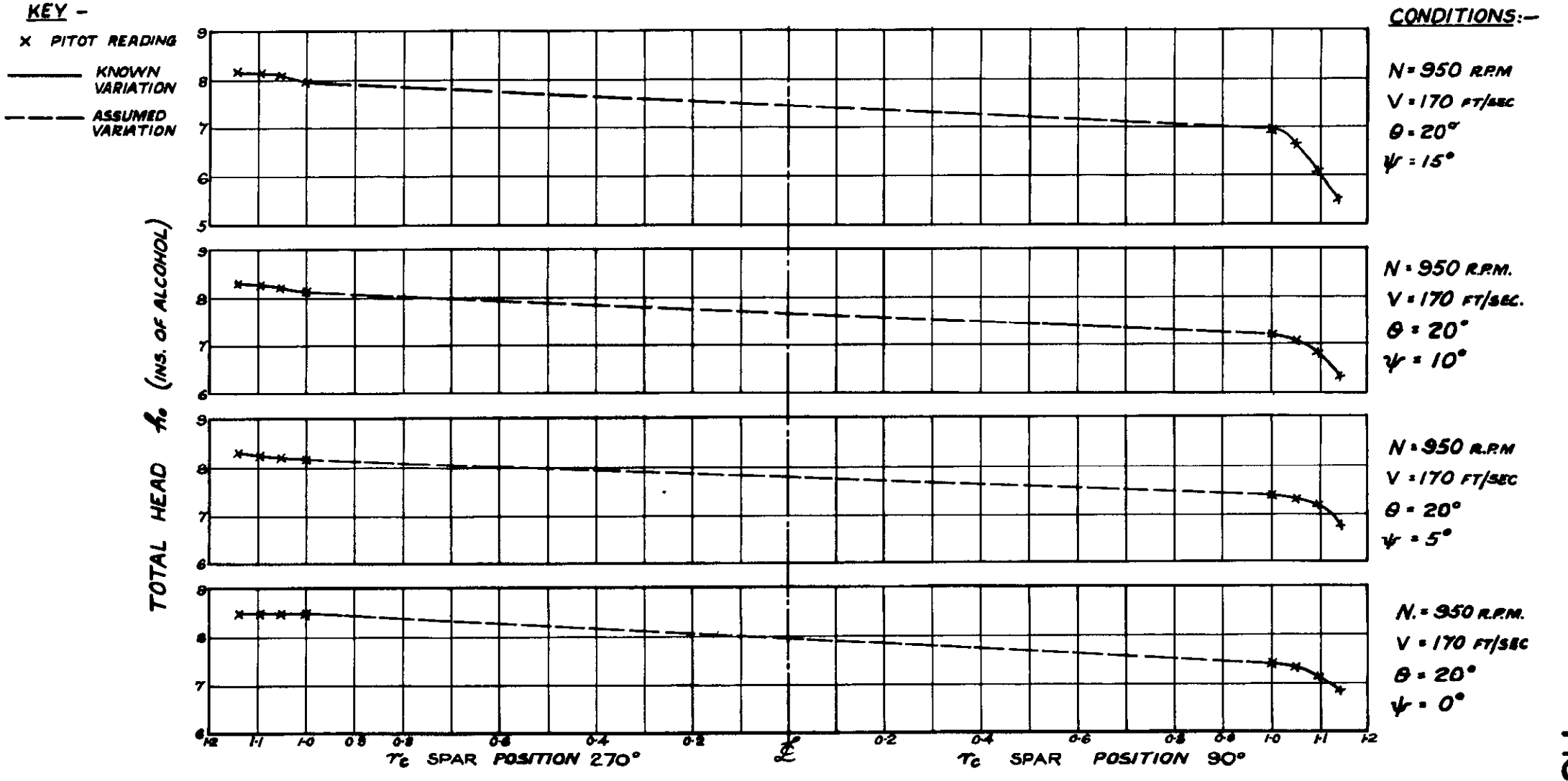

FIG. 8. ASSUMED VARIATION OF FREE STREAM TOTAL HEAD ACROSS PROPELLER DISC IN THE HORIZONTAL PLANE

FIG. 8.

FIG. 9.

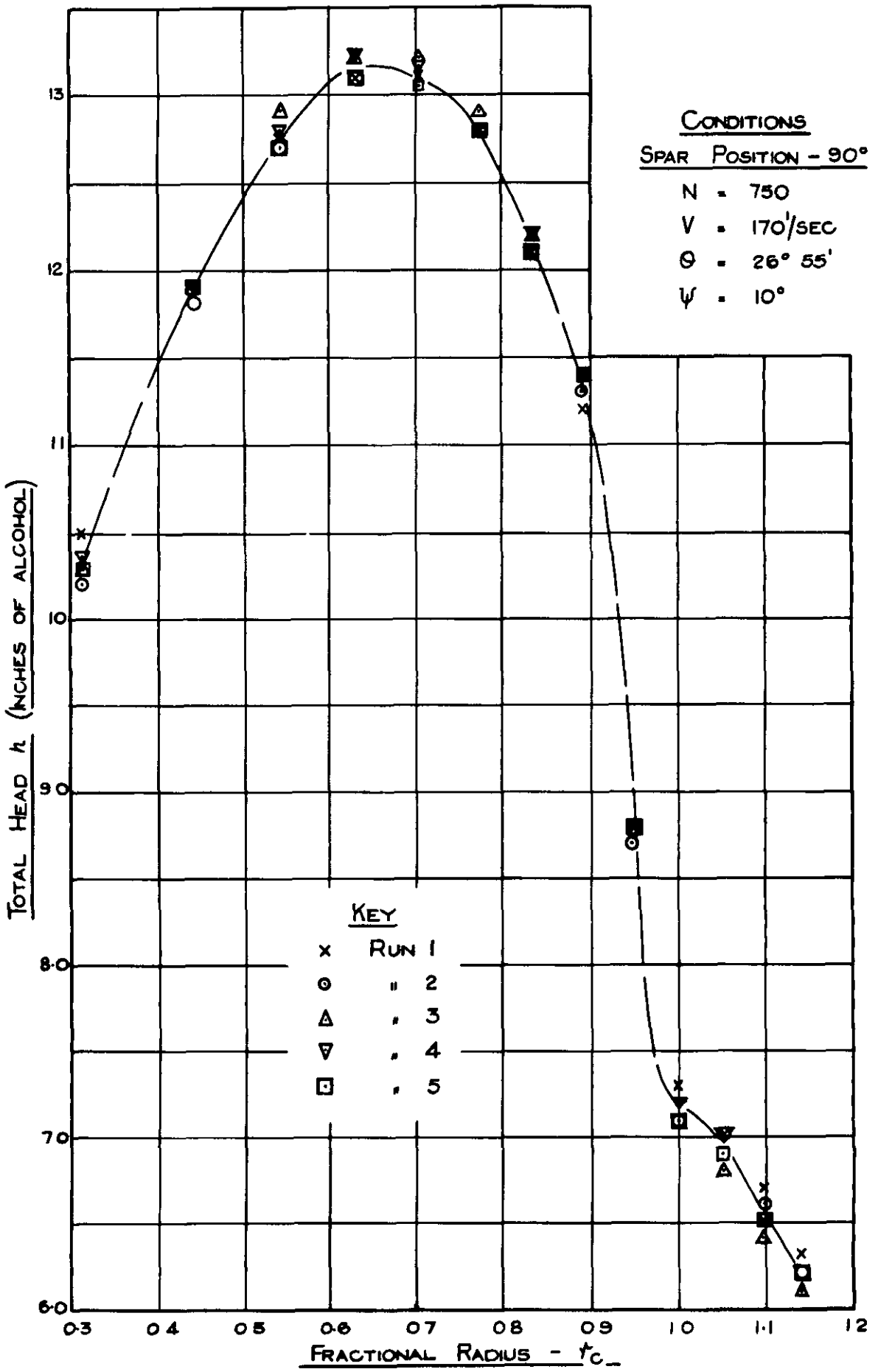

FIG. 9. ACTUAL MANOMETER READINGS FOR ONE SPAR POSITION SHOWING TEST SCATTER.

FIG.10,

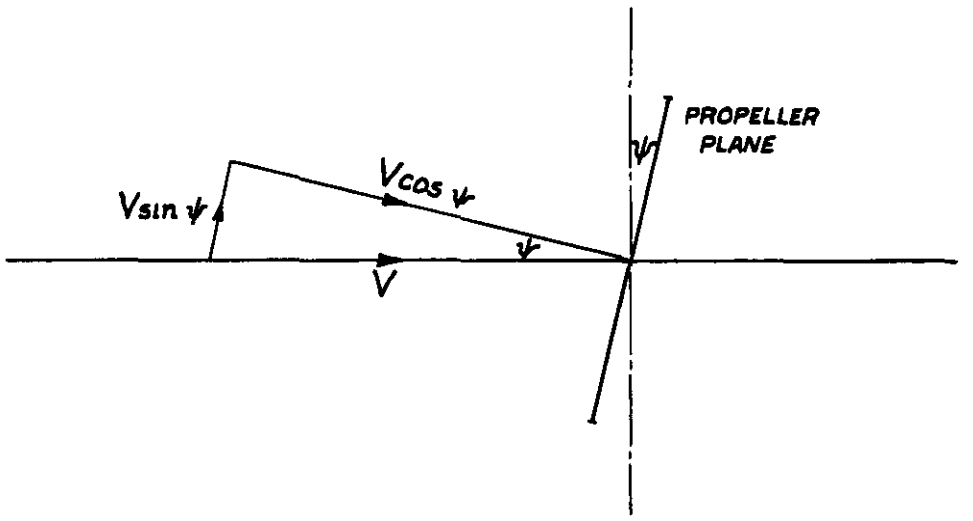

FIG.10a SIDE VIEW OF INCLINED PROPELLER

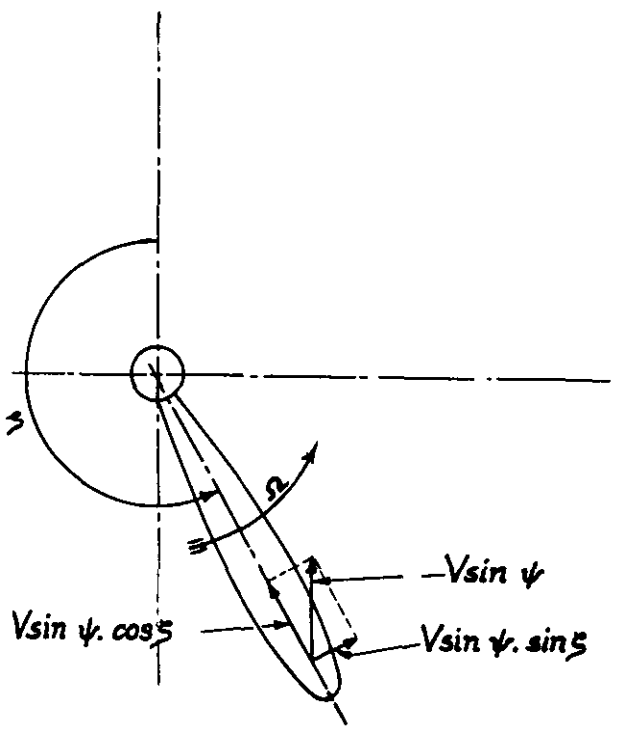

FIG.10b PROPELLER DISC VIEWED FROM REAR

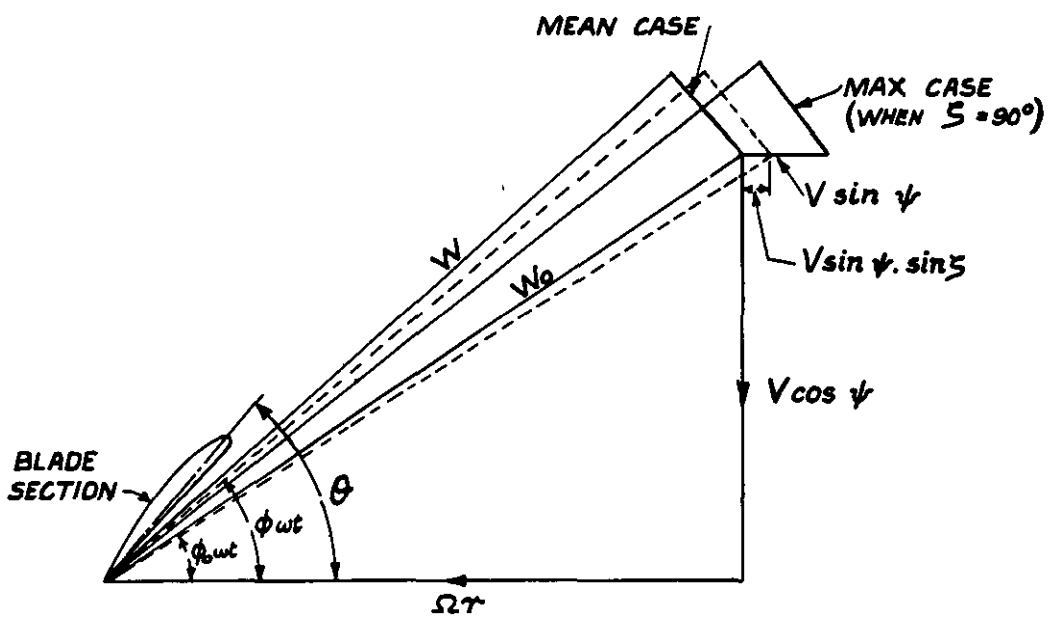

FIG.10c VELOCITY DIAGRAM OF INCLINED PROPELLER

FIG. 11.

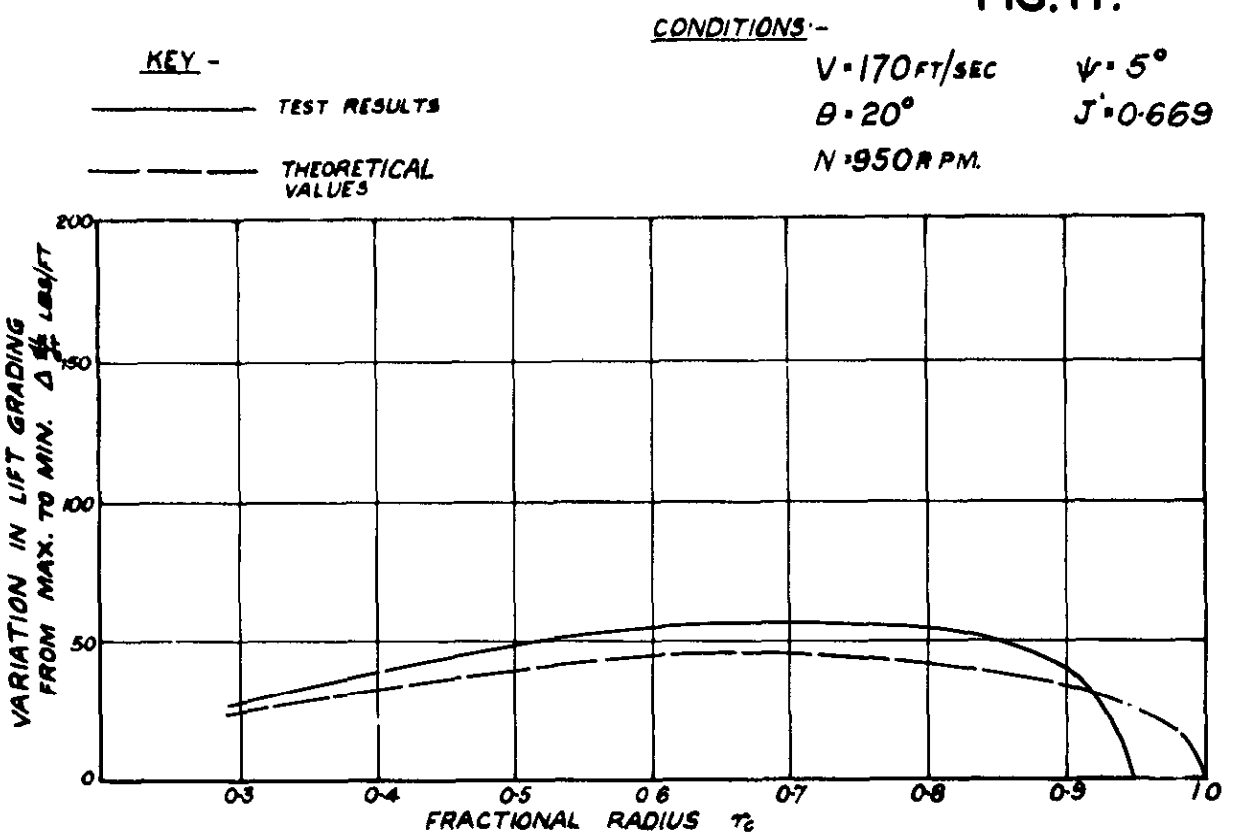

VARIATION IN LIFT GRADING FROM MAX. TO MIN.

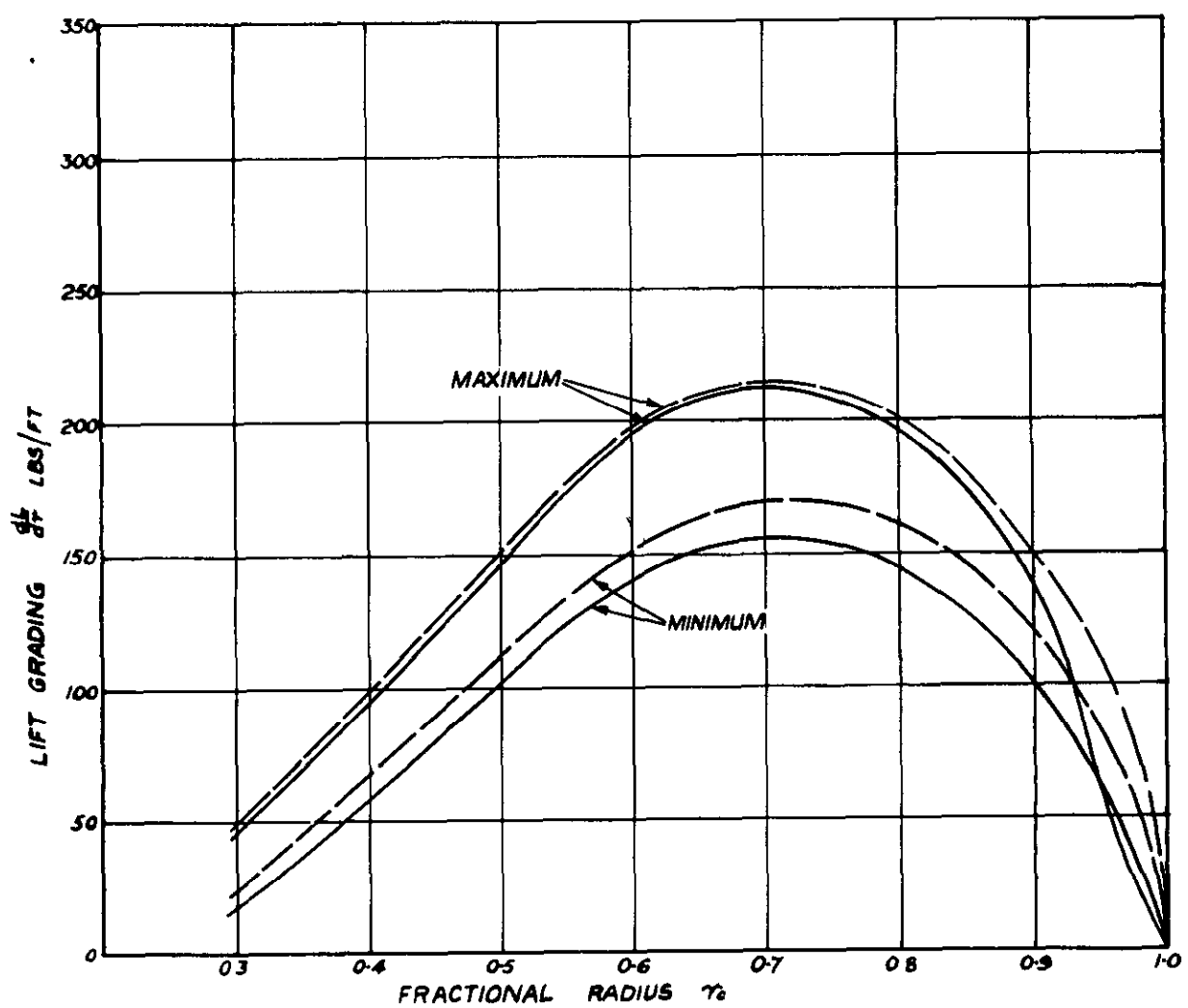

FIG. 11. COMPARISON OF EXPERIMENTAL AND ESTIMATED LIFT GRADING CURVES FOR AN INCLINED PROPELLER

FIG.12.

KEY:-

TEST RESULTS

THEORETICAL VALUES

CONDITIONS:-

V = 170 FT/SEC ψ = 10°

θ = 20° J' = 0·661

N = 950 R.P.M.

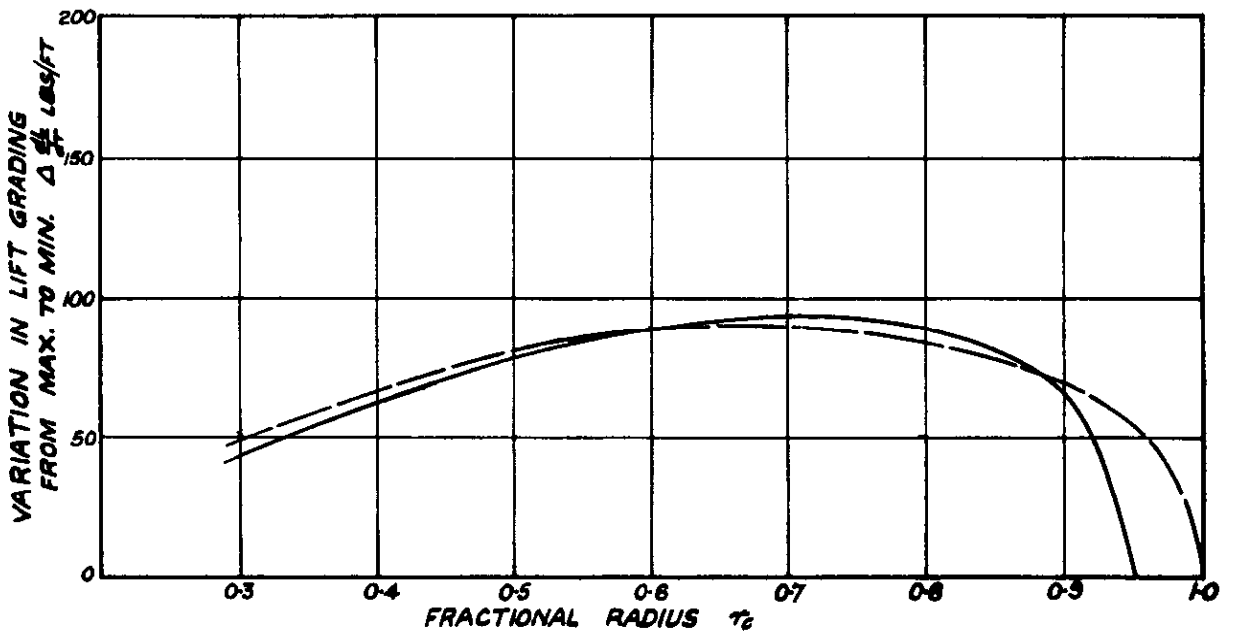

VARIATION IN LIFT GRADING FROM MAX. TO MIN.

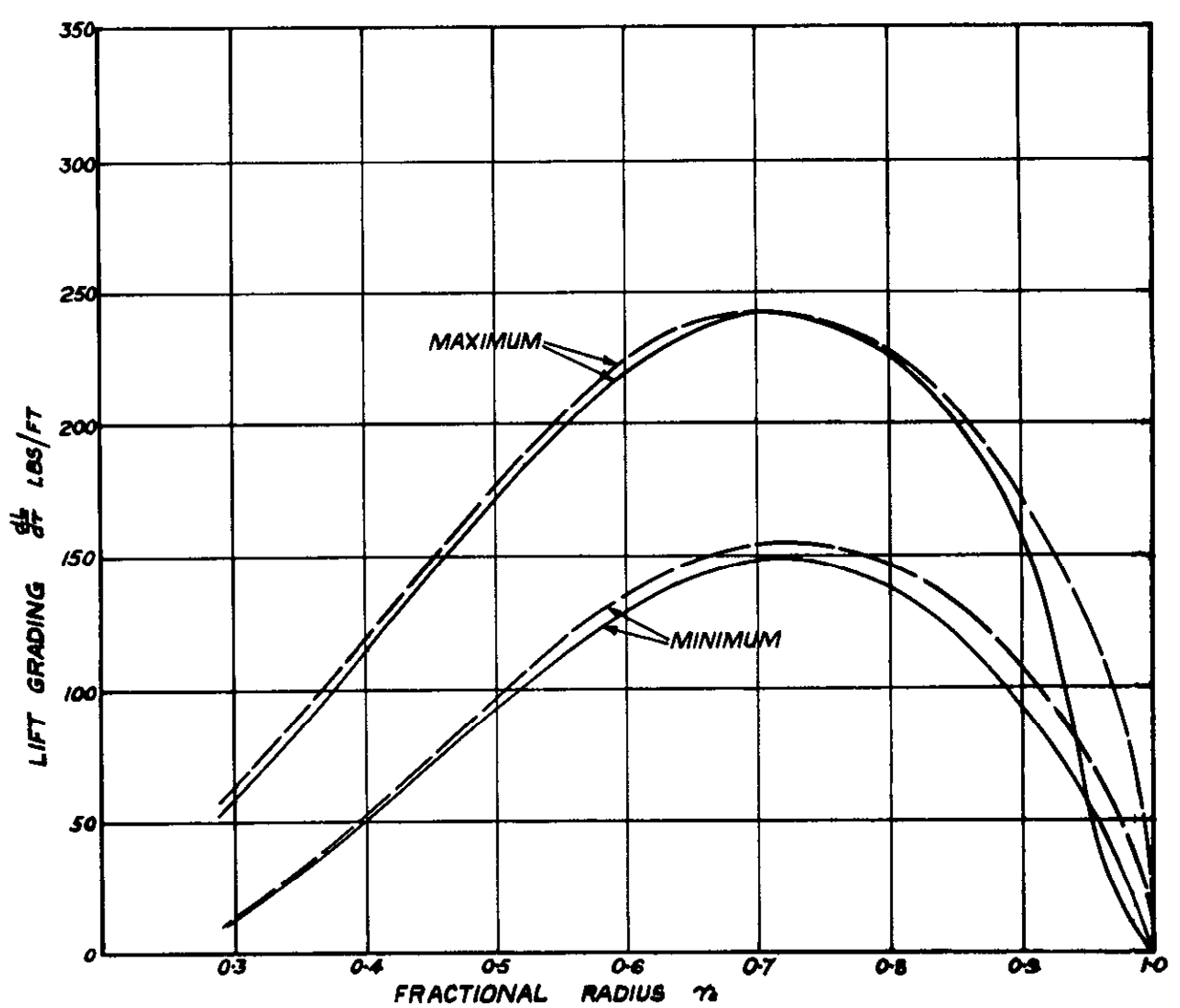

FIG.12. COMPARISON OF EXPERIMENTAL AND ESTIMATED LIFT GRADING CURVES FOR AN INCLINED PROPELLER

FIG.13.

KEY -

——— TEST RESULTS

— — — — THEORETICAL VALUES

CONDITIONS -

V = 170 FT/SEC ψ = 15°

θ = 20° J' = 0·648

N = 950 R.P.M.

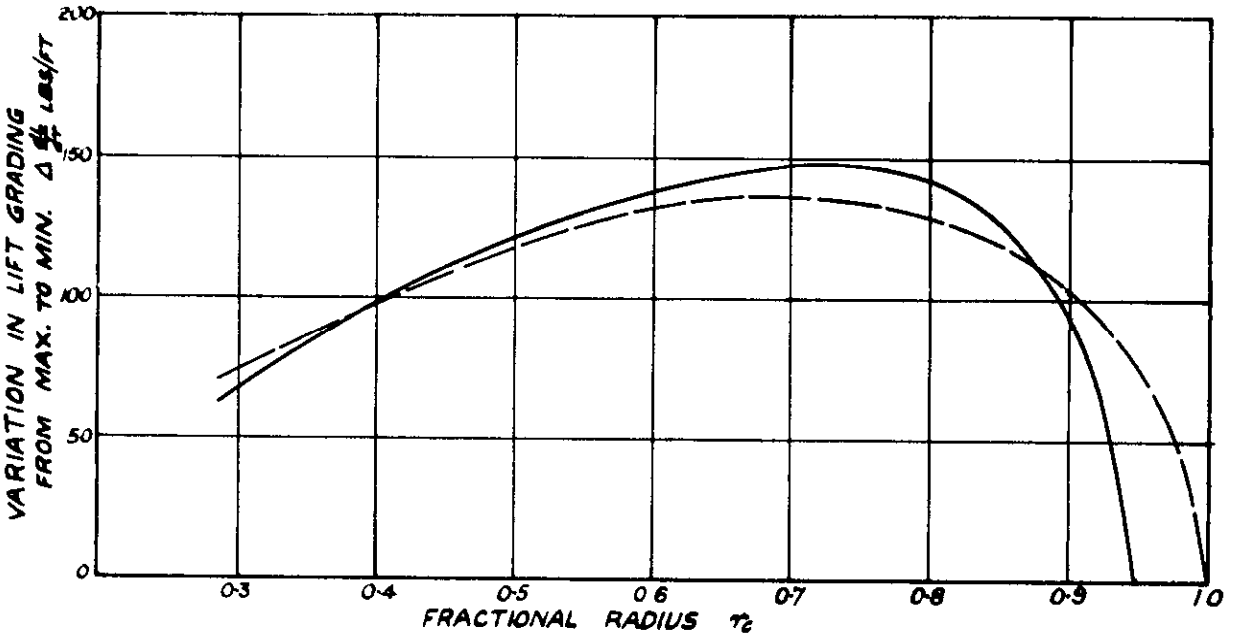

VARIATION IN LIFT GRADING FROM MAX. TO MIN.

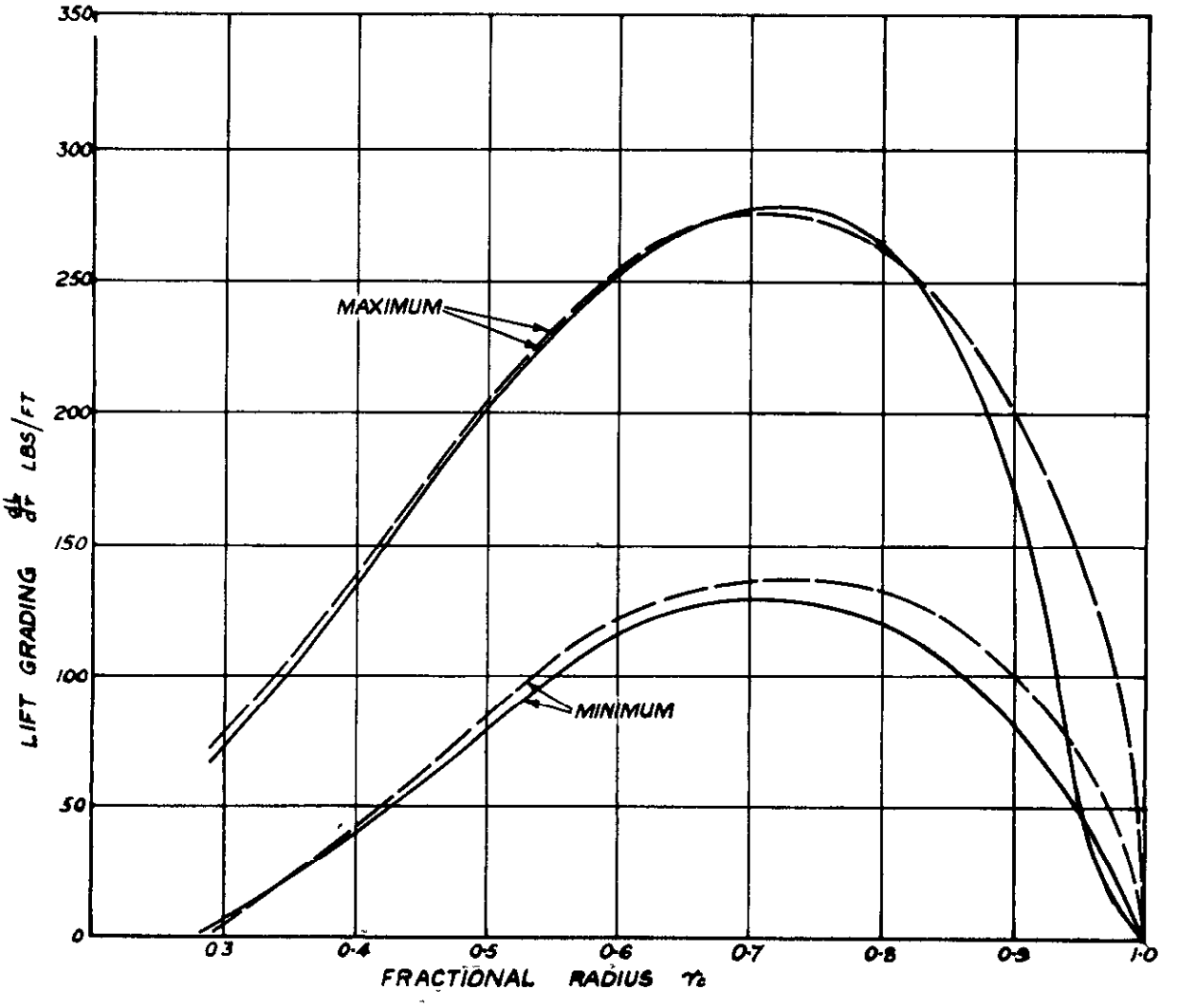

FIG.13. COMPARISON OF EXPERIMENTAL AND ESTIMATED LIFT GRADING CURVES FOR AN INCLINED PROPELLER

FIG.14.

KEY.-

TEST RESULTS

THEORETICAL VALUES

CONDITIONS:-

V = 170 FT/SEC ψ = 5°

θ = 23° J' = 0·749

N = 850 R.P.M.

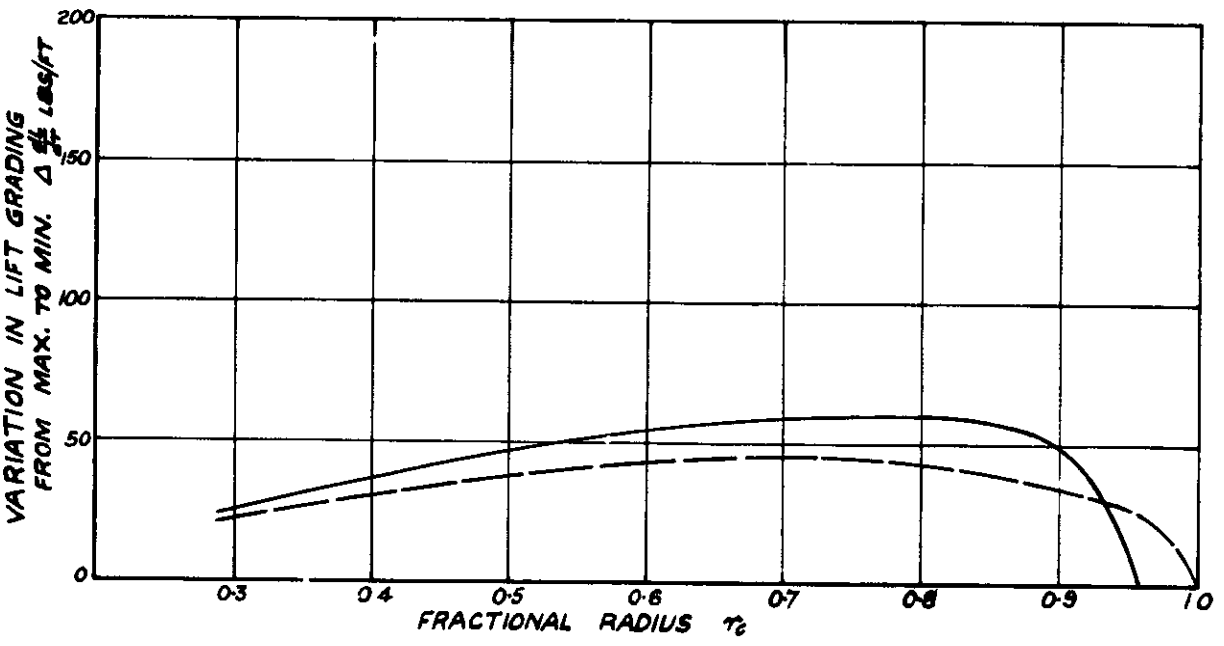

VARIATION IN LIFT GRADING FROM MAX. TO MIN.

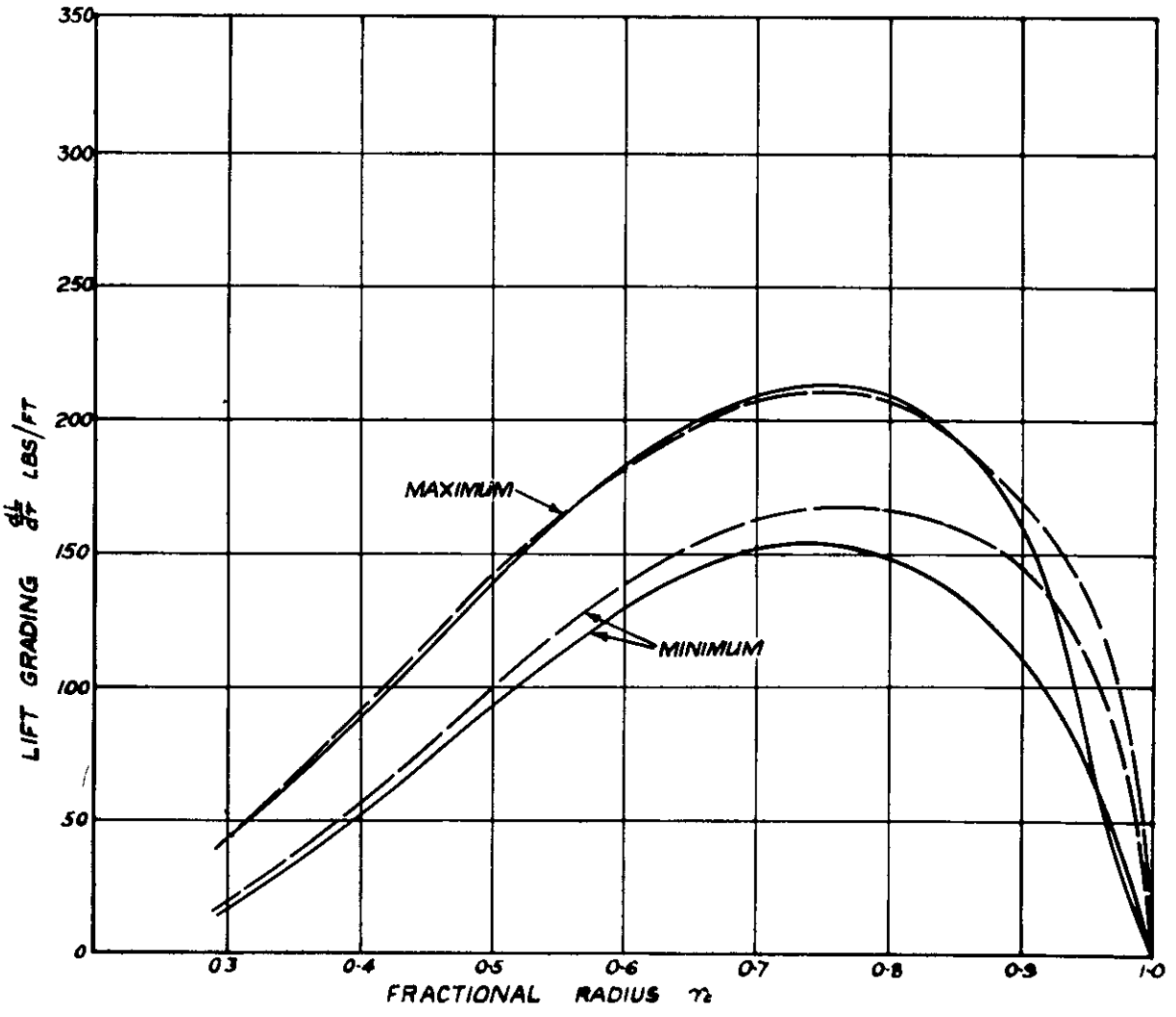

FIG.14. COMPARISON OF EXPERIMENTAL AND ESTIMATED LIFT GRADING CURVES FOR AN INCLINED PROPELLER

FIG.15

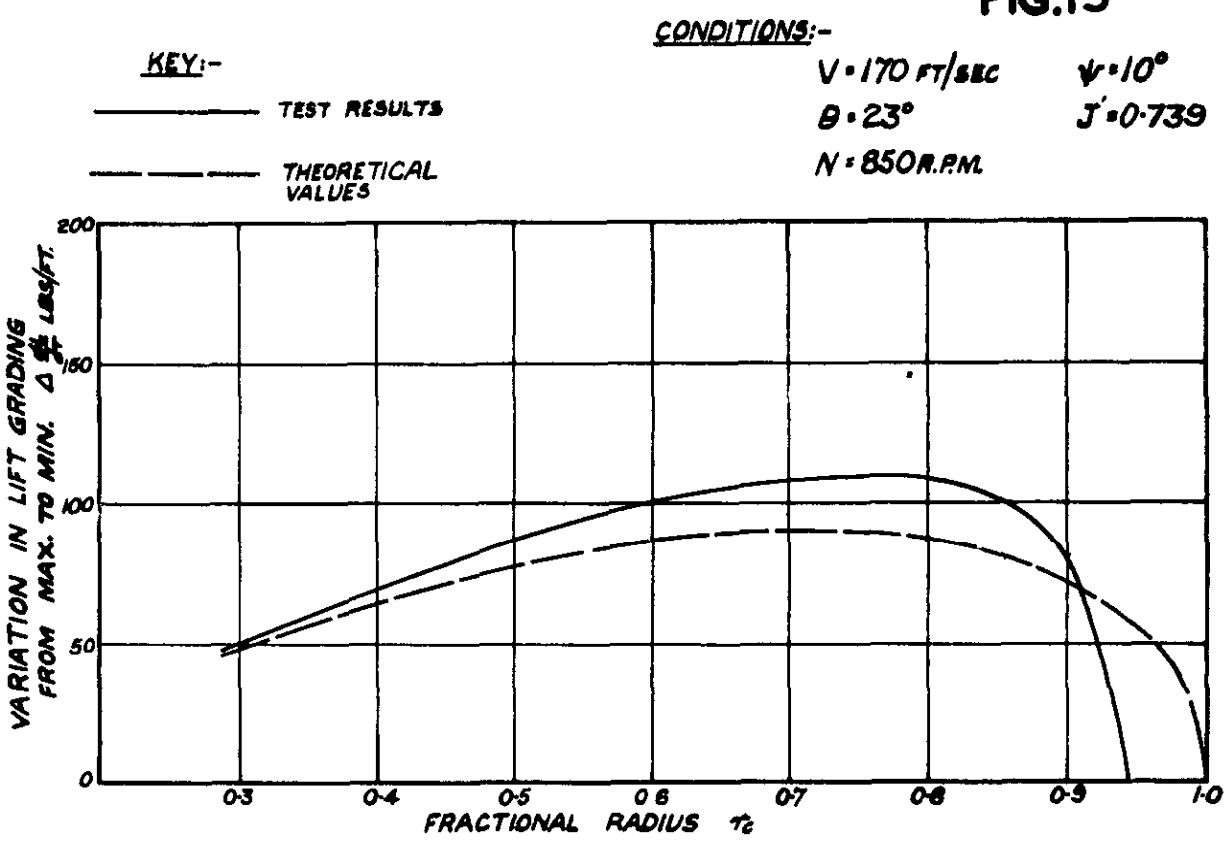

VARIATION IN LIFT GRADING FROM MAX. TO MIN.

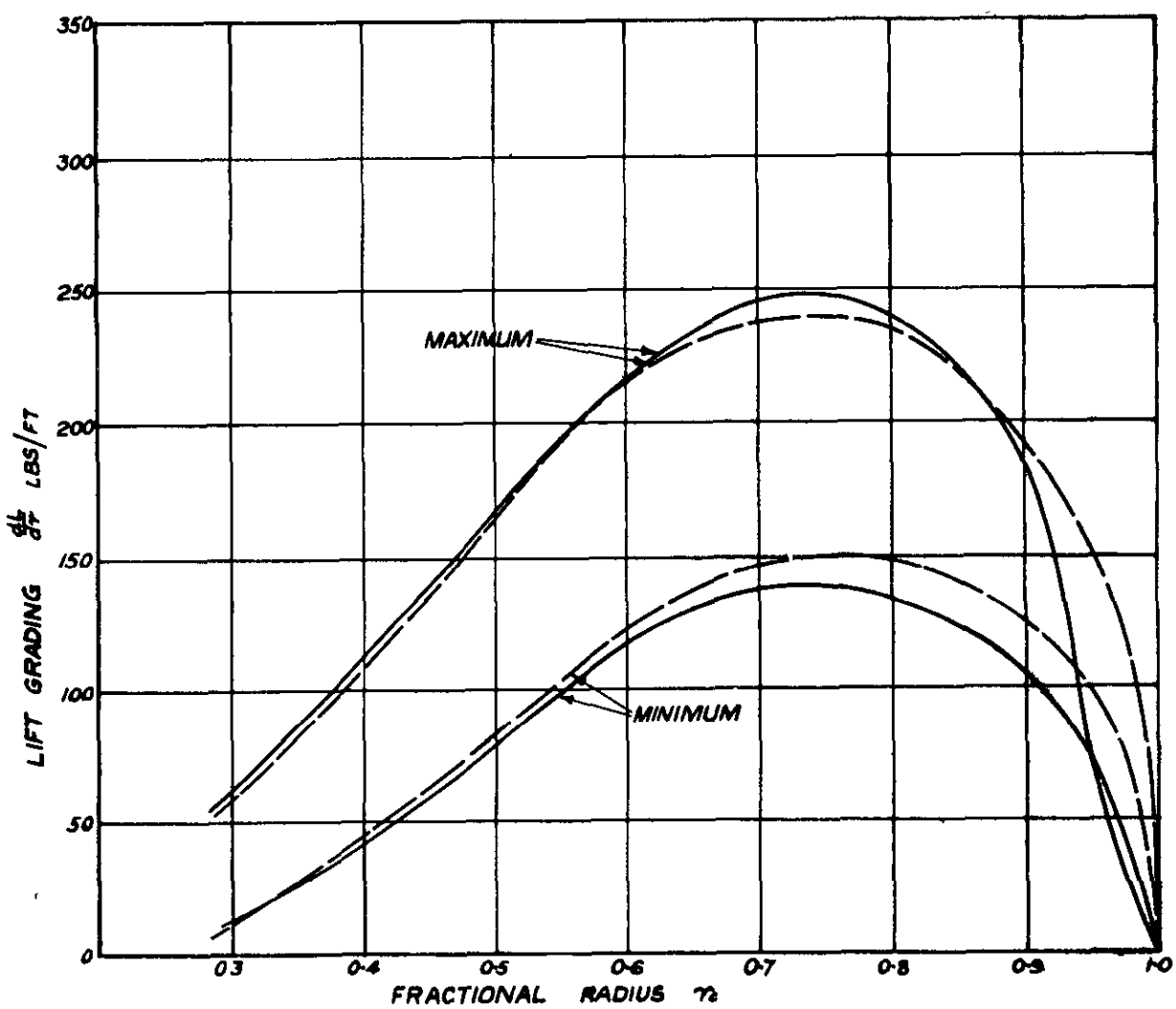

FIG.15. COMPARISON OF EXPERIMENTAL AND ESTIMATED LIFT GRADING CURVES FOR AN INCLINED PROPELLER

FIG. 16.

KEY:-

TEST RESULTS

THEORETICAL VALUES

CONDITIONS:-

V = 170 FT/SEC ψ = 15°

θ = 23° J' = 0·724

N = 850 R.P.M.

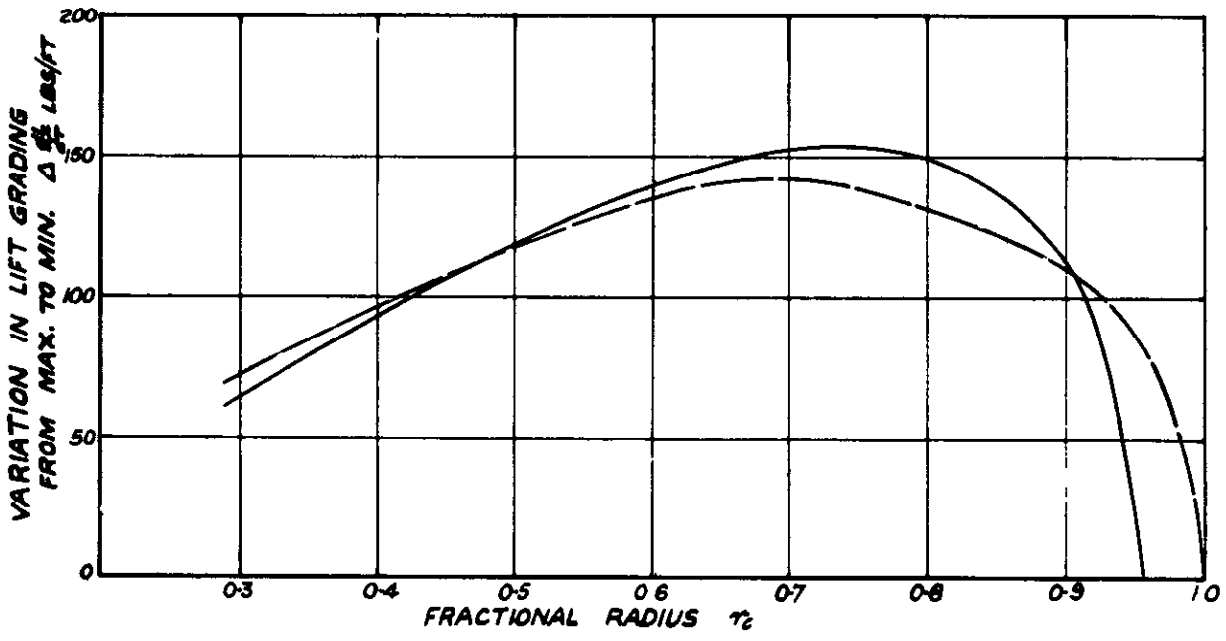

VARIATION IN LIFT GRADING FROM MAX. TO MIN.

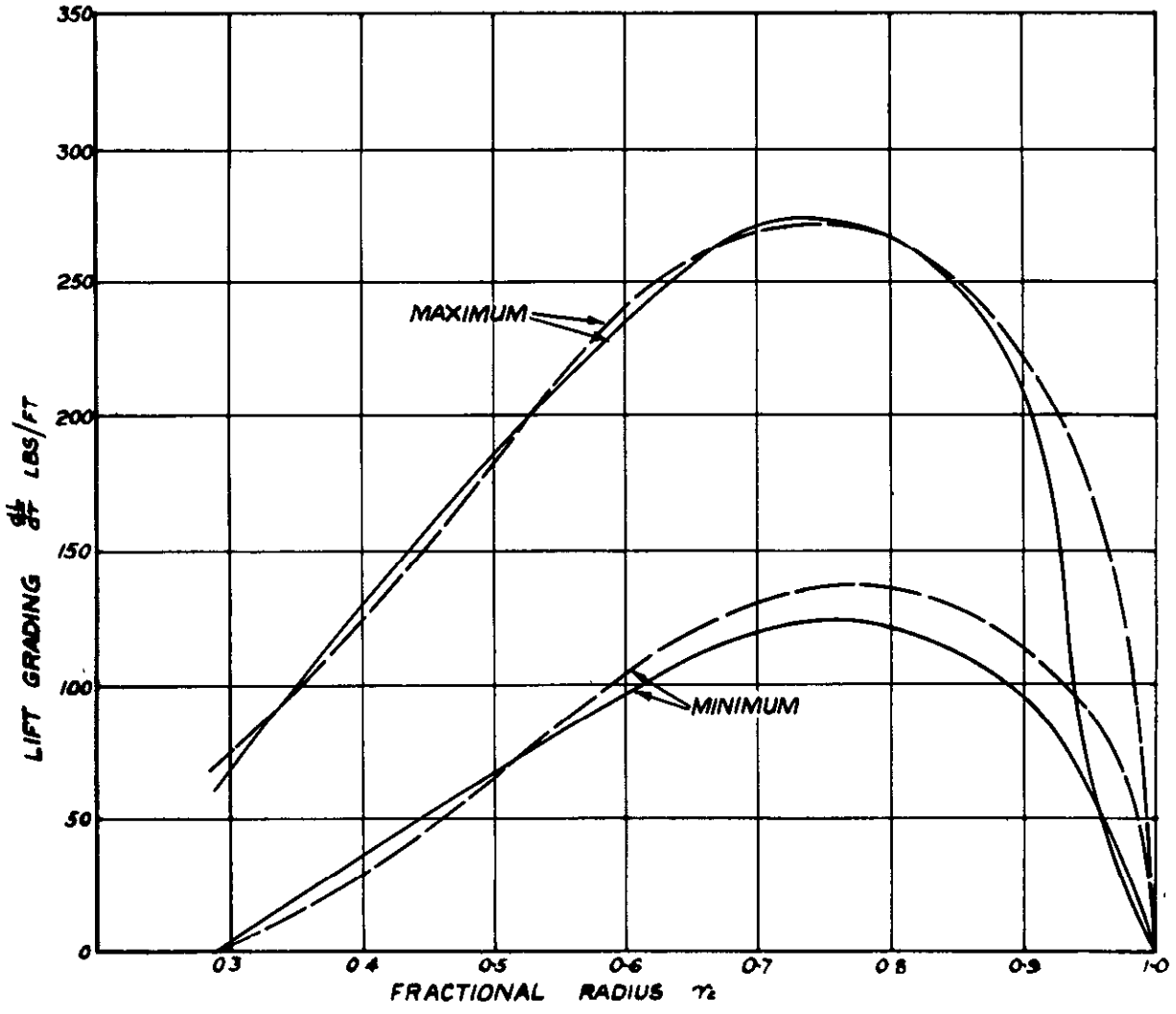

FIG. 16. COMPARISON OF EXPERIMENTAL AND ESTIMATED LIFT GRADING CURVES FOR AN INCLINED PROPELLER

FIG.17.

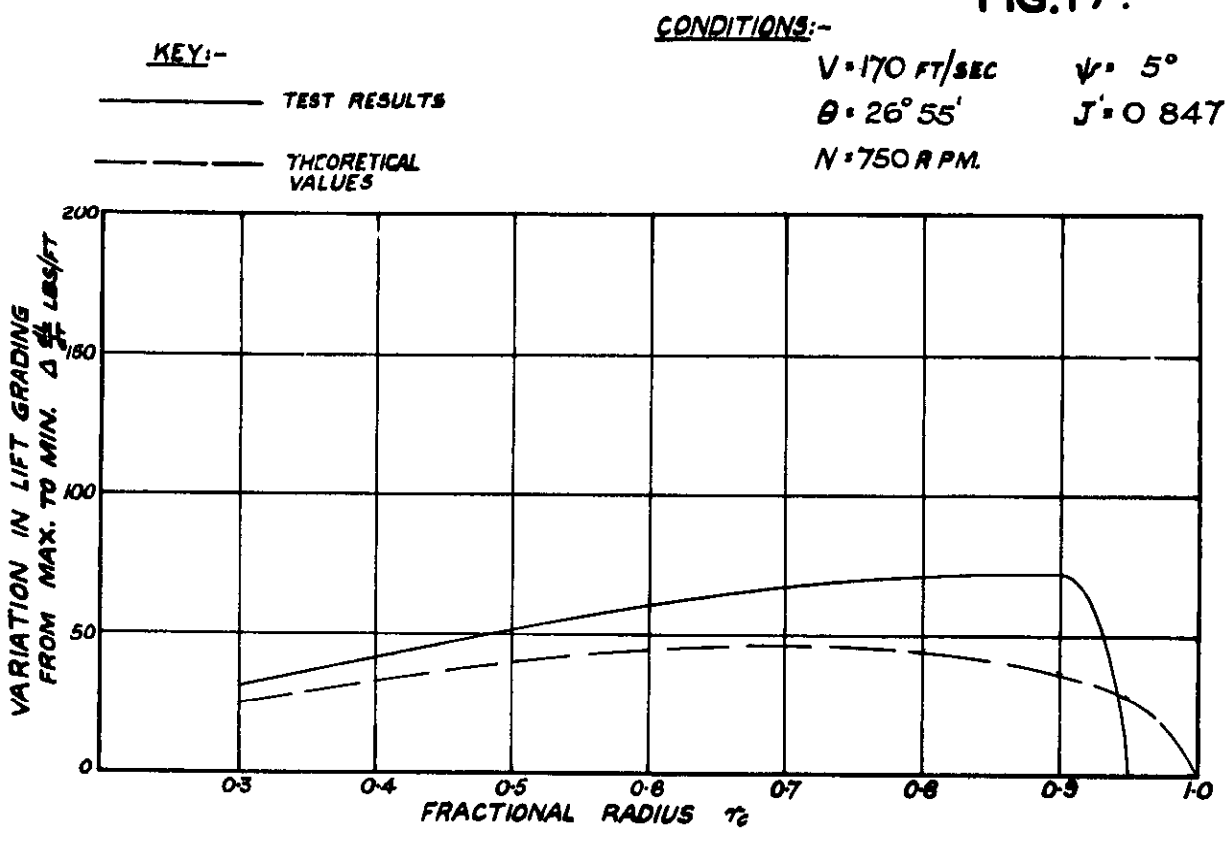

VARIATION IN LIFT GRADING FROM MAX. TO MIN.

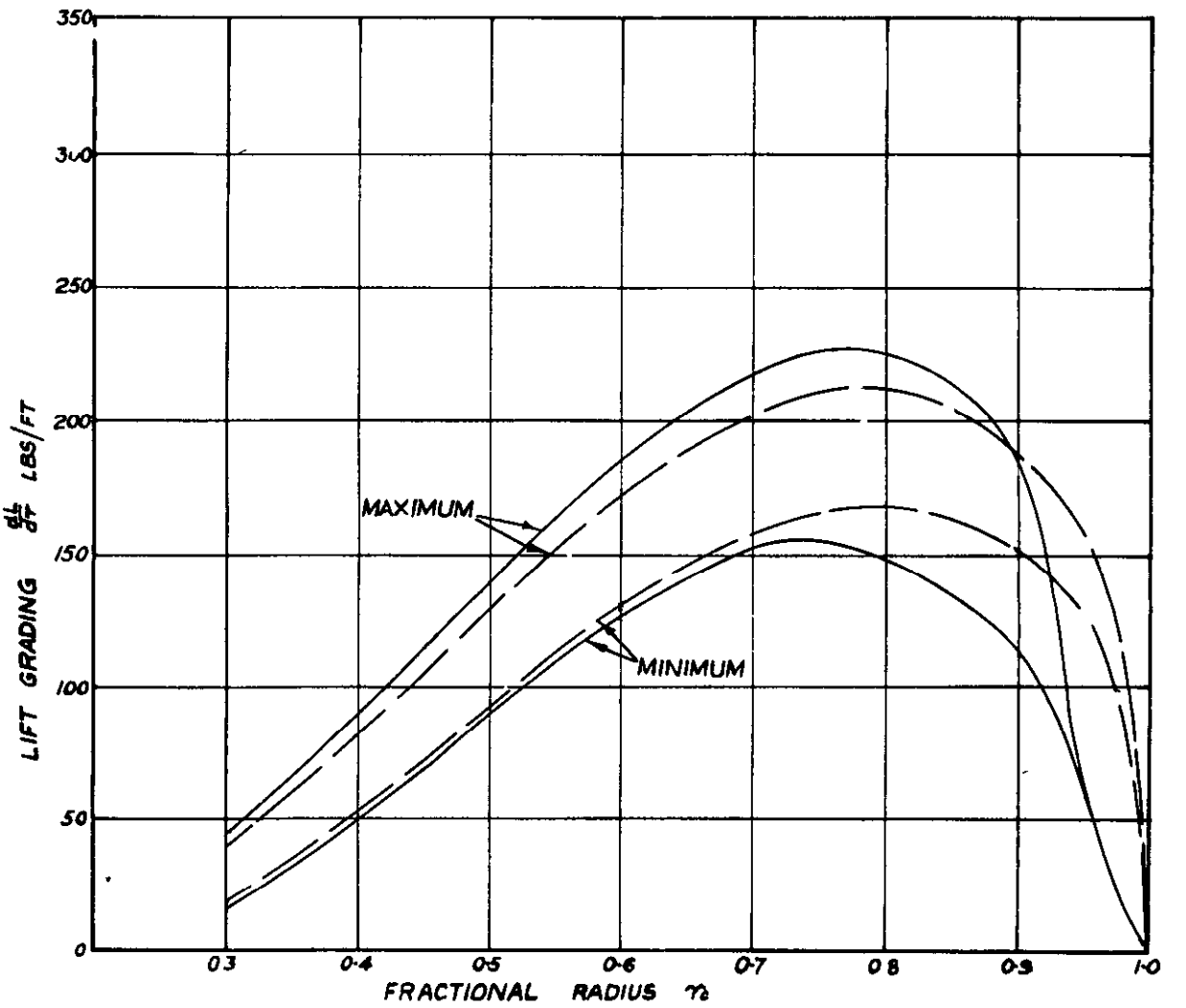

FIG.17. COMPARISON OF EXPERIMENTAL AND ESTIMATED LIFT GRADING CURVES FOR AN INCLINED PROPELLER

FIG.18.

KEY:-

——— TEST RESULTS

— — — — THEORETICAL VALUES

CONDITIONS:-

V = 170 FT/SEC ψ = 10°

θ = 26° 55' J = 0·837

N = 750 R.P.M.

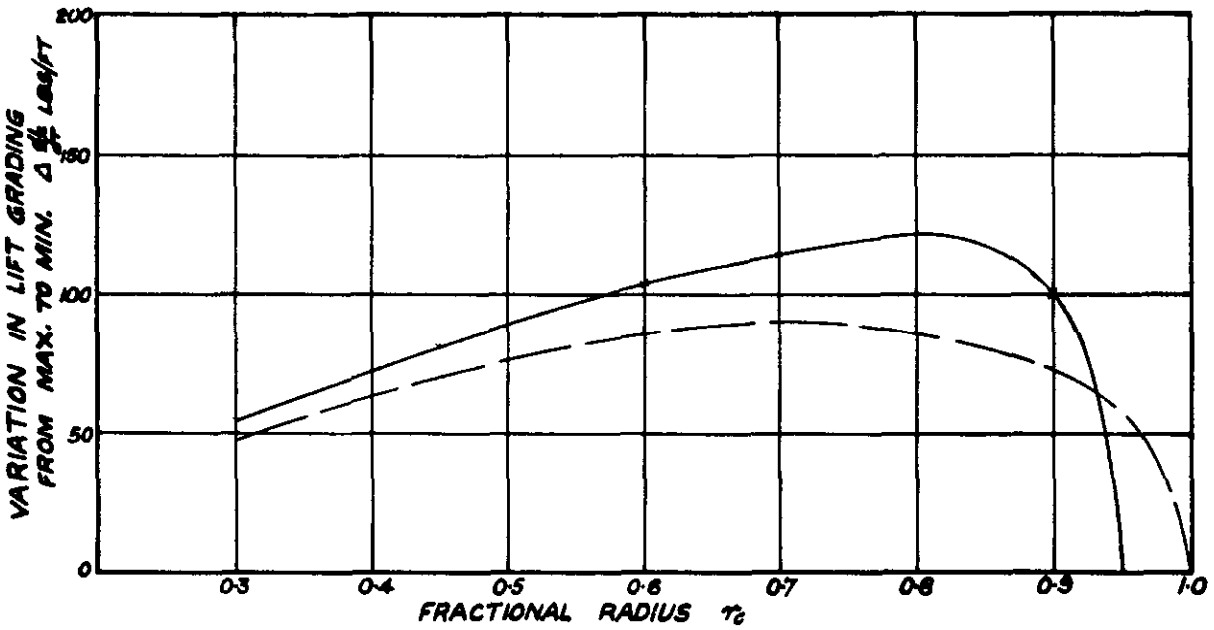

VARIATION IN LIFT GRADING FROM MAX. TO MIN.

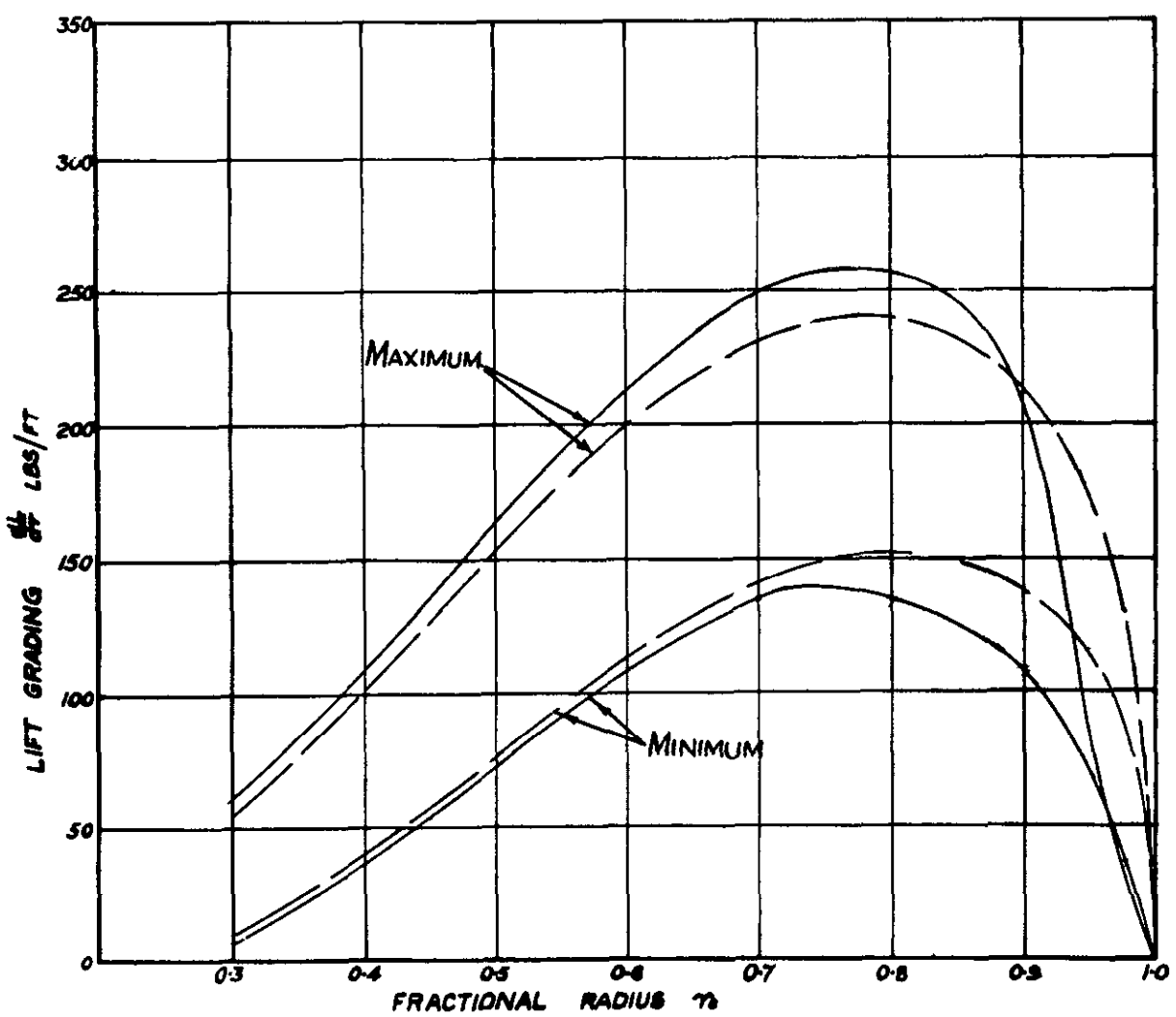

FIG.18. COMPARISON OF EXPERIMENTAL AND ESTIMATED LIFT GRADING CURVES FOR AN INCLINED PROPELLER

FIG. 19.

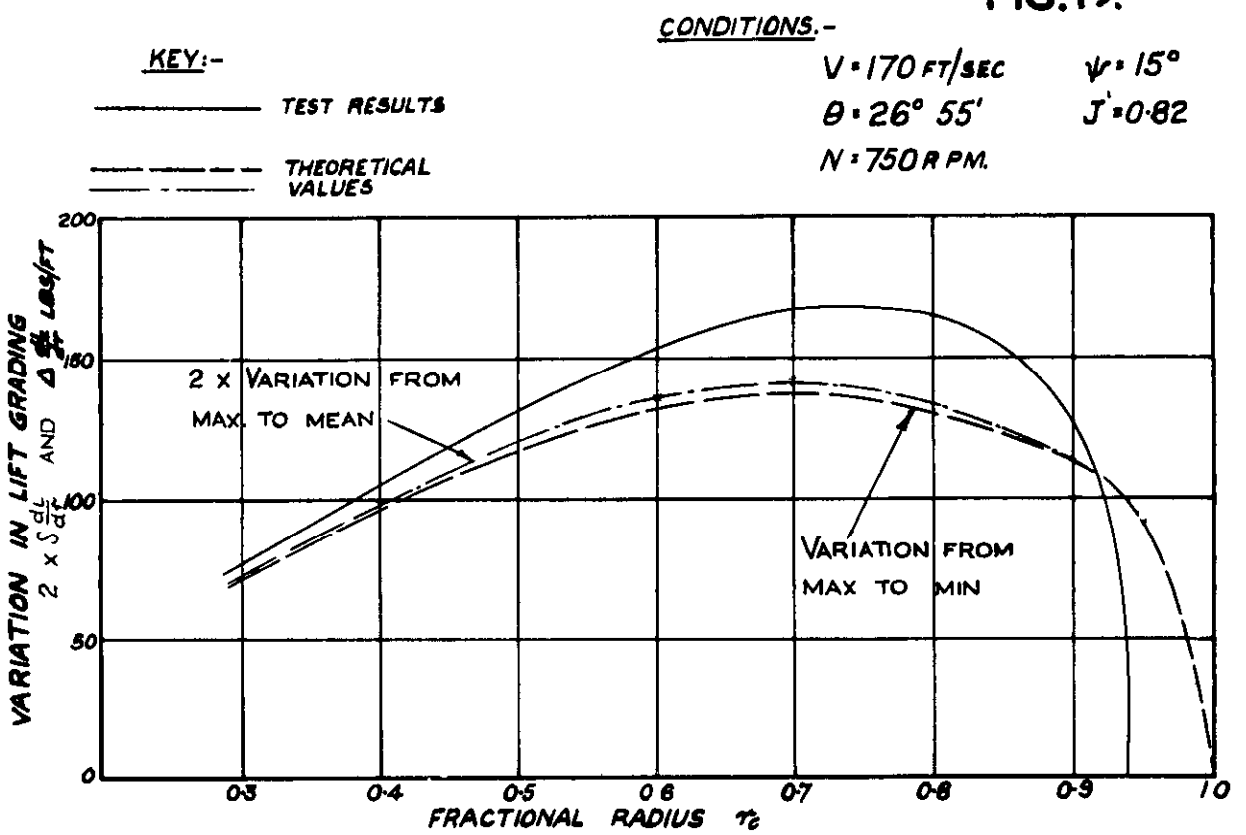

VARIATION IN LIFT GRADING

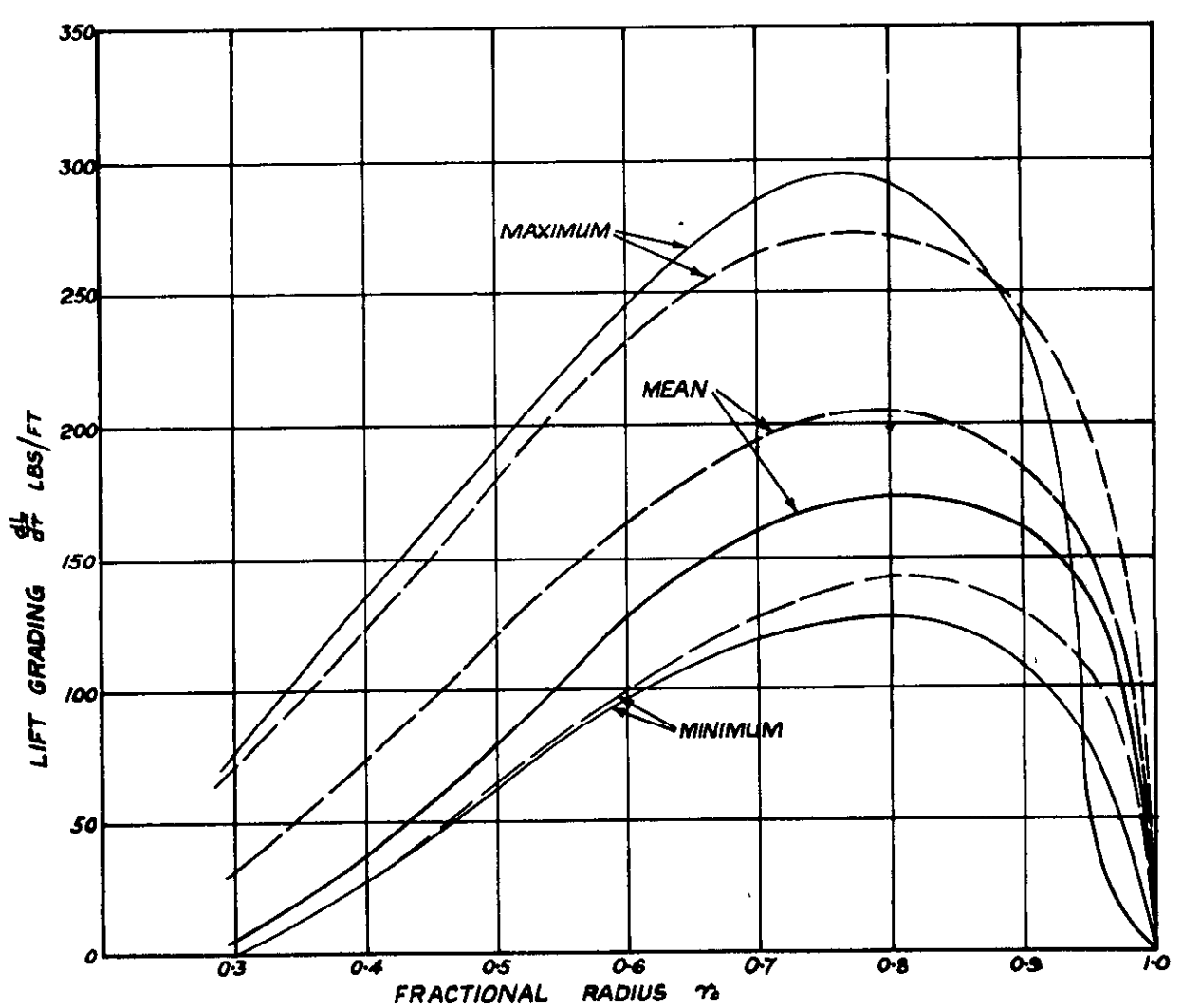

FIG. 19. COMPARISON OF EXPERIMENTAL AND ESTIMATED LIFT GRADING CURVES FOR AN INCLINED PROPELLER

FIG. 20.

KEY:-

TEST RESULTS

THEORETICAL VALUES

CONDITIONS:-

V = 100 FT/SEC ψ = 10°

θ = 20° J' = 0·5679

N = 650 R.P.M.

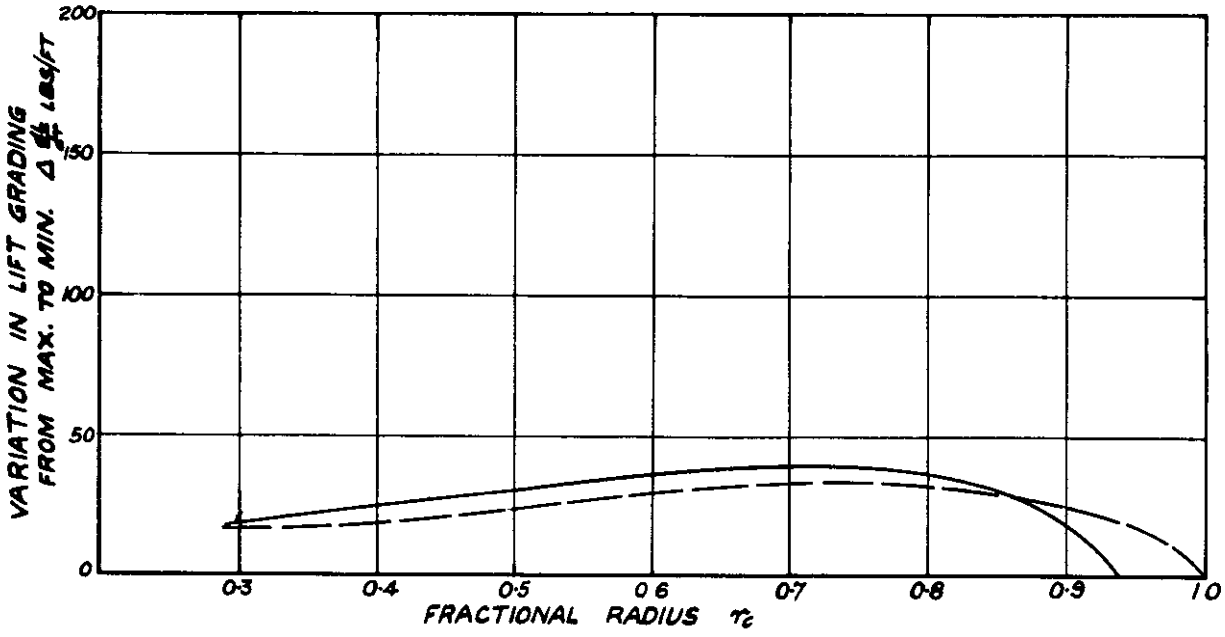

VARIATION IN LIFT GRADING FROM MAX. TO MIN.

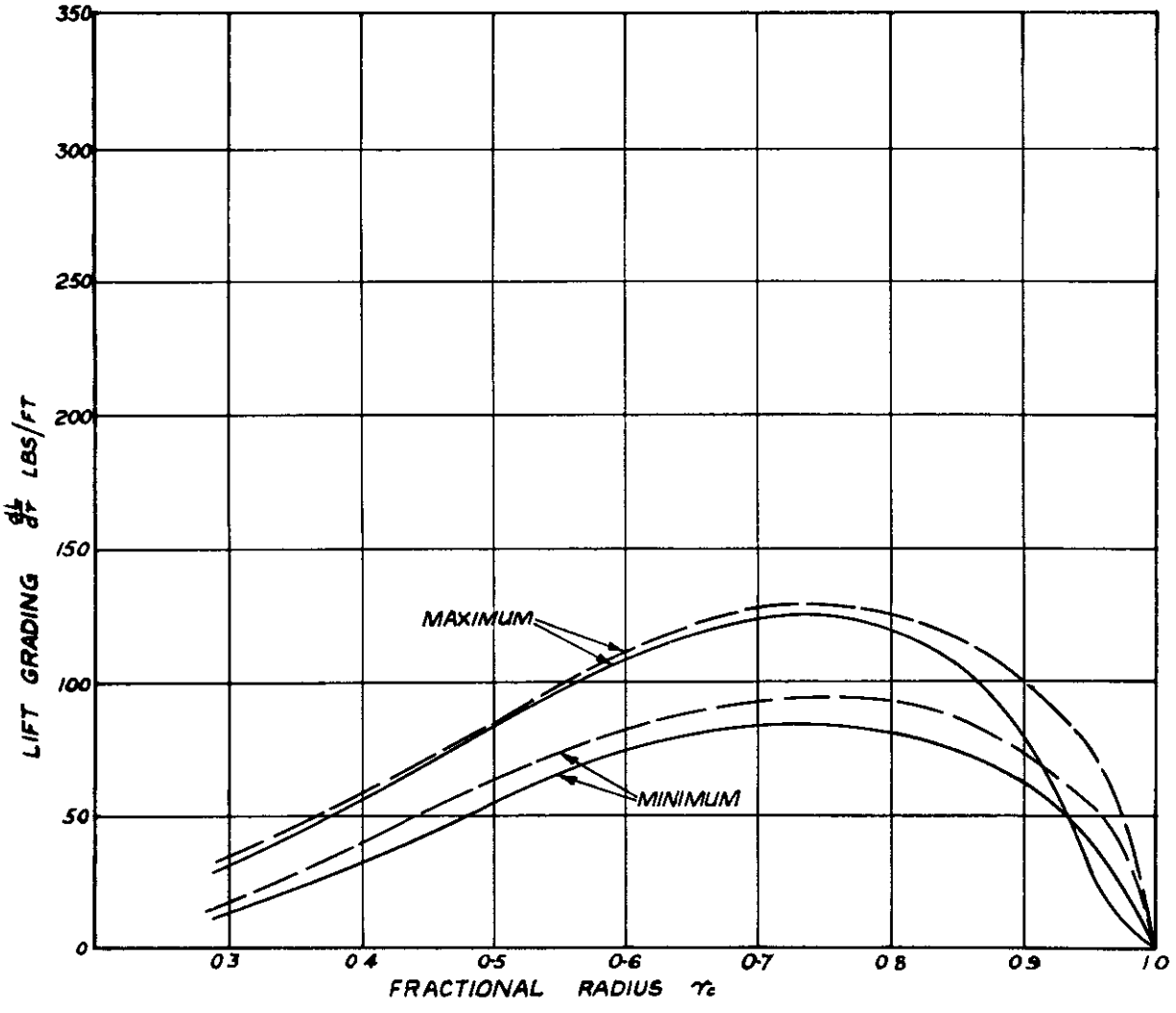

FIG. 20. COMPARISON OF EXPERIMENTAL AND ESTIMATED LIFT GRADING CURVES FOR AN INCLINED PROPELLER

FIG. 21.

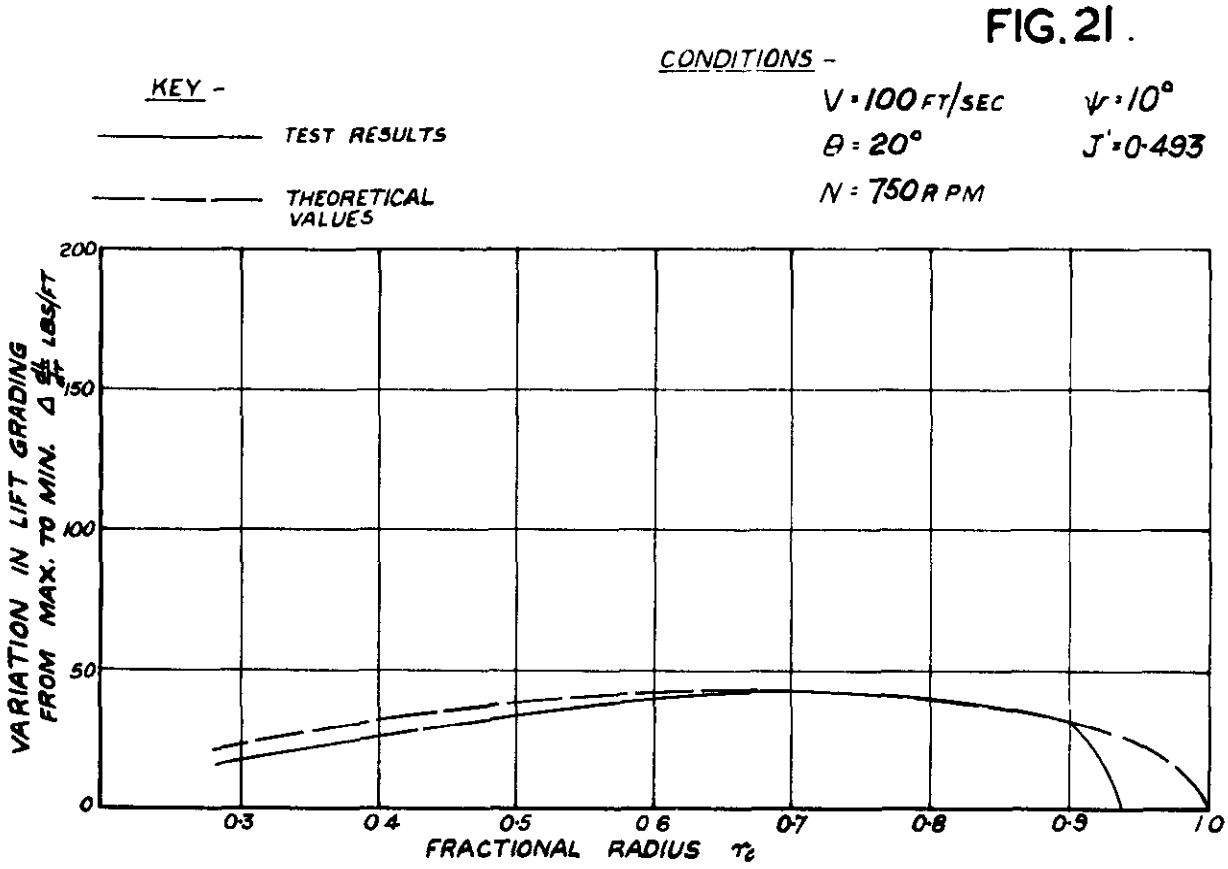

VARIATION IN LIFT GRADING FROM MAX. TO MIN.

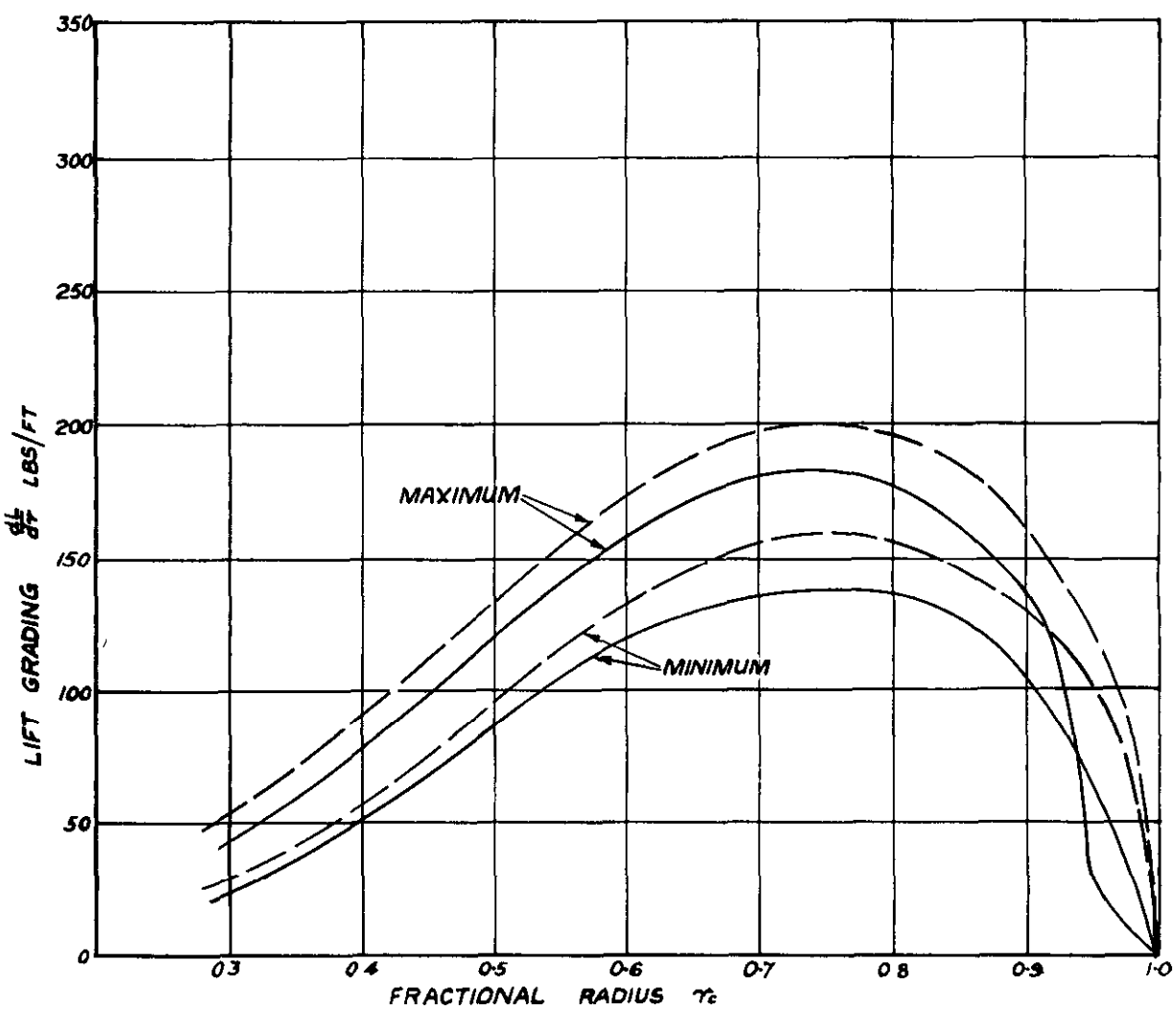

FIG. 21. COMPARISON OF EXPERIMENTAL AND ESTIMATED LIFT GRADING CURVES FOR AN INCLINED PROPELLER

FIG. 22.

KEY:-

TEST RESULTS

THEORETICAL VALUES

CONDITIONS:-

$V = 100$ FT/SEC $\quad \psi = 10°$

$\theta = 20°$ $\quad J' = 0.422$

$N = 875$ R.P.M.

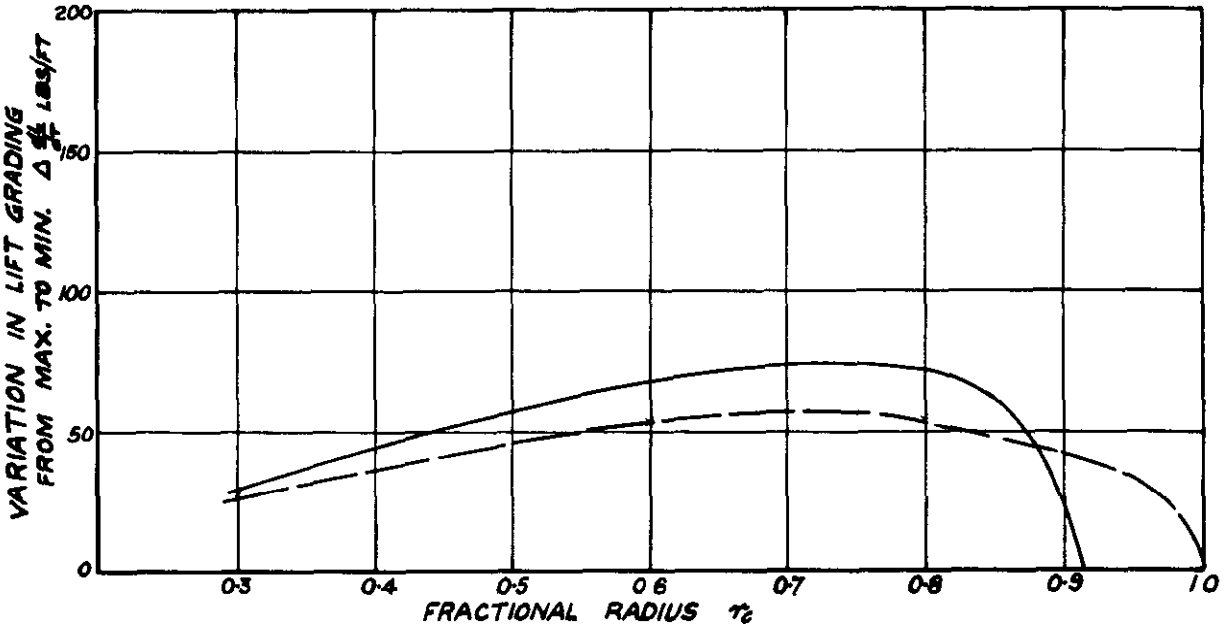

VARIATION IN LIFT GRADING FROM MAX. TO MIN.

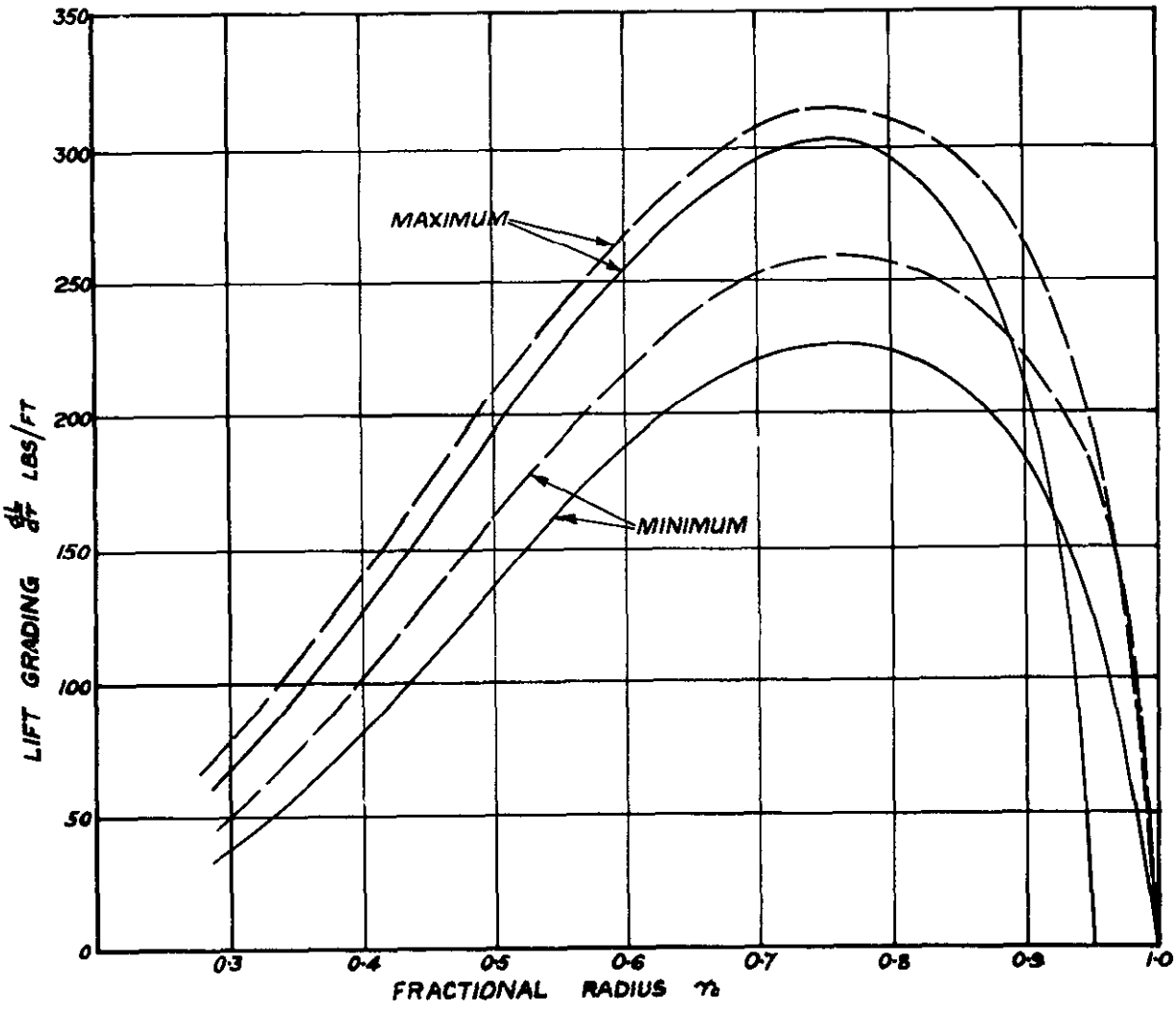

FIG.22. COMPARISON OF EXPERIMENTAL AND ESTIMATED LIFT GRADING CURVES FOR AN INCLINED PROPELLER

FIG.23.

CONDITIONS:-

V = 170 FT/SEC ψ = 10°

θ = 20° J' = 0·837

N = 750 R.P.M.

KEY:-

——— TEST RESULTS

— — — THEORETICAL VALUES

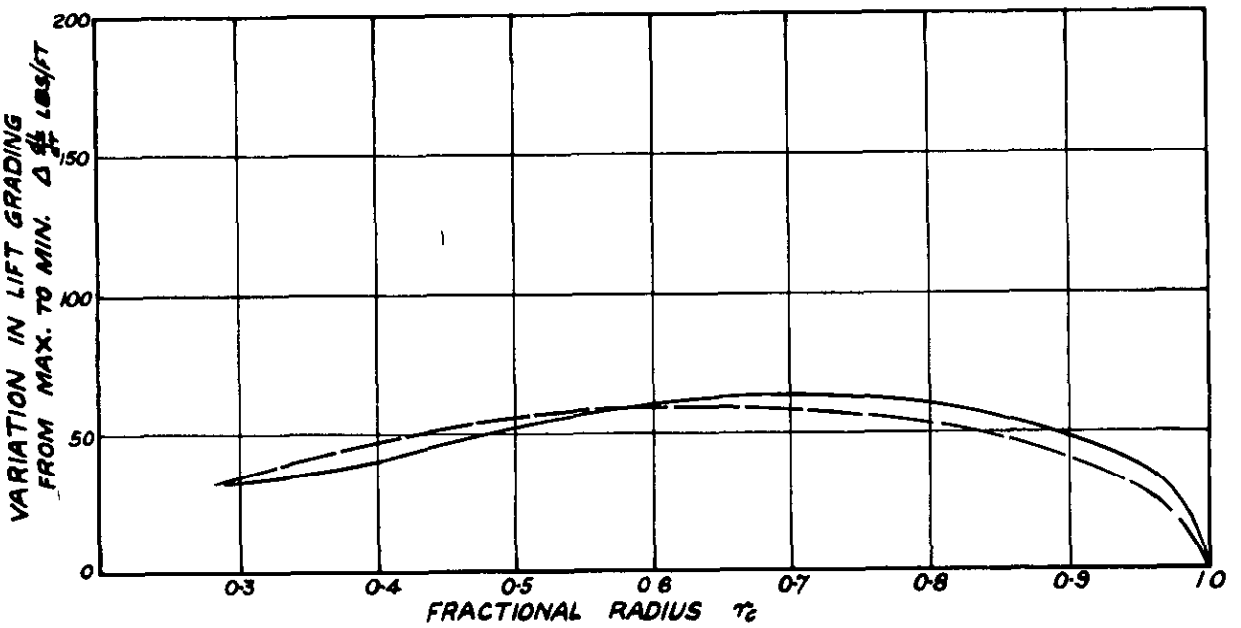

VARIATION IN LIFT GRADING FROM MAX. TO MIN.

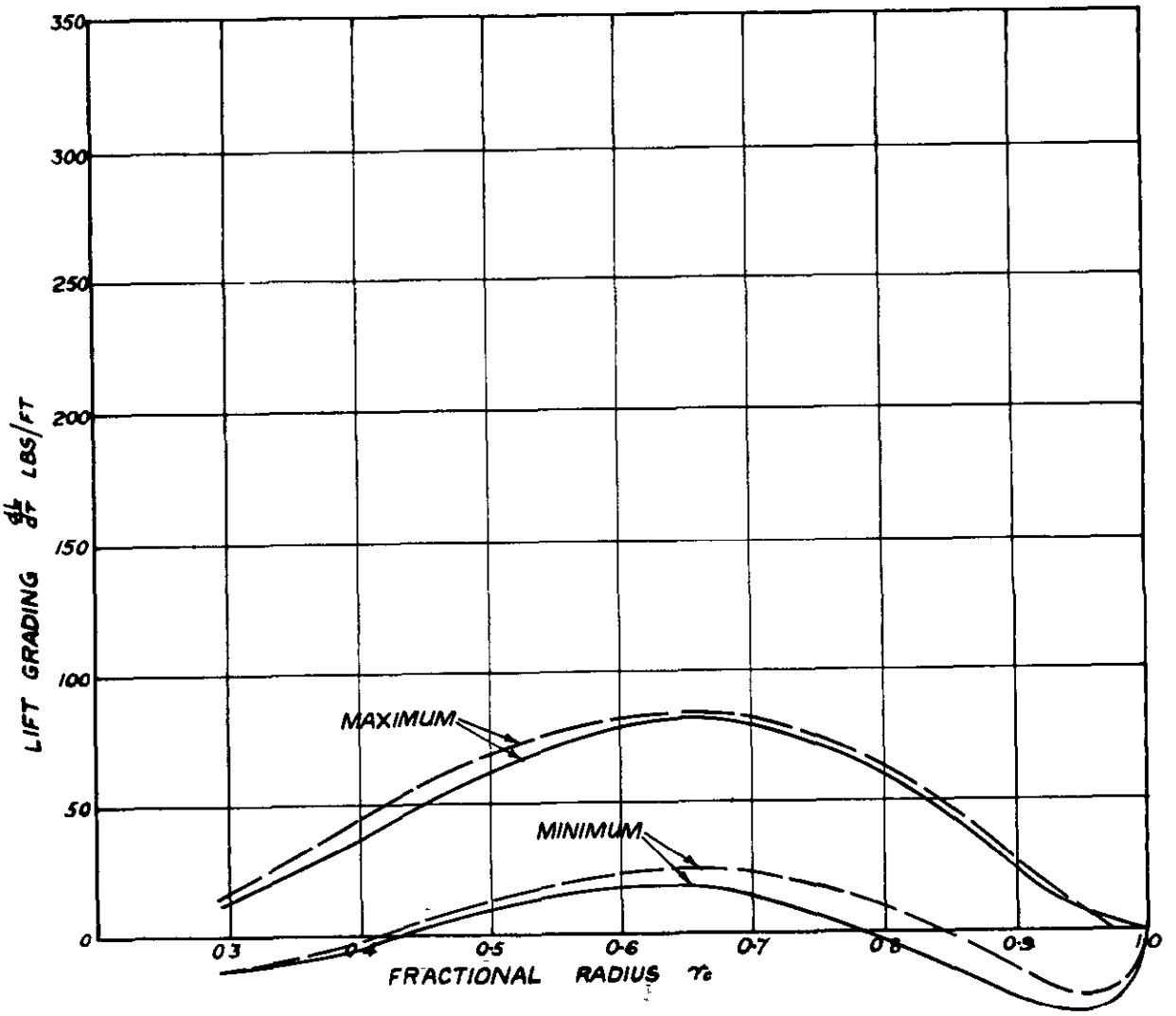

FIG.23. COMPARISON OF EXPERIMENTAL AND ESTIMATED LIFT GRADING CURVES FOR AN INCLINED PROPELLER

FIG.24

KEY:-

TEST RESULTS

THEORETICAL VALUES

CONDITIONS:-

V = 170 FT/SEC ψ = 10°

θ = 20° J' = 0.739

N = 850 R.P.M.

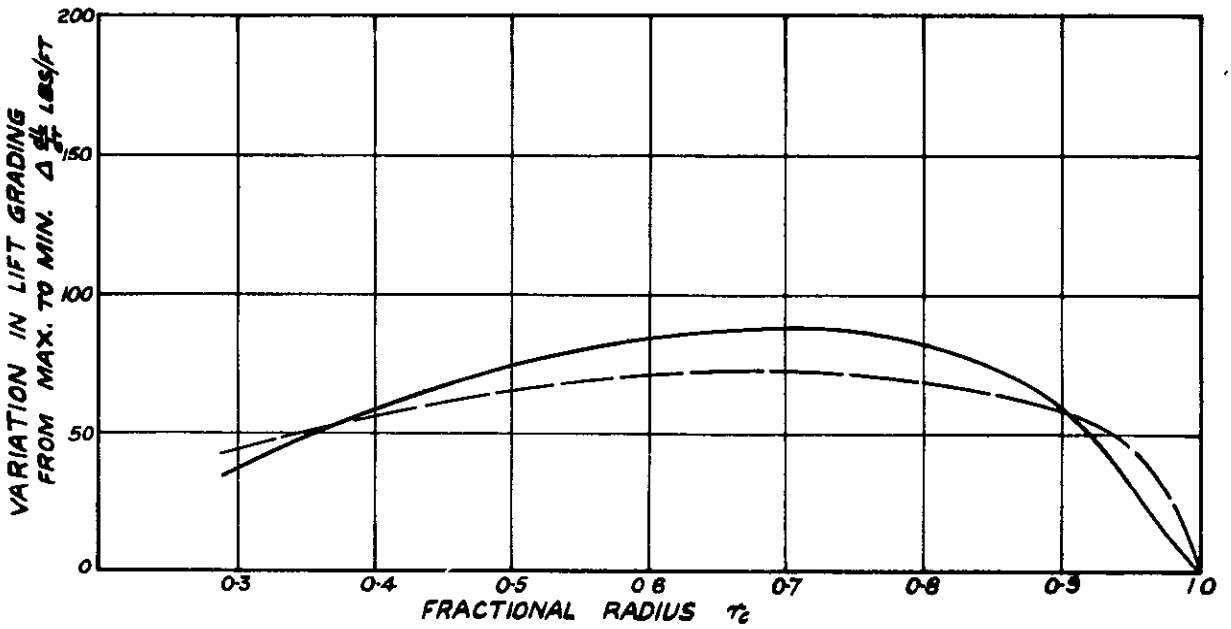

VARIATION IN LIFT GRADING FROM MAX. TO MIN.

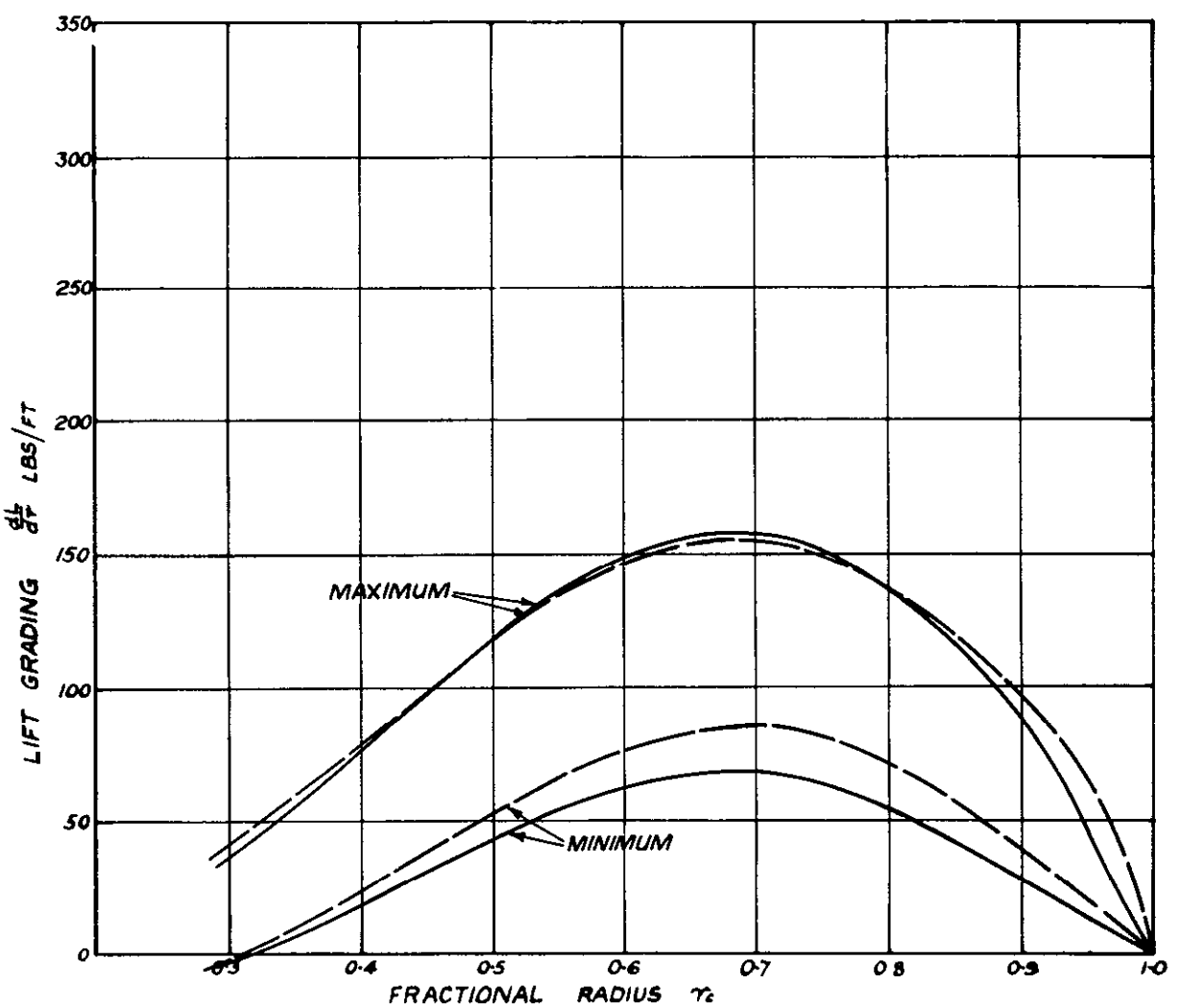

FIG.24. COMPARISON OF EXPERIMENTAL AND ESTIMATED LIFT GRADING CURVES FOR AN INCLINED PROPELLER

FIG.25.

KEY -

TEST RESULTS

THEORETICAL VALUES

CONDITIONS -

$V = 100$ FT/SEC $\quad \psi = 5°$

$\theta = 23°$ $\quad J = 0.498$

$N = 750$ R P M

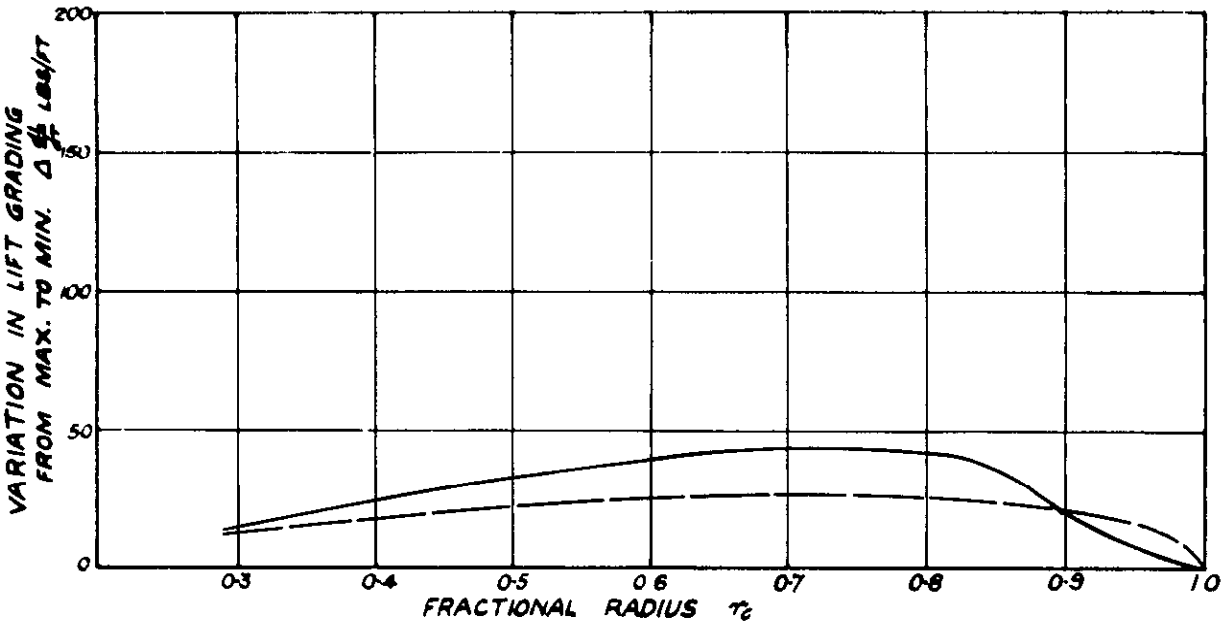

VARIATION IN LIFT GRADING FROM MAX. TO MIN.

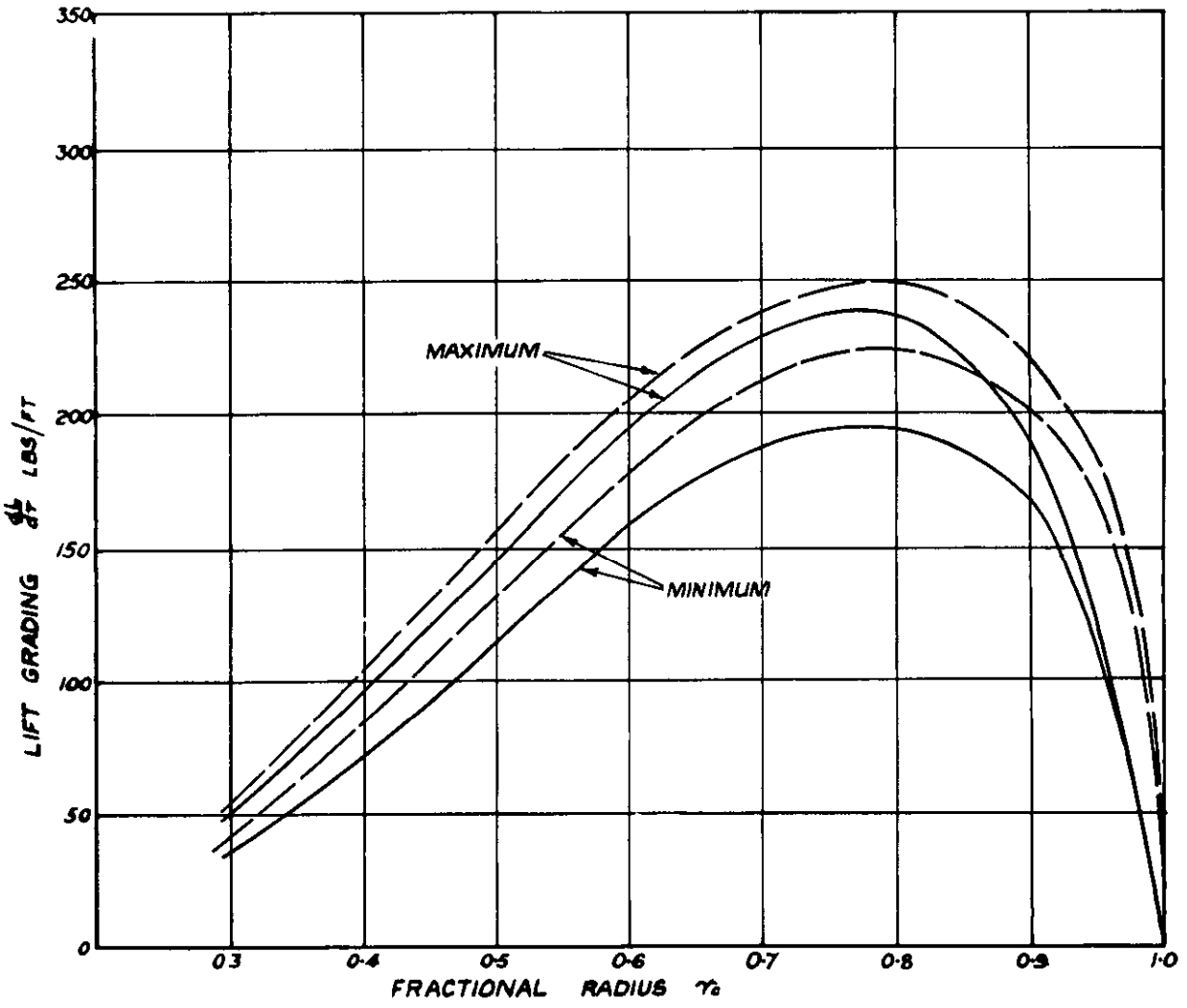

FIG.25. COMPARISON OF EXPERIMENTAL AND ESTIMATED LIFT GRADING CURVES FOR AN INCLINED PROPELLER

FIG. 26.

KEY.-

TEST RESULTS

THEORETICAL VALUES

CONDITIONS:-

V = 100 FT/SEC ψ = 15°

B = 26° 55' J' = 0·5574

N = 650 R.P.M.

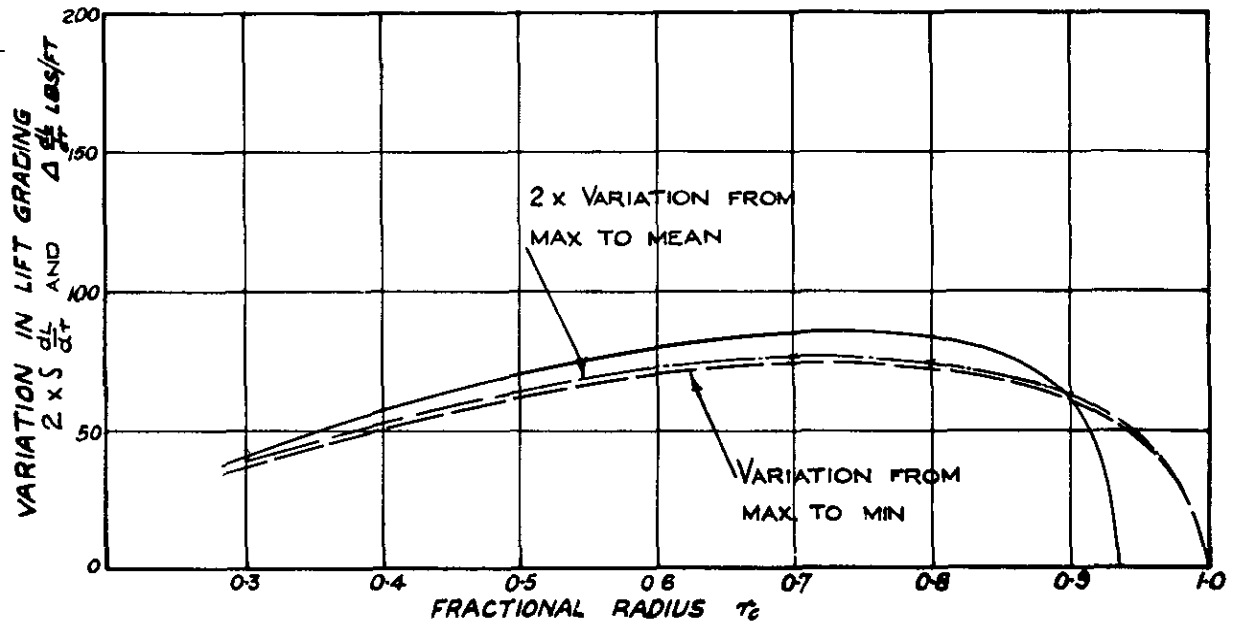

VARIATION IN LIFT GRADING

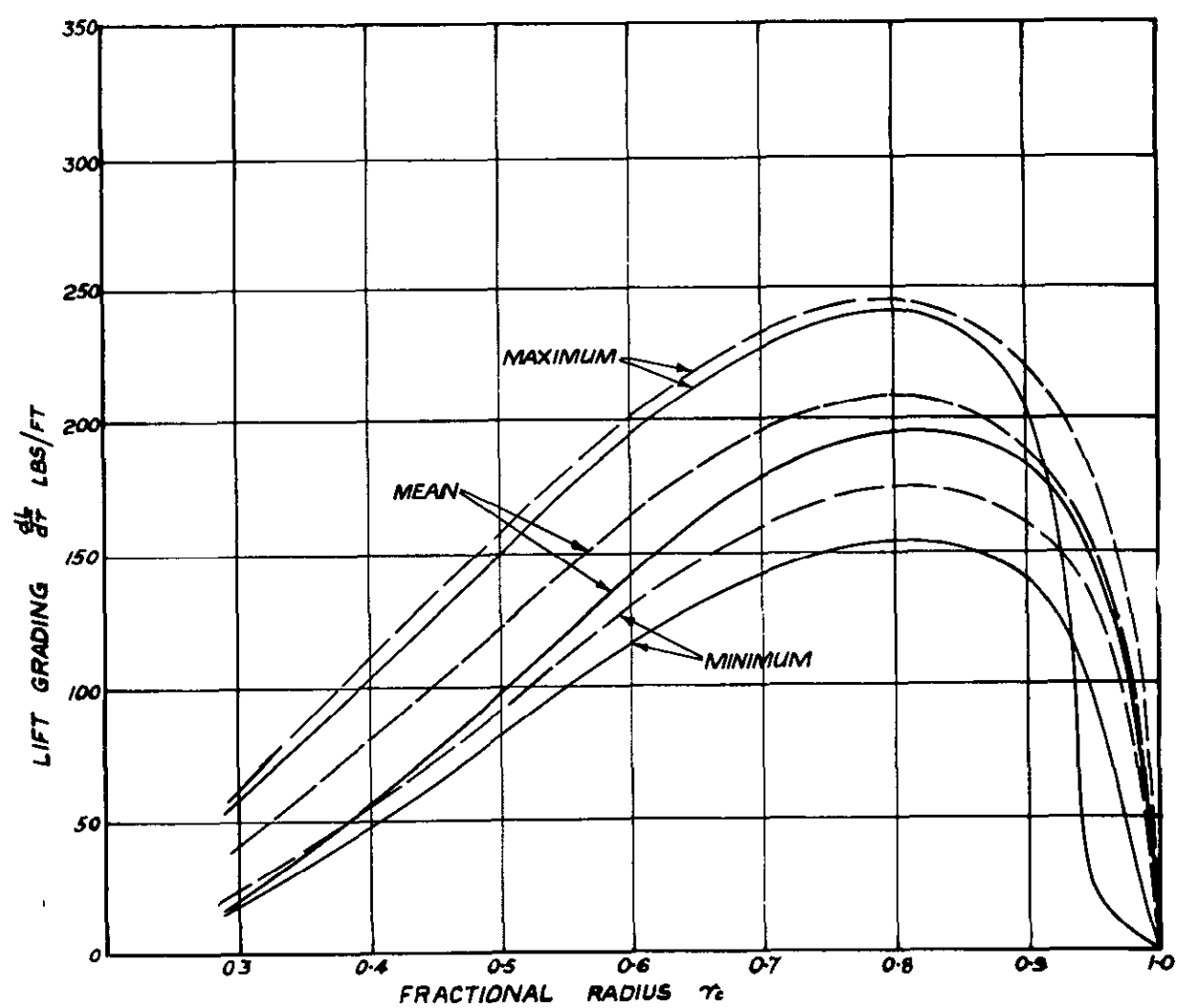

FIG. 26. COMPARISON OF EXPERIMENTAL AND ESTIMATED LIFT GRADING CURVES FOR AN INCLINED PROPELLER

FIG.27.

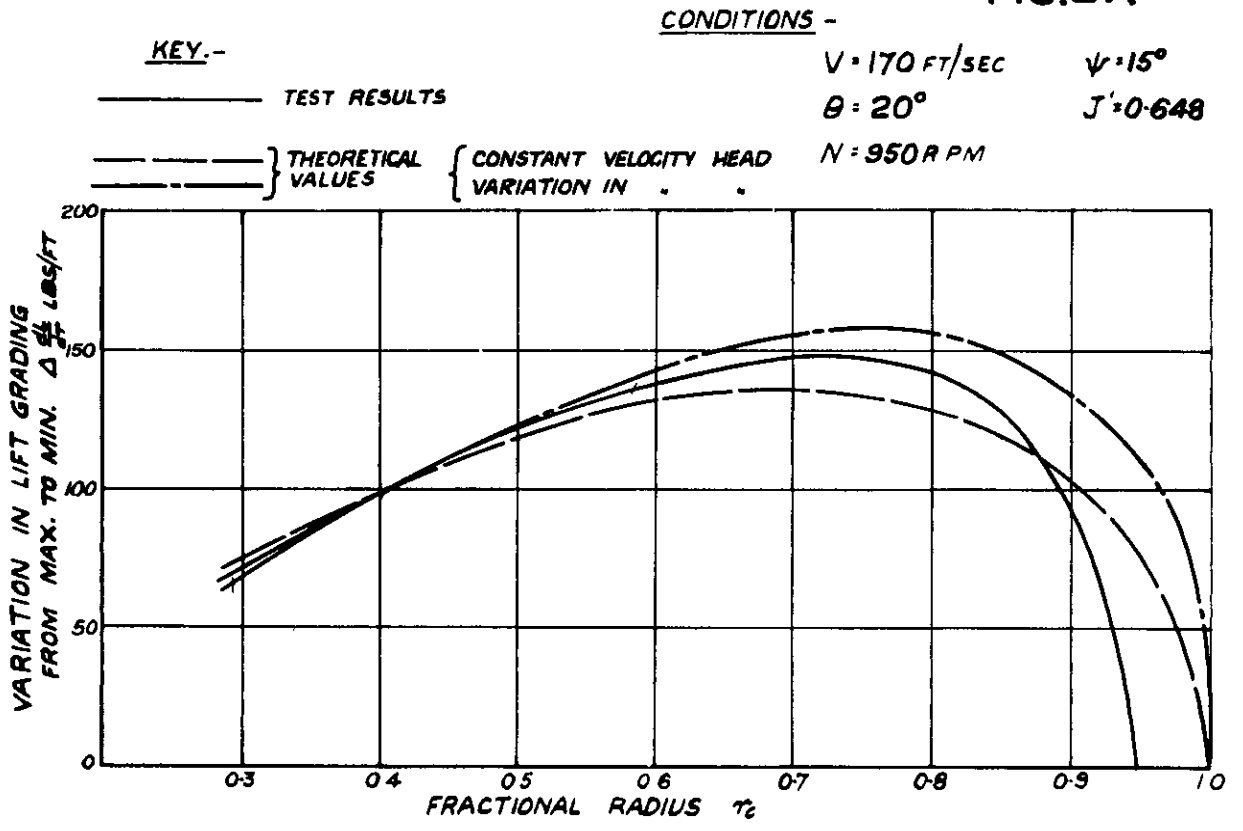

VARIATION IN LIFT GRADING FROM MAX. TO MIN.

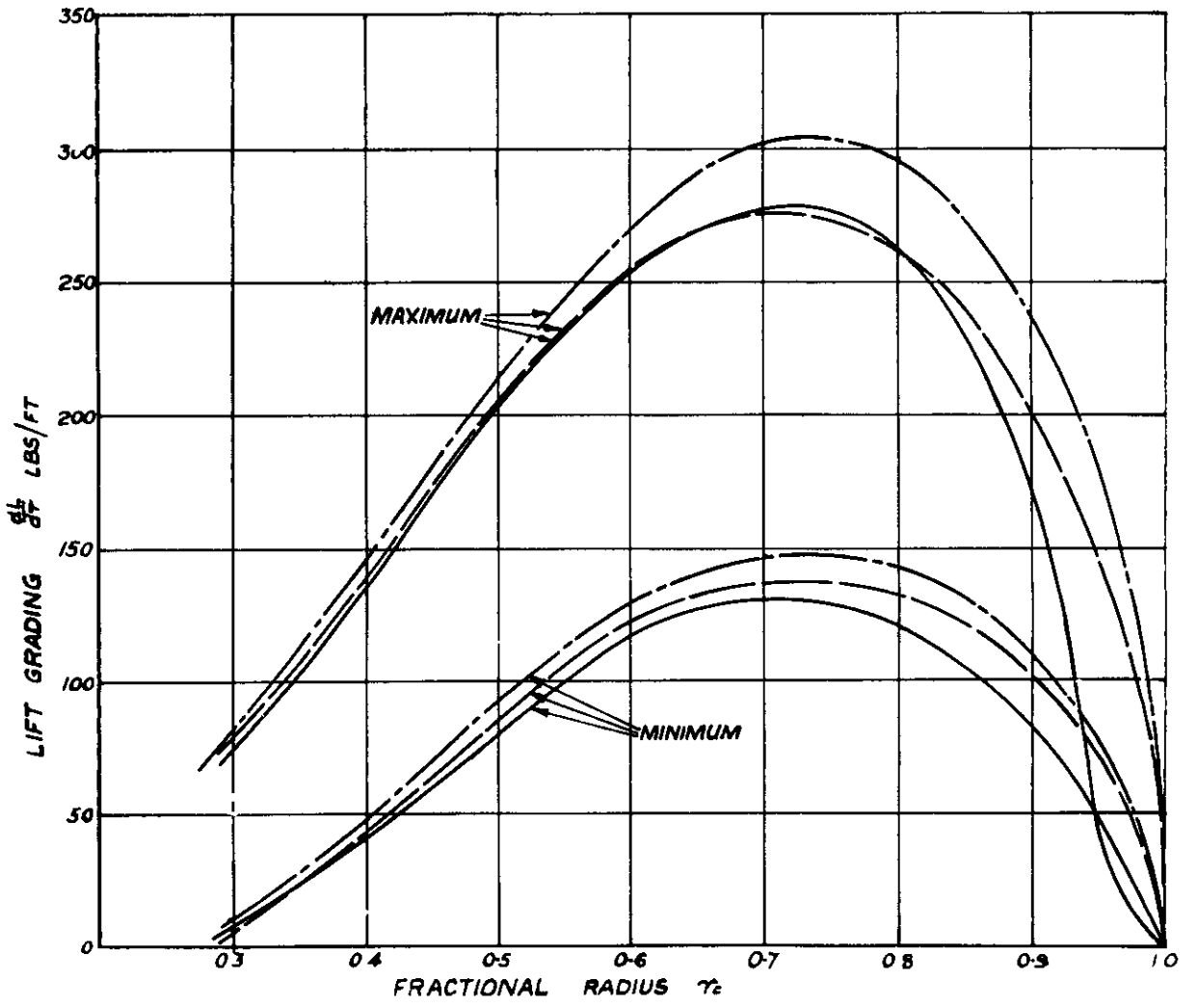

FIG.27. COMPARISON OF EXPERIMENTAL AND ESTIMATED LIFT GRADING CURVES FOR AN INCLINED PROPELLER

FIG.28.

CONDITIONS.-

KEY -

TEST RESULTS

THEORETICAL VALUES

CONSTANT VELOCITY HEAD

VARIATION IN " "

$V = 170$ FT/SEC $\psi = 15°$

$\theta = 23°$ $J' = 0.724$

$N = 850$ R.P.M.

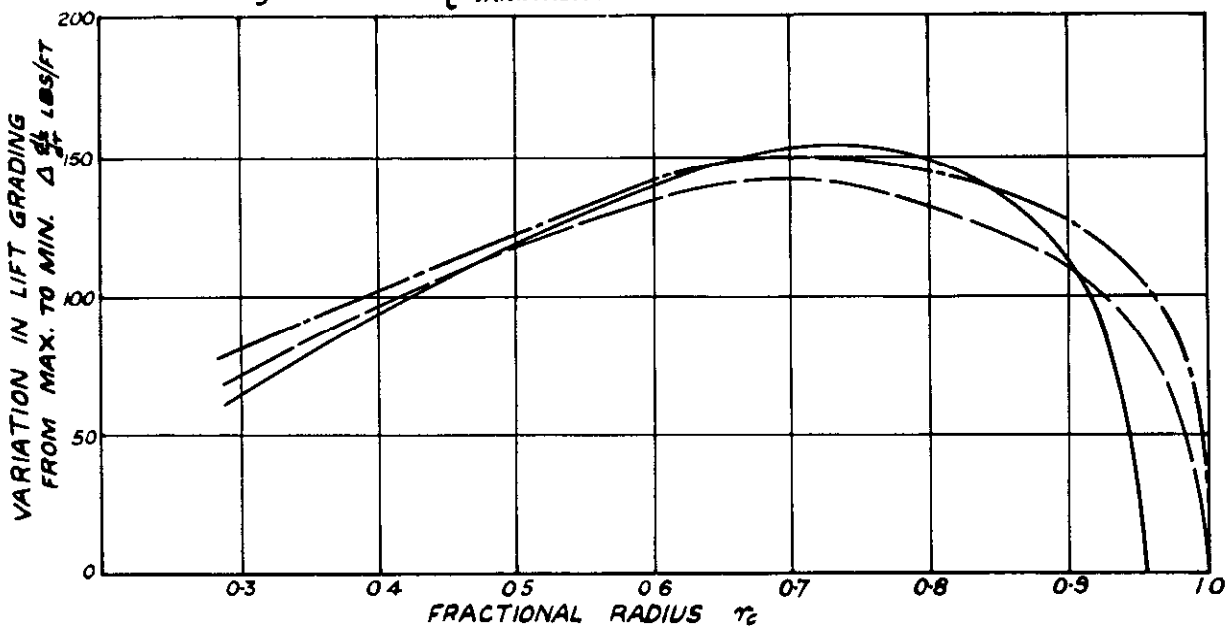

VARIATION IN LIFT GRADING FROM MAX. TO MIN.

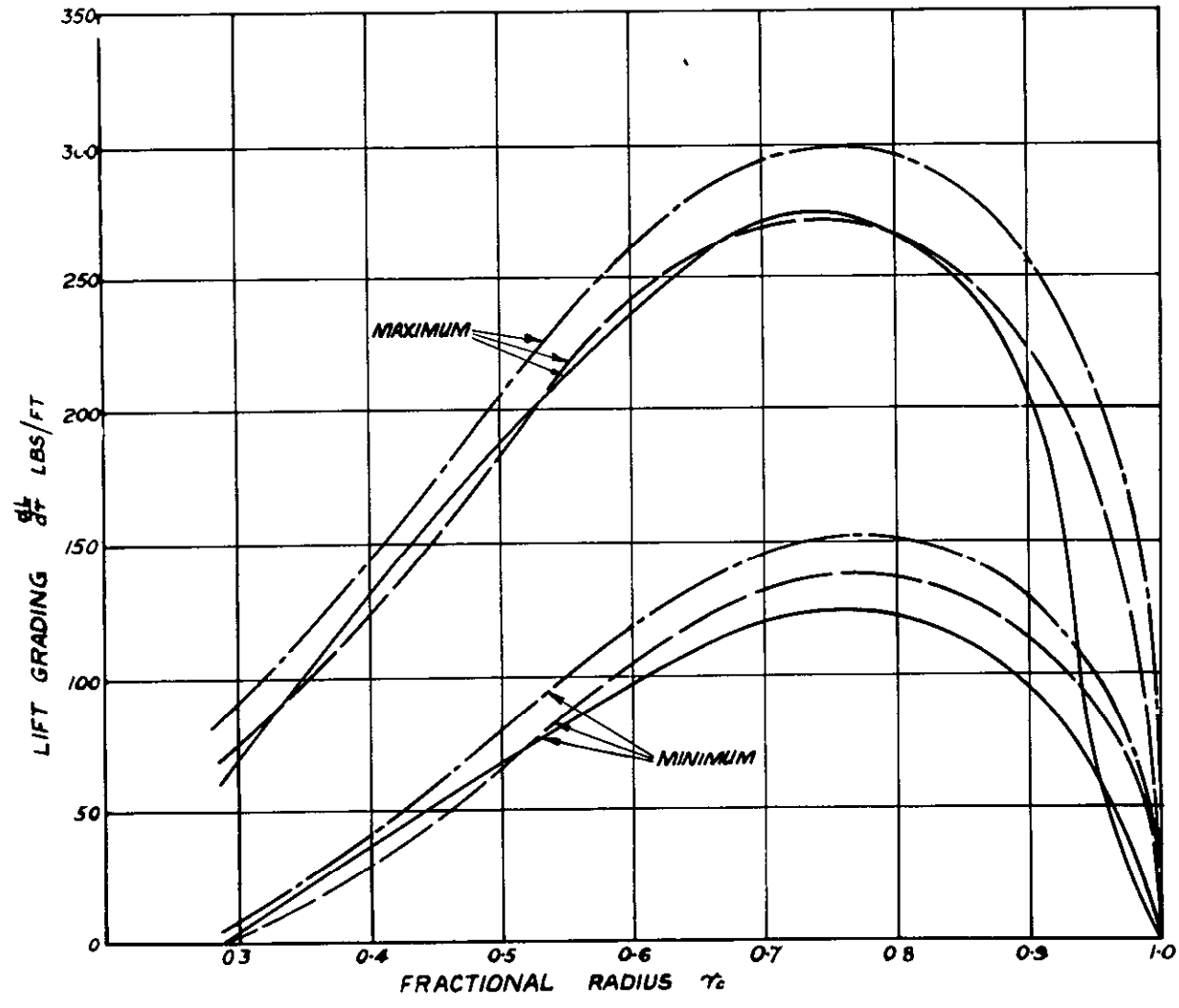

FIG. 28 COMPARISON OF EXPERIMENTAL AND ESTIMATED LIFT GRADING CURVES FOR AN INCLINED PROPELLER

FIG.29.

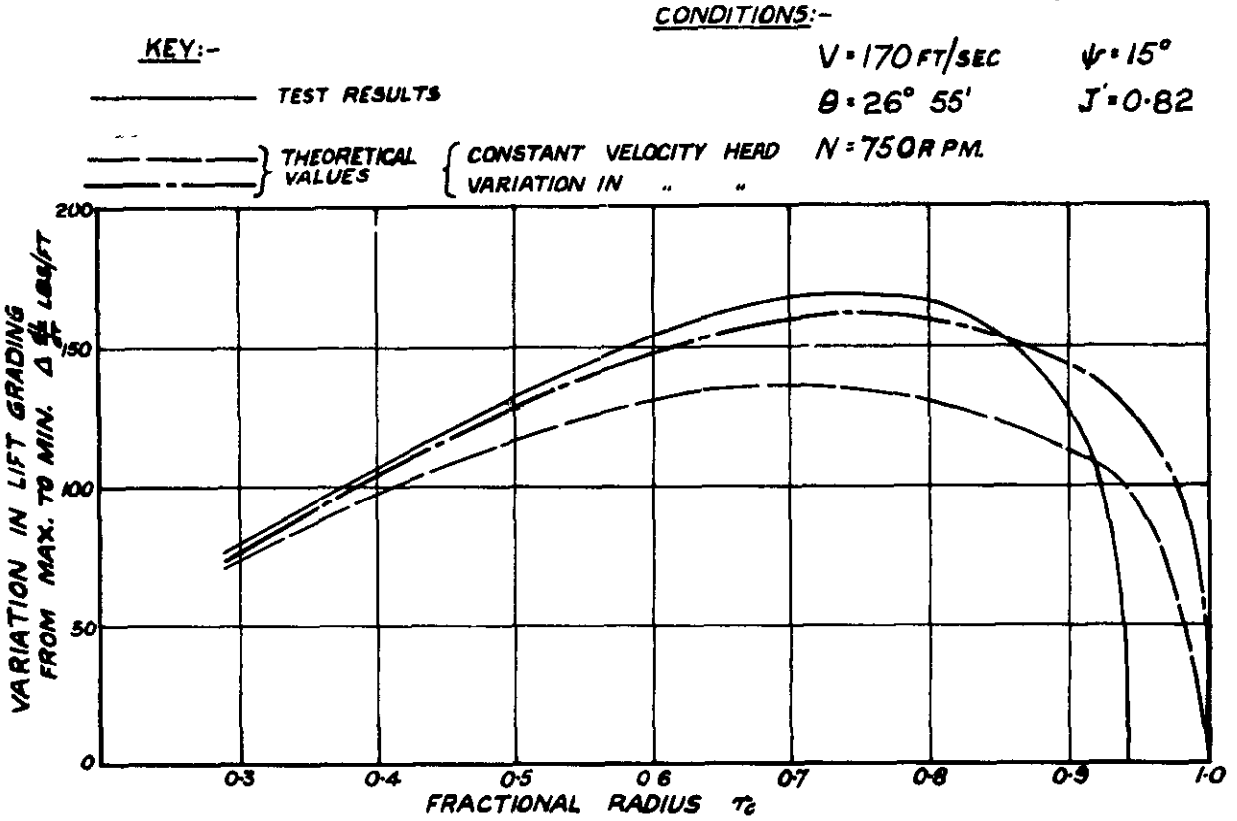

VARIATION IN LIFT GRADING FROM MAX. TO MIN.

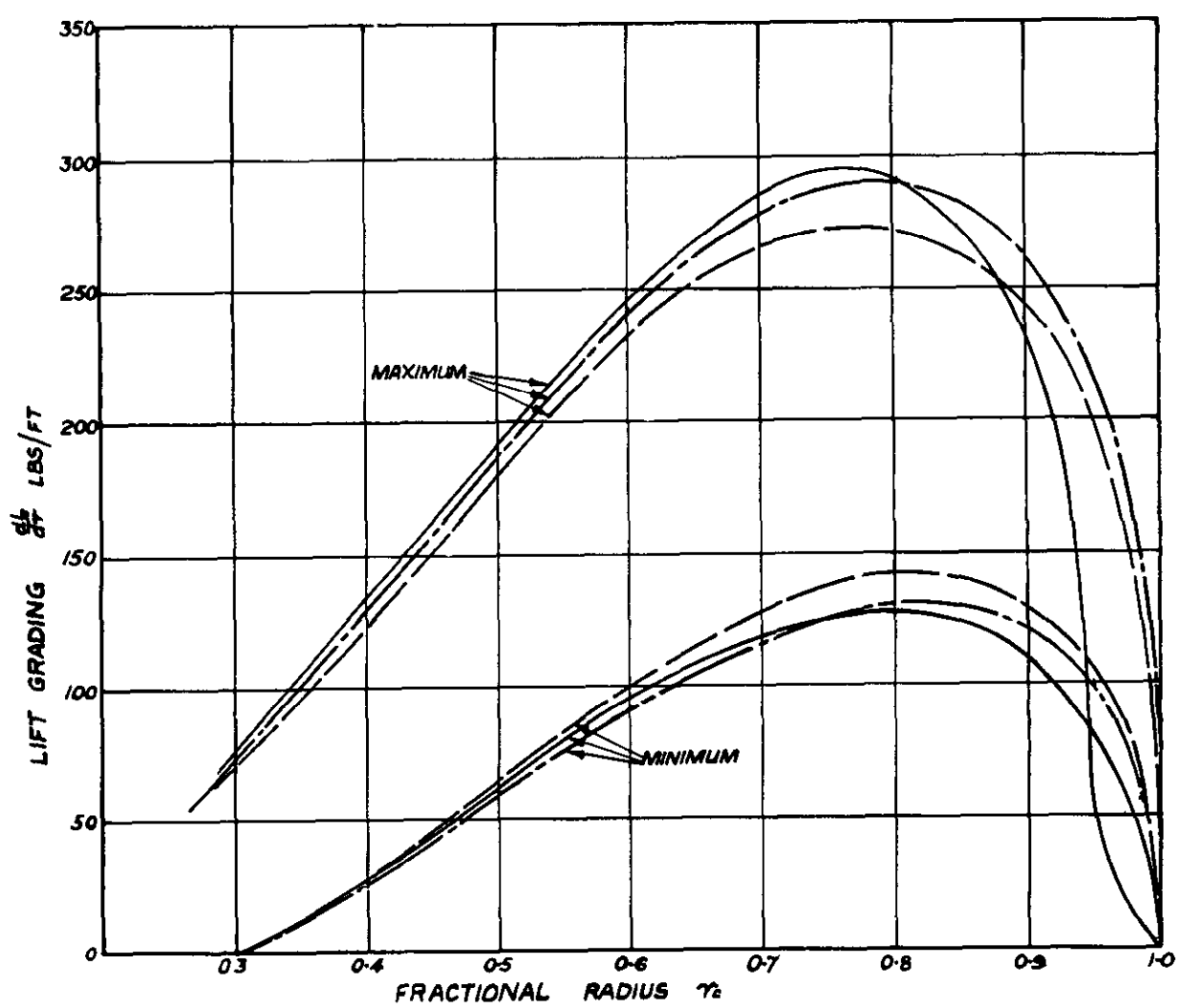

FIG.29. COMPARISON OF EXPERIMENTAL AND ESTIMATED LIFT GRADING CURVES FOR AN INCLINED PROPELLER

FIG. 30.

KEY:-

TEST RESULTS

THEORETICAL VALUES

CONDITIONS:-

V = 170 FT/SEC ψ = 0° & 15°

θ = 20°

N = 950 R.P.M.

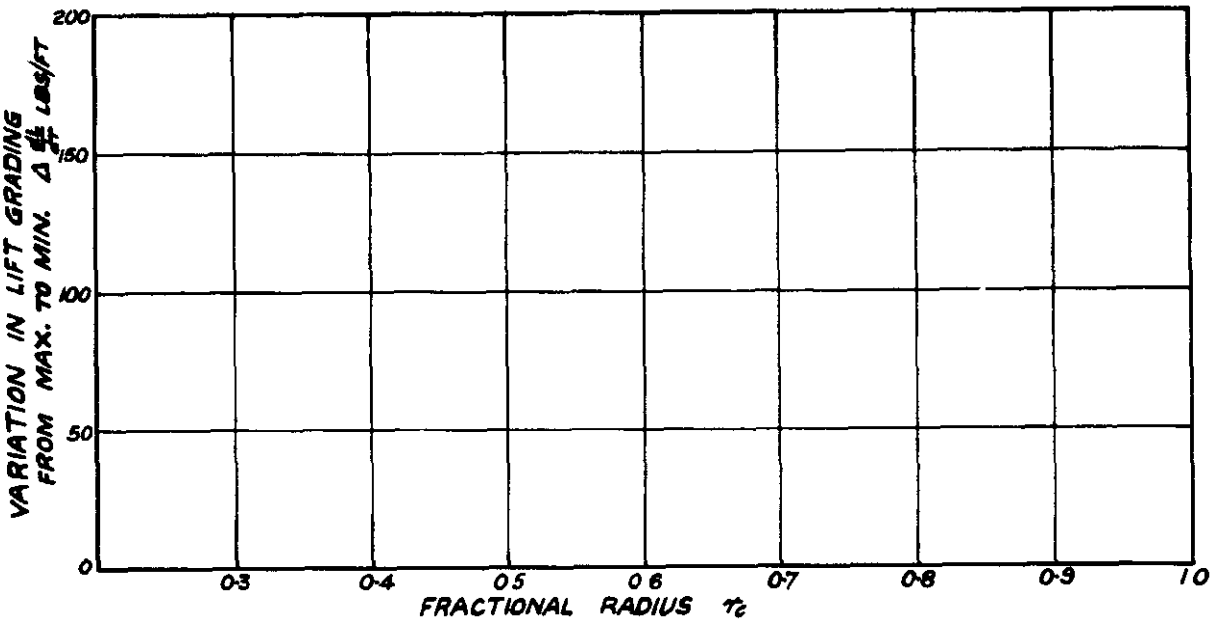

VARIATION IN LIFT GRADING FROM MAX. TO MIN.

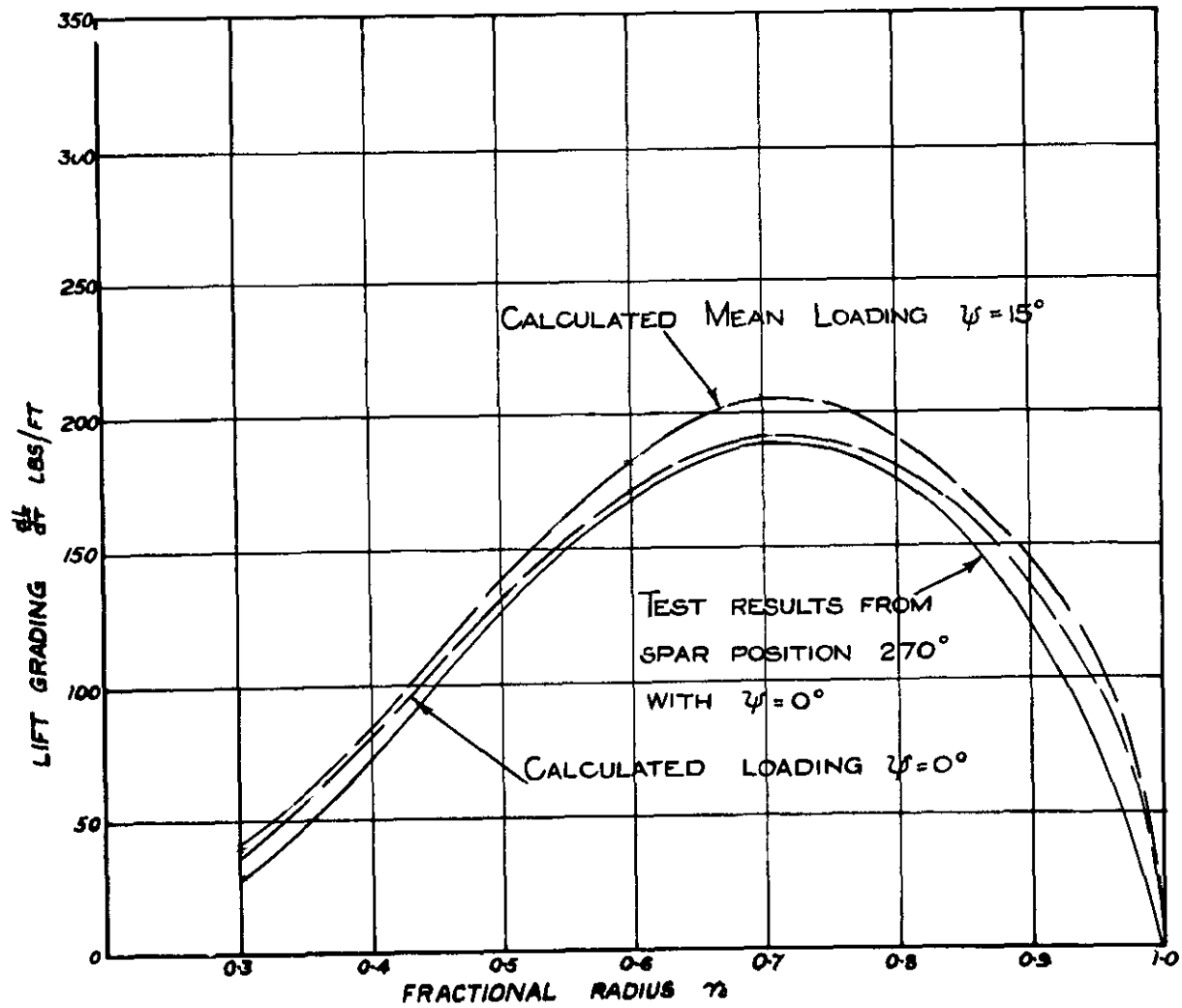

FIG. 30. COMPARISON OF EXPERIMENTAL AND ESTIMATED LIFT GRADING CURVES FOR AN INCLINED PROPELLER

FIG. 31.

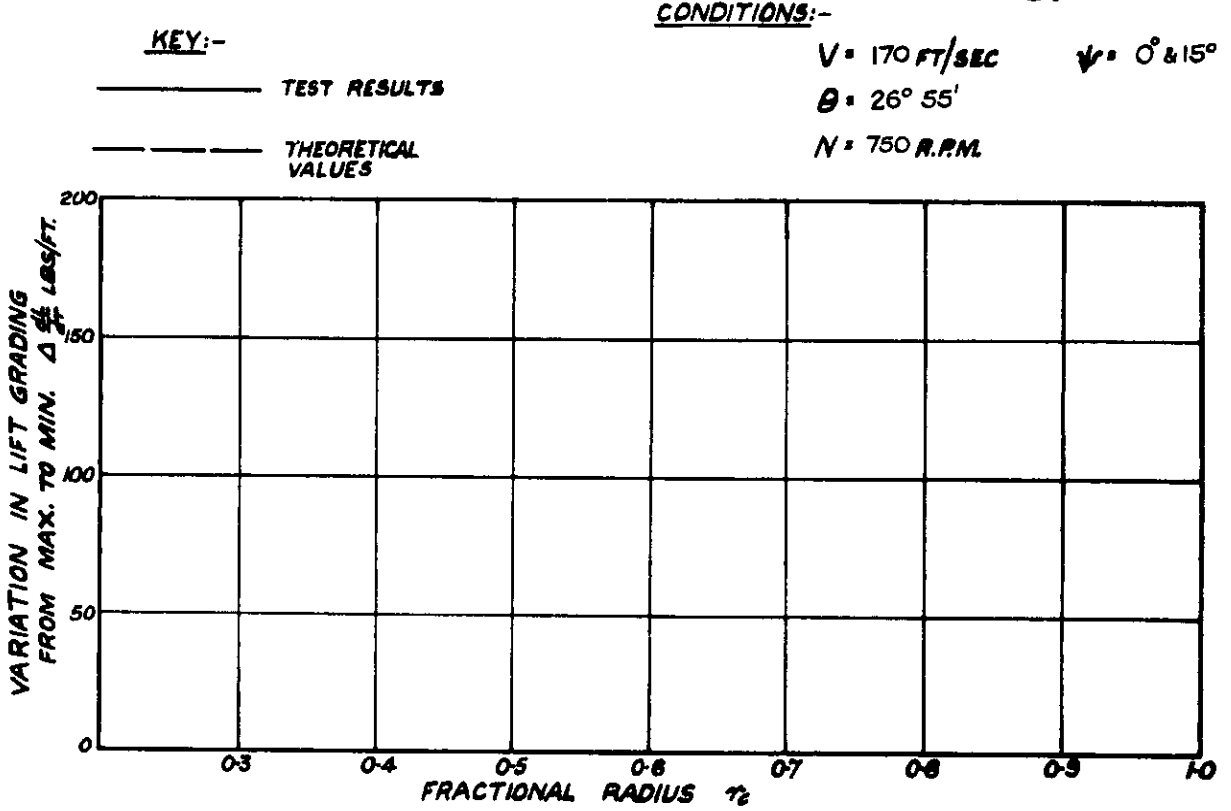

VARIATION IN LIFT GRADING FROM MAX. TO MIN.

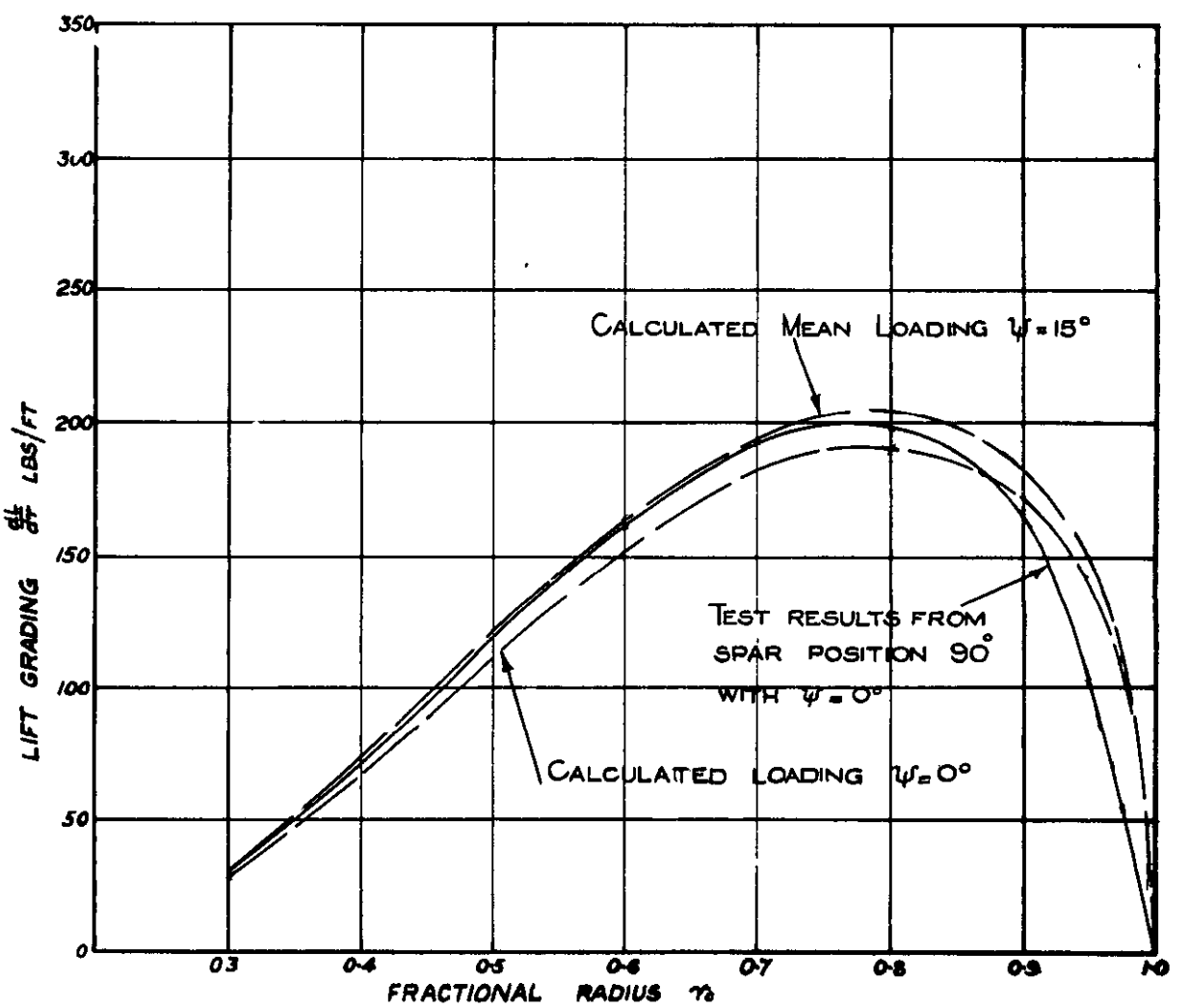

FIG. 31. COMPARISON OF EXPERIMENTAL AND ESTIMATED LIFT GRADING CURVES FOR AN INCLINED PROPELLER

FIG. 32.

KEY:-

——————— TEST RESULTS

— — — — THEORETICAL VALUES

CONDITIONS :-

V = 170 FT. SEC.

θ = 20°

N = 950 R.P.M.

ψ = 0°, 5°, 10° & 15°

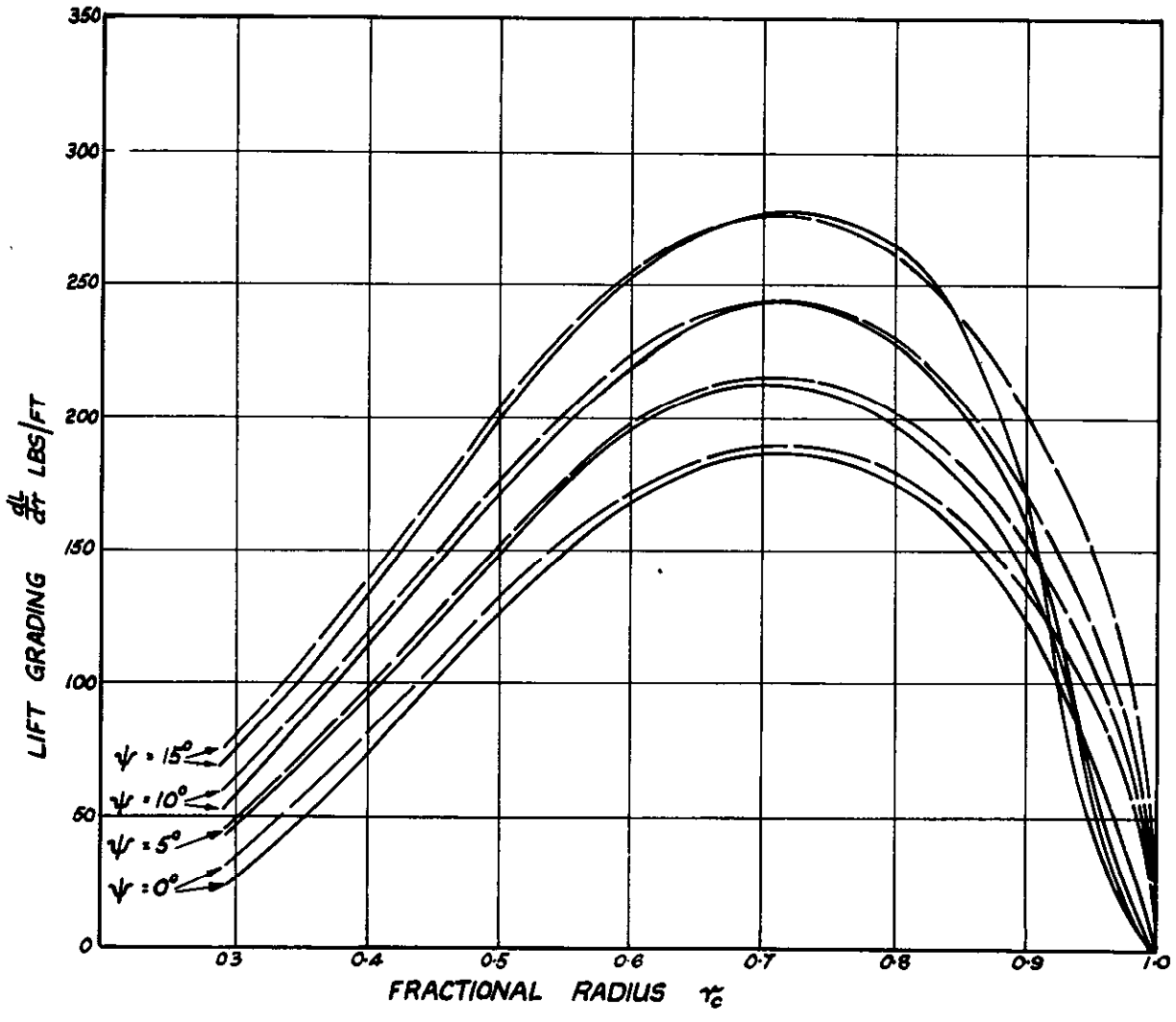

FIG.32. EFFECT OF INCLINATION ψ ON MAXIMUM LIFT GRADING.

KEY:-

——— TEST RESULTS

— — — — THEORETICAL VALUES

CONDITIONS:-

V = 170 FT/SEC.

θ = 23°

N = 850 R.P.M.

ψ = 5°, 10° & 15°

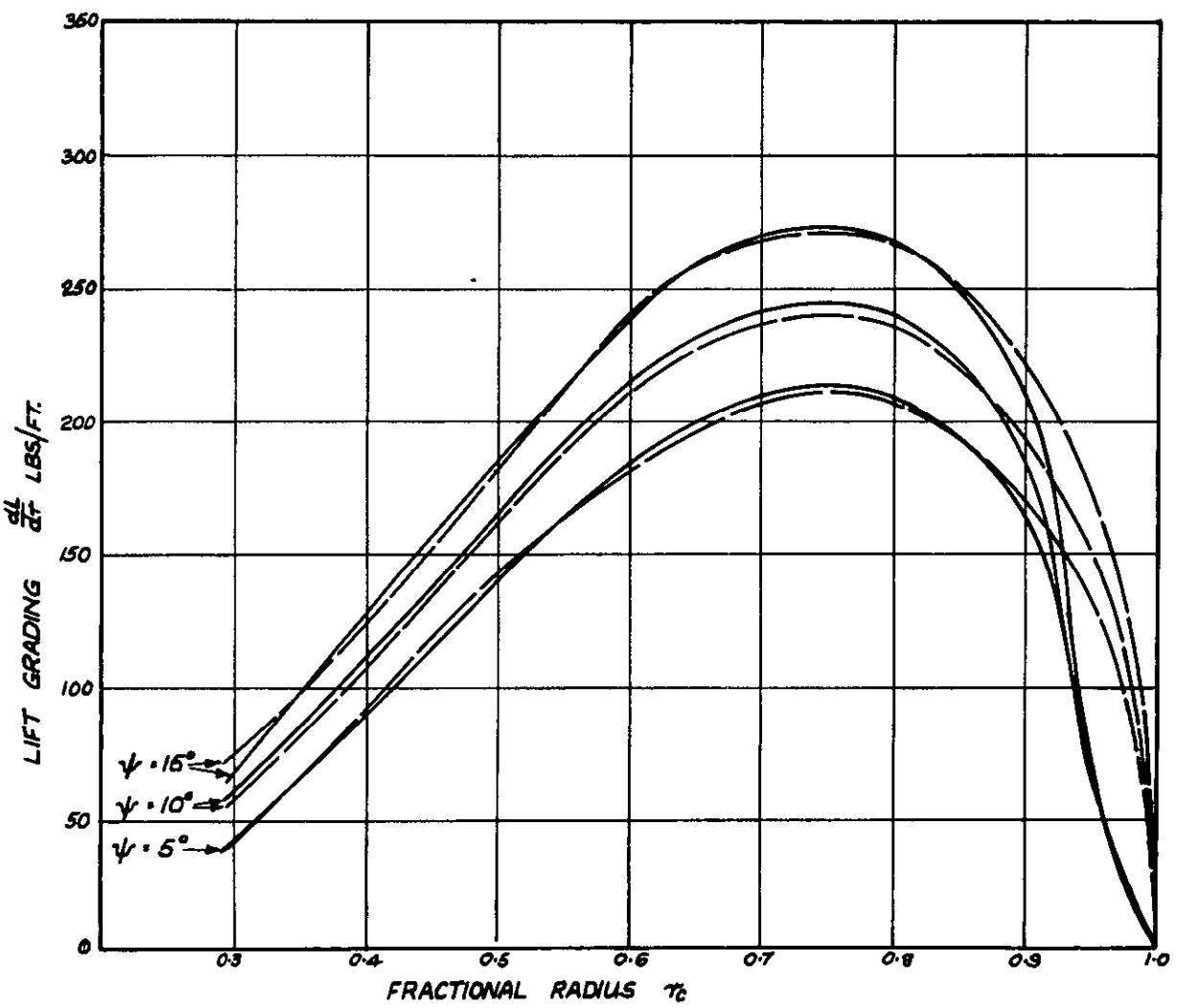

FIG.33. EFFECT OF INCLINATION ψ ON MAXIMUM LIFT GRADING

FIG. 34.

KEY:-

TEST RESULTS

THEORETICAL VALUES

CONDITIONS -

V = 170 FT/SEC.

θ = 26° 55'

N = 750 R.P.M

ψ = 0°, 5°, 10° & 15°

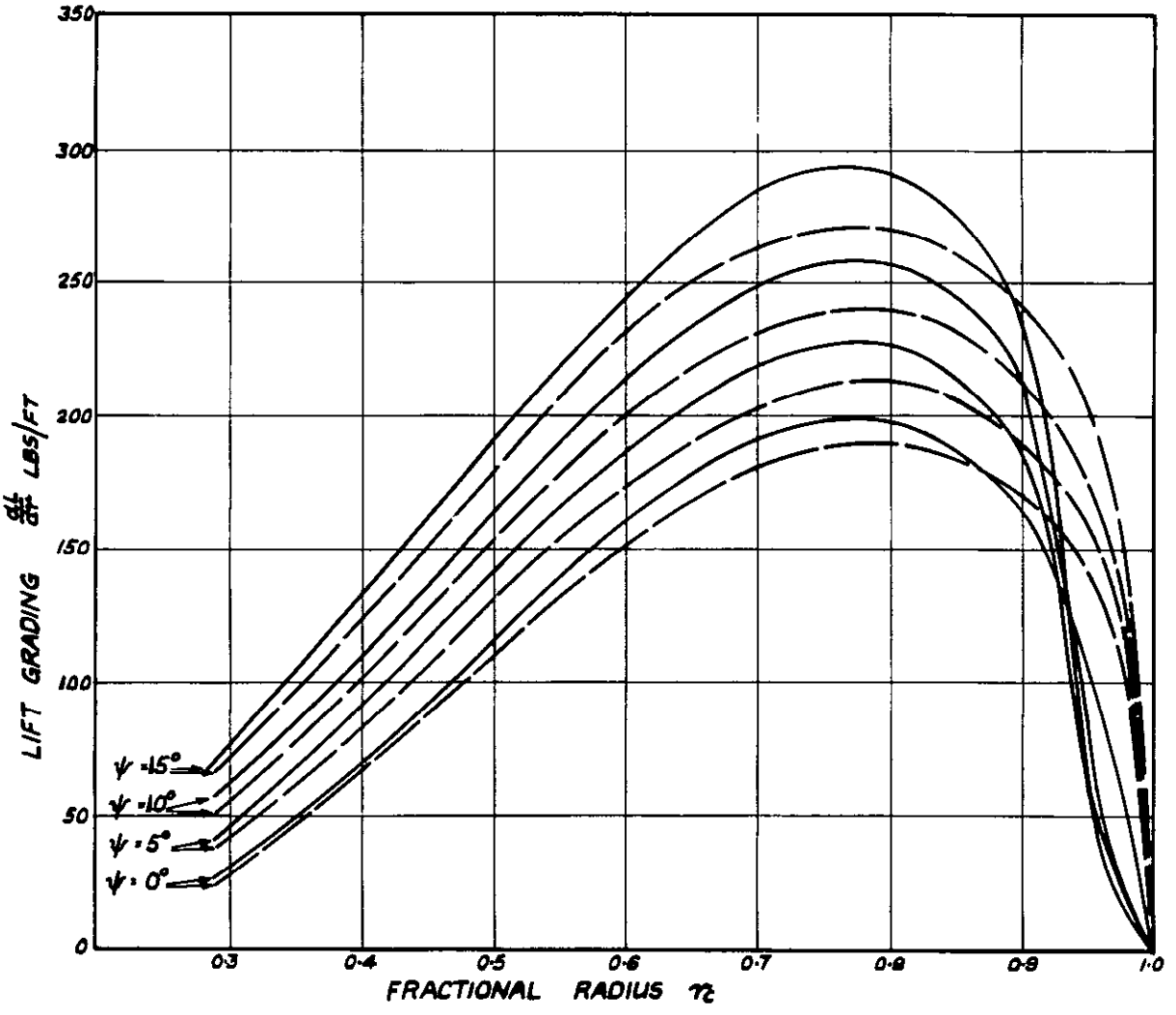

FIG. 34. EFFECT OF INCLINATION ψ ON MAXIMUM LIFT GRADING

KEY:—

——————— TEST RESULTS

— — — — — THEORETICAL VALUES

CONDITIONS:—

V = 170 FT./SEC.

θ = 20°

N = 750, 850 & 950 R.P.M

ψ = 10°

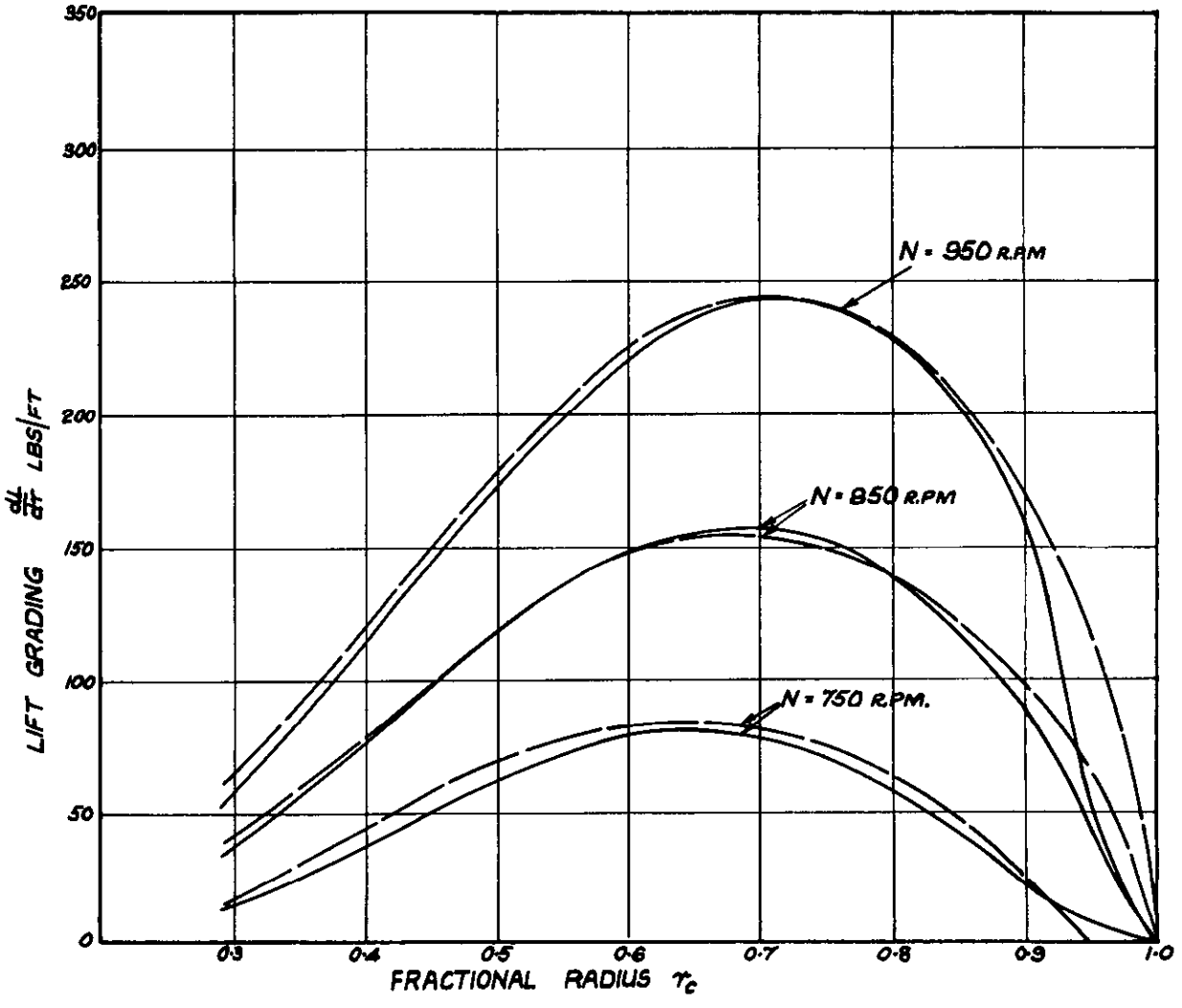

FIG. 35. EFFECT OF PROPELLER R.P.M. ON MAXIMUM LIFT GRADING

KEY:-

——————— TEST RESULTS

— — — — — THEORETICAL VALUES

CONDITIONS:-

V = 100 FT/SEC.

θ = 20°

N = 650, 750 & 875 R.P.M.

ψ = 10°

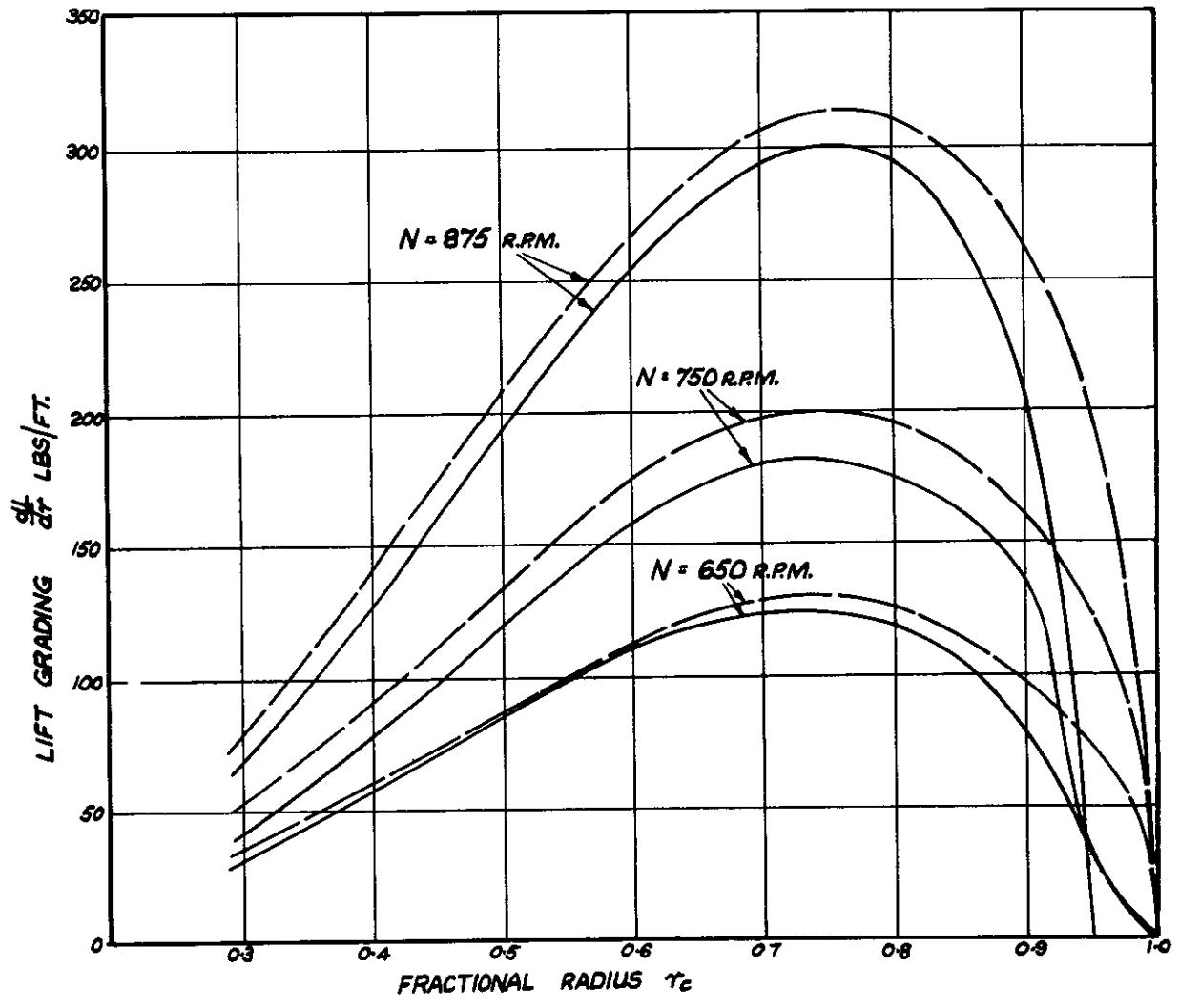

FIG.36. EFFECT OF PROPELLER R.P.M. ON MAXIMUM LIFT GRADING

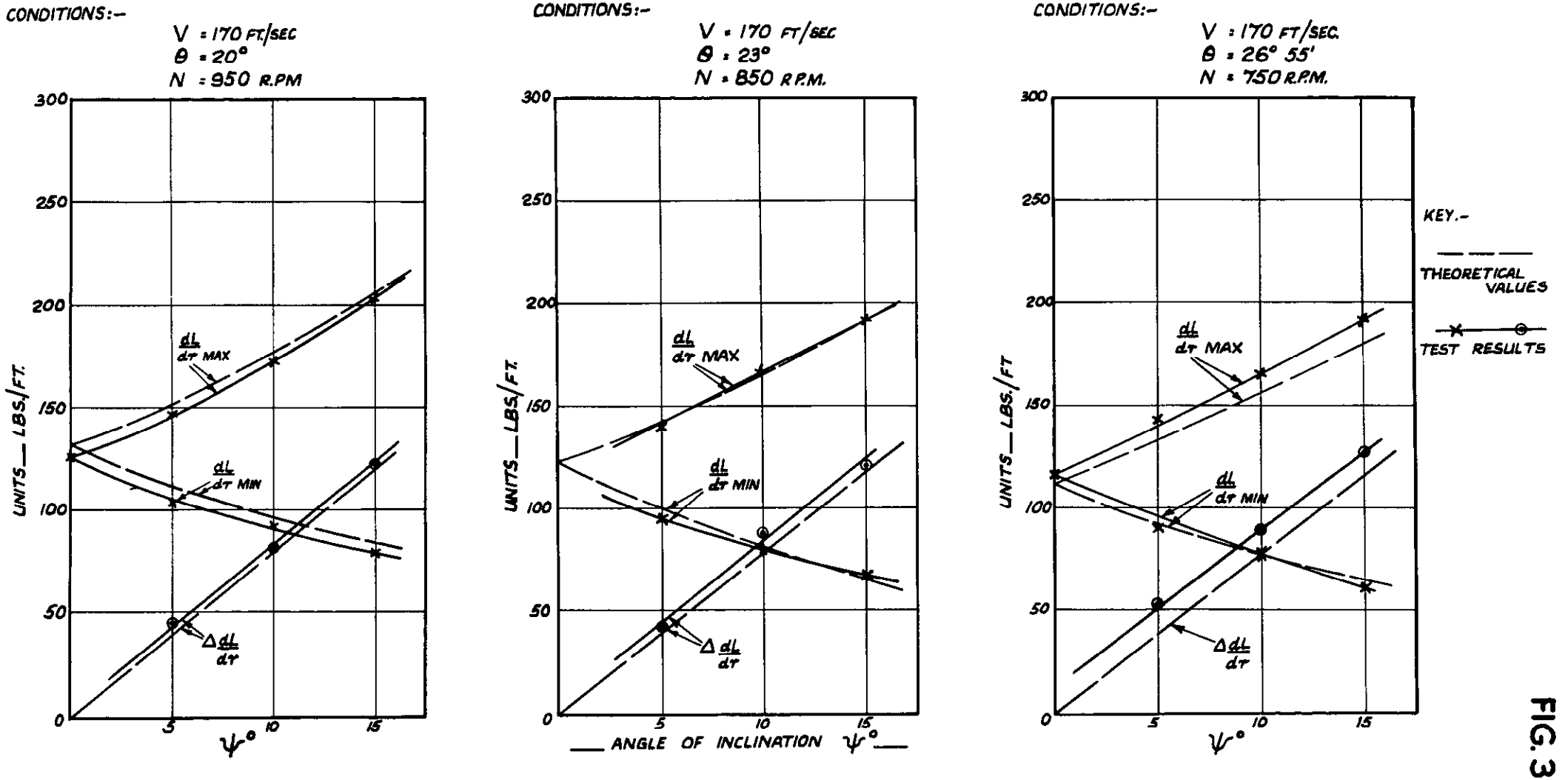

FIG.37.

FIG.37. EFFECT OF INCLINATION ψ ON THE LIFT GRADING AT $\tau_c = 0.5$

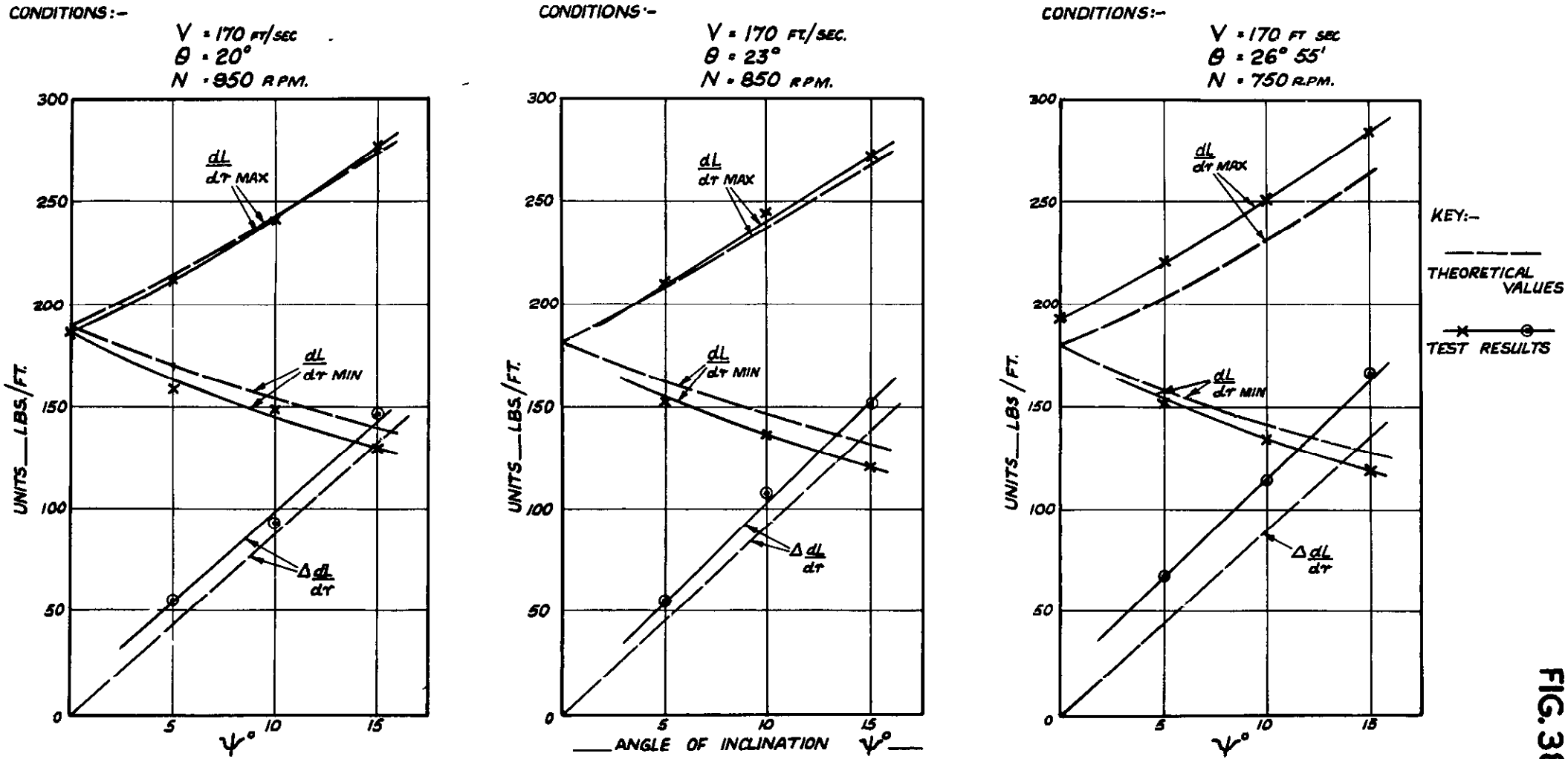

FIG. 38.

FIG. 38. EFFECT OF INCLINATION ψ ON THE LIFT GRADING AT $\tau_c = 0.7$

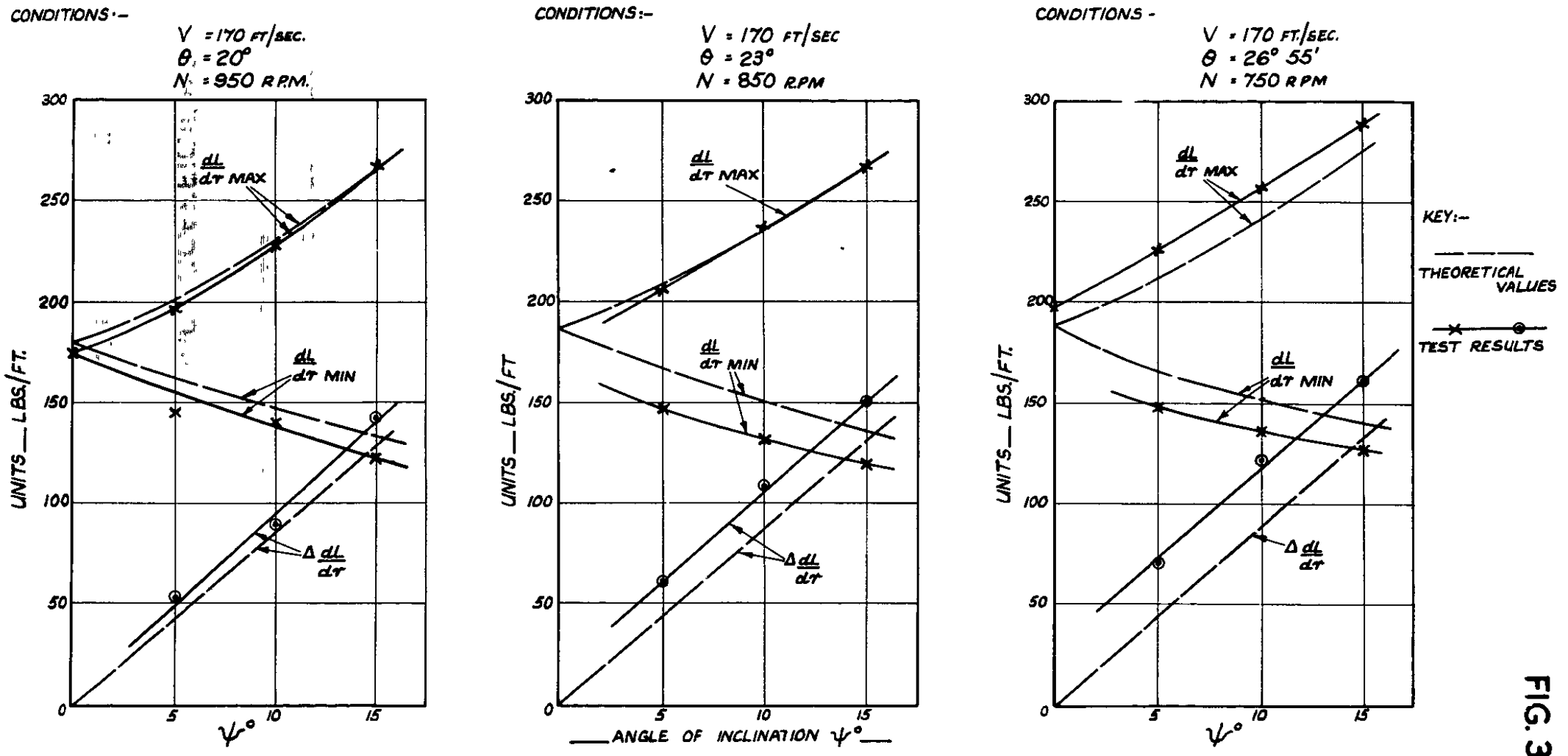

FIG. 39.

FIG.39. EFFECT OF INCLINATION ψ ON THE LIFT GRADING AT $\tau_c = 0.8$

FIG. 42.

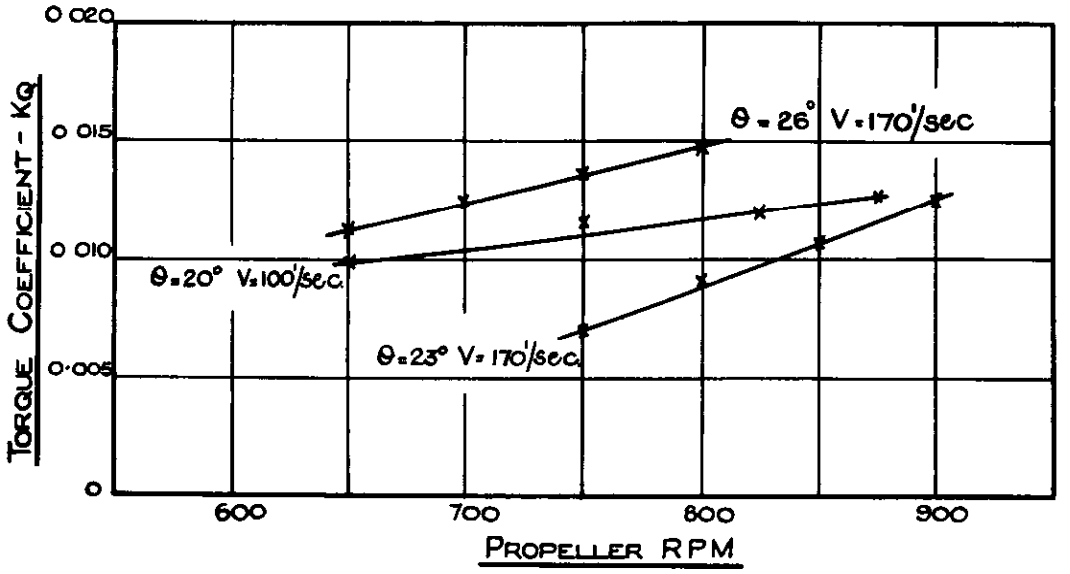

MEASURED Kq VALUES
RELATIVE TO THRUSTS SHOWN BELOW.

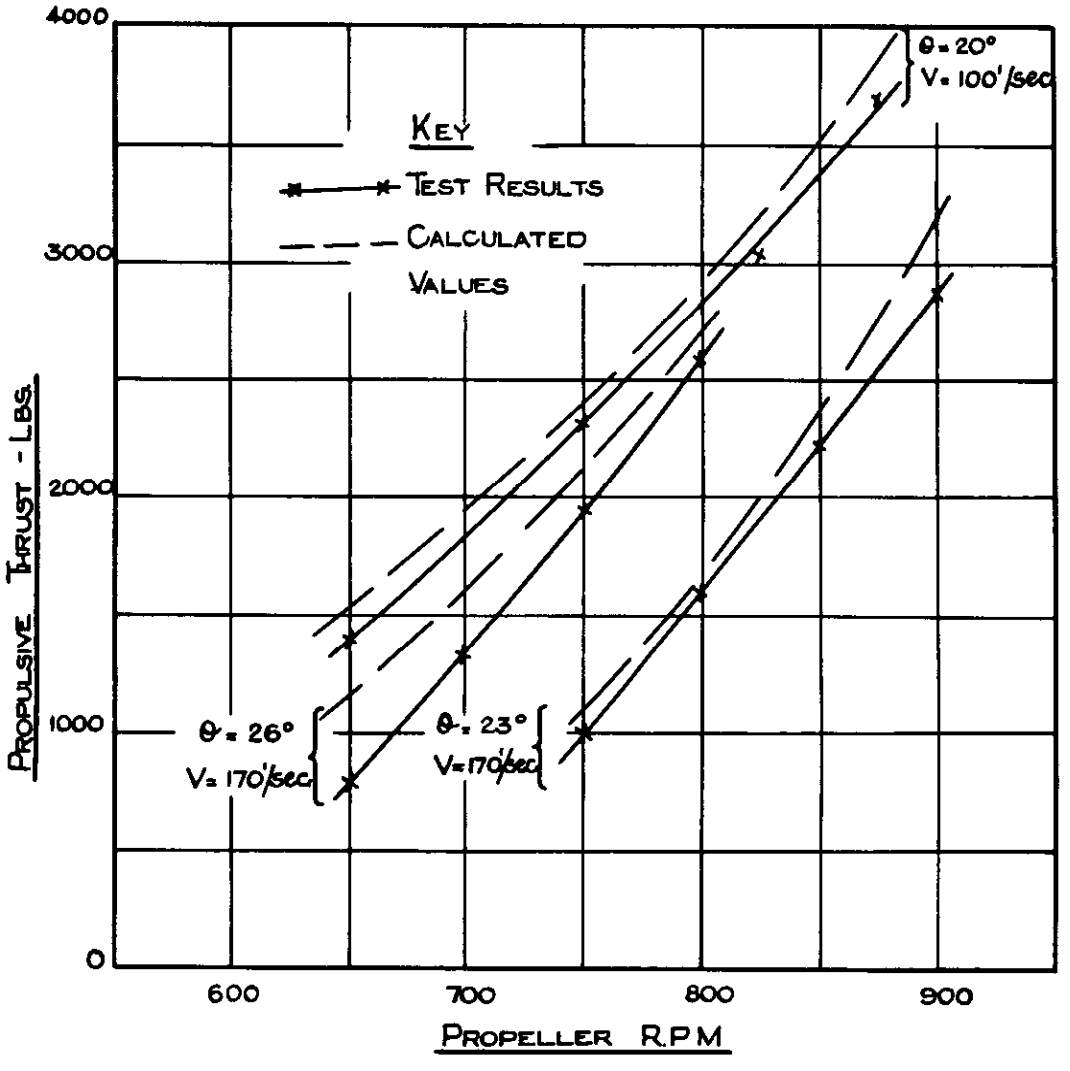

FIG. 42. COMPARISON OF MEASURED THRUSTS WITH VALUES CALCULATED BY USE OF THE S.B.A.C. METHOD.

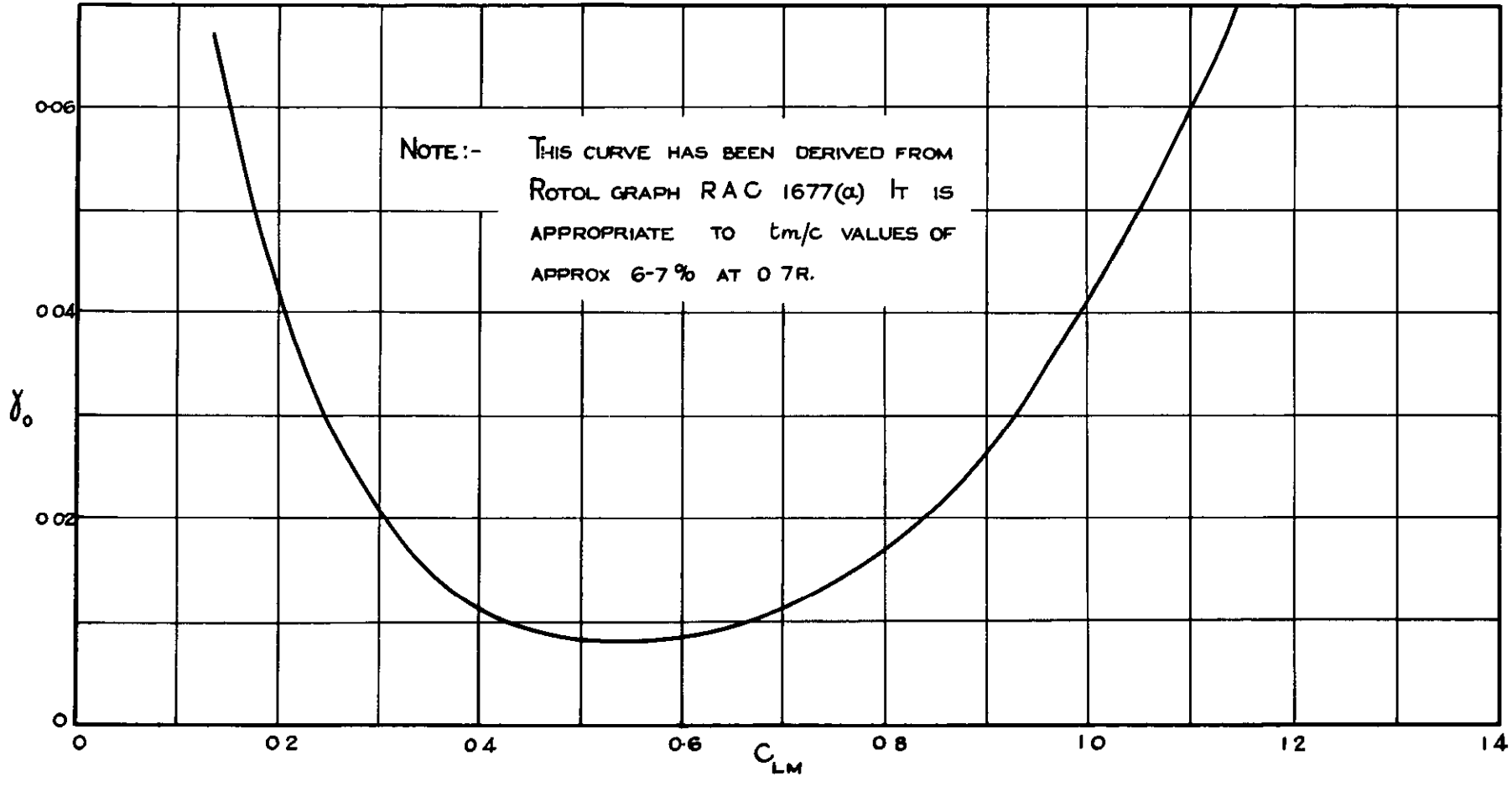

FIG. 43. VARIATION OF γ_0 WITH C_{LM} FOR BLADES HAVING NACA. SERIES 16 SECTIONS WITH DESIGN C_L OF 0·484 AT 0·7 R. (FOR USE WITH S.B.A.C. METHOD.)

FIG. 43.

C.P. No 117
(14,698)
A R C. Technical Report

PRINTED AND PUBLISHED BY HER MAJESTY'S STATIONERY OFFICE
To be purchased from
York House, Kingsway, LONDON, W C 2 423 Oxford Street, LONDON, W 1
P.O Box 569, LONDON, S E 1
13a Castle Street, EDINBURGH, 2 1 St. Andrew's Crescent, CARDIFF
39 King Street, MANCHESTER, 2 Tower Lane, BRISTOL, 1
2 Edmund Street, BIRMINGHAM, 3 80 Chichester Street, BELFAST
or from any Bookseller
1953
Price 9s 0d net
PRINTED IN GREAT BRITAIN

S O Code No 23-9007-17